Mapping Neural Function in *DCC* Mutation Carriers

Daniel Eric Vosberg

Integrated Program in Neuroscience (IPN)

Faculty of Medicine

McGill University, Montreal

A thesis submitted to McGill University in

partial fulfillment of the requirements of the degree of

Doctor of Philosophy (Ph.D.)

August, 2018

This thesis dissertation is dedicated to the memory of my bubbie, Mae Karsh Vosberg, who passed away on October 11th, 2018, at 97 years of age. Bubbie, you were incredibly bright, loving, funny, and unconditionally encouraging. I will love you and miss you forever.

Table of contents

Acknowledgments

I am extremely fortunate to have been supported throughout my doctoral studies by two outstanding supervisors. Dr. Marco Leyton, I appreciate your dedication, your kindness, your patience, your scrupulous feedback, and the confidence that you have inspired in me. You have mentored me to become a more effective science communicator, across a wide range of contexts. You have taught me to be resilient in the face of challenges and have enriched my understanding and application of scientific principles. Dr. Cecilia Flores, in addition to sharing these traits with Dr. Leyton, your expertise and passion have deepened my knowledge and appreciation of neuroscience at the molecular level, introducing me to the exciting field of axon guidance. You have provided the support for me to excel as a scientist and public speaker, supplying instrumental feedback on the content of my work as well as strengthening my capacities. Together, you have both acted as guidance cues, helping me to navigate the complex path towards completing a PhD. I also deeply appreciate the activities outside the lab, including fantastic dining experiences, skiing adventures, and disco parties.

I am grateful to the many collaborators who have provided mentorship and contributed to the projects described here. These remarkable individuals include Dr. Yu Zhang, Dr. Vincent Beaulé, Dr. Angélica Torres Berrío, Aurore Menegaux, Amanda Chalupa, Dominique Allard, France Durand, Dr. Sylvia Cox, Dr. Natalia Jaworska, Dr. Simone Zehntner, Dr. Colleen Manitt, Conrad Eng, Kristina DeDuck, Dr. Donatella Tampieri, Dr. Roberta La Piana, Dr. Barry J. Bedell, Dr. Alain Dagher, Dr. Chawki Benkelfat, Dr. Myriam Srour, Dr. Ridha Joober, Dr. Franco Lepore, Dr. Guy Rouleau, and Dr. Hugo Théoret. I would particularly like to acknowledge Amanda who began the recruitment of the study, and who is a wonderful friend. I would also like to thank Dominique for her incredible dedication to the study as well as for her

kindness, helping me through challenging times. A special thanks to Sylvia as well who was always eager to help when I had questions and who has enriched all the projects in the lab.

I am grateful to my terrific lab mates and friends at McGill for their support and comradery, including Kelly Smart, Luca Posa, Maria Tippler, Stephanie Scala, Valérie D'Amour-Horvat, Jen Lissemore, Jose Maria Restrepo, Dr. Daniel Hoops, Dr. Santiago Cuesta, Lauren Reynolds, Andrea Pantoja Urbán, Sonia Israel, Dominique Nouel, Alice Morgunova, Dr. Danilo De Gregorio, Dr. Martha López-Canul, Dr. Fernanda Pérez Gay Juárez, and John Aspler.

I'd like to acknowledge my undergraduate Honor's supervisor, Dr. Jim Pfaus, whose passion and creativity helped encourage me to pursue post-graduate studies. I am thankful to Dr. Paul Clarke, who made me passionate about statistics, enriching my love of rigorous science and sharpening my skepticism. I'm also grateful to my high school physics teacher, Mr. Bernie Lawetz, who made high school challenging and fascinating, inspiring me to pursue science.

I would like to thank Elijah Paull, Pardeep Trehan, Rina Brodeur, Maria Santaguida, Robbie Zunenshine, Richie Starr, and Nathaniel Mayer-Heft for their support throughout my graduate studies. I would especially like to thank my amazing girlfriend, Abigail Cruz Cruz, for keeping me sane and inspiring me with her brilliance.

I would like to thank my family for their support and encouragement. I am particularly thankful to my wonderful parents, Ron and Camille, who have helped me persevere through difficult times and who have unconditionally supported me. I also want to thank my brother, Mike, one of my best friends. I would like to thank my cousin Marion for always encouraging me throughout my studies. I would also like to acknowledge my aunt, Lenore, who founded the Centre for the Arts in Human Development (CAHD) at Concordia University, and who has

inspired me by enriching the lives of those with developmental disabilities. Finally, I would like to recognize the memory of my dog Jasper, who passed away earlier this year.

Abstract

Background: During development, axon guidance molecules direct axonal pathfinding, organize neuronal connectivity, neuronal function, transmitter release, and, ultimately, behavior. In the course of preparing the current thesis, I have had the rare opportunity to investigate these effects due to (1) the previous identification of a four-generational Quebec family, half of whom are haploinsufficient (+/-) for the axon guidance molecule receptor gene, *DCC*, and (2) well-characterized DCC-deficient transgenic mouse models. Previous work indicates that transgenic mice with impaired DCC function exhibit (i) a mirror-type hopping gait, (ii) failure of interhemispheric crossing of commissural and corticospinal axons, and (iii) increased dopamine pathway innervation to the medial prefrontal cortex coupled with blunted striatal dopamine release and diminished sensitivity to stimulant drugs. Among the members of the aforementioned Quebec family, two-thirds of the $DCC^{+/-}$ mutation carriers exhibit "mirror movements". In these individuals, voluntary movements on one side of the body elicit simultaneous, involuntary movements on the contralateral side. Given DCC's role in axon guidance, it was first hypothesized that $DCC^{+/-}$ mutation carriers with mirror movements would exhibit evidence of multiple connectivity alterations including atypical motor activations in the "mirroring" hemisphere, reduced interhemispheric inhibition, a greater functional ipsilateral corticospinal tract, and altered commissural white matter integrity. Secondly, it was hypothesized that $DCC^{+/-}$ mutation carriers would exhibit altered mesocorticolimbic features affecting connectivity, volumes, and associated behaviors. Finally, it was predicted that *DCC* mutation carriers would have reduced *DCC* mRNA expression.

Methods: Fifty-six participants were tested, including 13 $DCC^{+/-}$ mutation carriers with mirror movements, 7 $DCC^{+/-}$ mutation carriers without mirror movements, 16 $DCC^{+/+}$ relatives, and 20

unrelated healthy volunteers (UHV). Neuroimaging modalities included functional magnetic resonance imaging (fMRI), structural MRI, diffusion tensor imaging (DTI), transcranial magnetic stimulation (TMS), and resting state fMRI. Employing a translational approach, automated morphometric analyses of mesocorticolimbic regional brain volumes were conducted in *DCC* haploinsufficient humans and mice.

Results: As anticipated, $DCC^{+/-}$ mutation carriers with mirror movements exhibited functional ipsilateral corticospinal tracts, more bilateral motor representations, reduced interhemispheric inhibition, and reduced *DCC* mRNA expression. Both $DCC^{+/-}$ mutation carrier subgroups exhibited reductions in white matter integrity of the corpus callosum and one $DCC^{+/-}$ mutation carrier without mirror movements exhibited partial agenesis of the corpus callosum. Within the mesocorticolimbic system, both $DCC^{+/-}$ mutation carrier groups exhibited reductions in anatomical connectivity between the midbrain and target sites in both the striatum and prefrontal cortex, as well as reduced novelty seeking and cigarette smoking. Finally, striatal volumetric reductions were observed in both $DCC^{+/-}$ haploinsufficient humans and mice.

Conclusions: The translational investigations described here provide evidence that the axon guidance molecule receptor, DCC, alters brain connectivity, structure, function, and behavior in humans. The findings have implications for our understanding of differential susceptibility to putative mesocorticolimbic and brain connectivity related neuropsychiatric disorders.

Résumé

Contexte: Au cours du développement, les molécules de guidage axonal dirigent la détection des axones en organisant la connectivité et la fonction neuronale, la libération du transmetteur et, finalement, le comportement. J'ai eu la rare occasion d'étudier ces effets au moyen (1) de l'identification d'une famille québécoise de quatre générations, dont la moitié des individus est haploinsuffisante (+/-) pour le gène du récepteur de la molécule axonale *DCC* et (2) des modèles de souris transgéniques déficients en *DCC*. Des travaux antérieurs indiquent que les souris transgéniques avec la fonction du gène DCC altérée présentent (i) une allure de saut du type miroir, (ii) une défaillance du croisement interhémisphérique des axones commissuraux et corticospinaux et (iii) une augmentation de l'innervation de la voie dopaminergique vers le cortex frontal médial associée à une réduction de la libération de la dopamine dans le striatum et à une diminution de la sensibilité aux médicaments stimulants. Parmi les membres identifiés de la famille québécoise, les deux tiers des porteurs de la mutation $DCC^{+/-}$ présentent des «mouvements en miroir». Chez ces individus, les mouvements volontaires d'un côté du corps provoquent des mouvements involontaires simultanés du côté controlatéral. On a d'abord supposé que les porteurs de la mutation $DCC^{+/-}$ présentant des mouvements en miroir montreraient aussi : des altérations de connectivité multiples incluant des activations motrices atypiques dans l'hémisphère "miroir", une inhibition interhémisphérique réduite, une augmentation de la fonctionnalité de la voie corticospinale, et une altération de l'intégrité de la substance blanche commissurale. Deuxièmement, on a formulé l'hypothèse que les porteurs de la mutation $DCC^{+/-}$ présenteraient des caractéristiques mésocorticolimbiques altérées affectant la connectivité, les volumes et les comportements associés. Enfin, on a prédit que les porteurs de la mutation *DCC* auraient une expression réduite de l'ARNm *DCC*.

Méthodes: Cinquante-six participants ont été testés, dont 13 étant porteurs de la mutation *DCC*$^{+/-}$ avec mouvements en miroir, 7 étant porteurs de la mutation *DCC*$^{+/-}$ sans mouvements miroir, 16 étant porteurs *DCC*$^{+/+}$ dans la famille et 20 étant volontaires sains sans relation familiale. Les modalités de neuro-imagerie ont compris l'imagerie par résonance magnétique fonctionnelle (IRMf), l'IRM structurelle, l'imagerie du tenseur de diffusion, la stimulation magnétique transcrânienne (SMT) et l'IRMf au repos. Des analyses morphométriques automatisées des volumes cérébraux régionaux mésocorticolimbiques ont été effectuées chez des souris et des humains haploinsuffisants en *DCC*.

Résultats: Les porteurs des mutations *DCC*$^{+/-}$ présentant des mouvements en miroir ont montré des voies corticospinales ipsilatérales fonctionnelles, des représentations motrices plus bilatérales, une inhibition interhémisphérique réduite et une expression réduite de l'ARNm *DCC*. Les deux sous-groupes de porteurs de mutations *DCC*$^{+/-}$ ont présenté des réductions dans l'intégrité de la substance blanche du corps calleux et un seul porteur de la mutation *DCC*$^{+/-}$ sans mouvements en miroir a présenté une agénésie partielle du corps calleux. Dans le système mésocorticolimbique, les porteurs de mutations *DCC*$^{+/-}$ ont présenté des réductions dans la connectivité anatomique, une réduction dans la recherche de nouveauté et dans le tabagisme. Finalement, des réductions volumétriques striatales ont été observées chez les humains et les souris présentant un *DCC*$^{+/-}$ haploinsuffisant.

Conclusions: Les recherches translationnelles décrites ici montrent que le récepteur de la molécule à guidage axonal, le DCC, modifie la connectivité, la structure, la fonction et le comportement du cerveau chez l'homme. Ces résultats ont des implications pour la compréhension de la susceptibilité différentielle aux troubles neuropsychiatriques associées à la connectivité cérébrale et mésocorticolimbique.

Contribution of Authors

Chapter I: Daniel E. Vosberg wrote the general introduction under the supervision of Dr. Marco Leyton and Dr. Cecilia Flores.

Chapter II: Daniel E. Vosberg wrote the introduction, results, discussion, and methodology sections (Participants, Genetics, MRI, Statistical Analyses), created the figures, recruited and screened participants, conducted the MRI testing sessions, analyzed the fMRI data, and conducted statistical analyses for all the modalities. Dr. Vincent Beaulé wrote the TMS methodology, analyzed the TMS data, and conducted the TMS sessions. Dr. Angélica Torres Berrío wrote the qPCR methodology and conducted the qPCR. Danielle Cooke, Dr. Alvaro Pascual-Leone, and Dr. Michael Fox analyzed the resting state fMRI data. Amanda Chalupa, Dominique Allard, and France Durand recruited and screened participants. Dr. Natalia Jaworska, Dr. Sylvia ML Cox, Kevin Larcher, and Dr. Yu Zhang assisted in the analyses of the MRI data. Dr. Donatella Tampieri and Dr. Roberta La Piana evaluated the anatomical MRIs for neurological anomalies. Dr. Alain Dagher, Dr. Chawki Benkelfat, Dr. Myriam Srour, Dr. Ridha Joober, Dr. Franco Lepore, and Dr. Guy Rouleau participated in the design of the study. Dr. Cecilia Flores, Dr. Hugo Théoret, and Dr. Marco Leyton supervised the project, designed the study, provided critical feedback, and contributed to the writing of the manuscript.

Chapter III: Daniel E. Vosberg wrote the introduction, results, discussion, and methodology sections (Participants, Genetics, MRI, Statistical Analyses, Mice sections), created the figures, recruited and screened participants, administered and analyzed personality tests, conducted the MRI testing sessions, conducted connectivity and volumetric MRI analyses, and conducted the statistical analyses for all the modalities. Dr. Yu Zhang designed and conducted connectivity and volumetric MRI analyses, wrote the human connectivity and volumetric methodology sections,

and made writing contributions throughout the manuscript. Aurore Menegaux and Dr. Simone Zehntner contributed to the analyses of the mice MRI data. Amanda Chalupa, Dominique Allard, and France Durand recruited and screened human participants. Dr. Colleen Manitt contributed to the running, design, and analysis of the mouse imaging study. Conrad Eng contributed to the running of the mouse imaging study. Kristina DeDuck contributed to the mouse imaging analyses. Dr. Barry J. Bedell contributed to the mouse MRI study design and analysis. Dr. Alain Dagher, Dr. Chawki Benkelfat, Dr. Myriam Srour, Dr. Ridha Joober, Dr. Franco Lepore, Dr. Guy Rouleau, and Dr. Hugo Théoret participated in the design of the study. Dr. Cecilia Flores and Dr. Marco Leyton supervised the project, designed the study, provided critical feedback, and contributed to the writing of the manuscript.

Chapter IV: Daniel E. Vosberg wrote the general discussion under the supervision of Dr. Marco Leyton and Dr. Cecilia Flores.

Contributions to Original Knowledge

Prior to the studies in the present manuscript-based PhD thesis dissertation, studies of human *DCC* mutation carriers focussed on the motor system, and particularly of participants who expressed mirror movements. The factors driving the partial penetrance of mirror movements among mutation carriers had not been explored. In Chapter II, the neurophysiology of the motor system is characterized in *DCC* mutation carriers, both with and without mirror movements. By employing generalized estimating equations, it was possible to examine which effects were attributable to mirror movements and which were best accounted for by the *DCC* mutation. Moreover, we identified a plausible candidate explanation for the partial penetrance of mirror movements, whereby decreased peripheral levels of *DCC* mRNA were seen in *DCC* mutation carriers with MM but not in those without MM. This first manuscript is currently under revision at the journal, *Annals of Neurology* (Impact factor: 10.2; ID: ANA-18-0177.R2).

In chapter III, I present the first investigation of the mesocorticolimbic system in humans carrying a mutation to *DCC*, guided by hypotheses that were based on the rapidly growing literature in *Dcc* mutant mice (Flores, 2011; Hoops and Flores, 2017). For the first time, I identified alterations in the connectivity of mesocorticolimbic pathways, the volumes of mesocorticolimbic terminal structures, and associated personality traits and behaviors. The human findings strikingly parallel the previously reported connectivity and behavioral findings in *Dcc* mutant mice. Moreover, the study includes evidence of reductions in striatal volume in *DCC* haploinsufficient humans and mice. Finally, by characterizing how alterations to *DCC* affect the mesocorticolimbic system, it may help elucidate the associations between genetic polymorphisms in *DCC* and psychiatric disorders long hypothesized to reflect disturbances to these pathways (Grant et al., 2012; Manitt et al., 2013; Dunn et al., 2016; Okbay et al., 2016;

Yan et al., 2016; Torres-Berrío et al., 2017; Ward et al., 2017; Zeng et al., 2017; Leday et al., 2018; Smeland et al., 2018; Wray et al., 2018). This second manuscript was published in the *Journal of Neuroscience* (Impact factor: 5.9) (Vosberg et al., 2018).

Chapter I: General Introduction

1.1 Overview

Ten years ago, a Quebec family was identified, one-third of whom exhibited a neurological phenomenon known as mirror movements, whereby intentional movements on one side of the body elicited concurrent involuntary movements on the other side (Srour et al., 2009). The affected individuals were subsequently found to possess a haploinsufficient mutation in a gene that encodes for a receptor called DCC (deleted in colorectal cancer) (Srour et al., 2010). DCC receptors play a critical role in axon guidance in rodents (Sun et al., 2011). The goal of my PhD thesis was to determine whether *DCC* haploinsufficiency in humans leads to disturbances in axonal pathfinding and neuronal connectivity. First, I hypothesized that the mirror movements exhibited by *DCC* mutation carriers might reflect alterations in commissural (Keino-Masu et al., 1996) and corticospinal pathways (Fazeli et al., 1997). Therefore, my first objective was to determine whether alterations to these pathways occur in humans.

Second, based on the work by Flores and colleagues showing that DCC receptors orchestrate the development of the mesocorticolimbic dopamine system in rodents (Flores et al., 2005; Flores, 2011; Hoops and Flores, 2017), I hypothesized that *DCC* mutation carriers might exhibit reorganization of mesocorticolimbic circuitry. Since mesocorticolimbic dopamine pathways are implicated in the regulation of mood and motivational states (Leyton 2010), and since a rapidly accumulating literature indicates that genetic variants and altered expression of *DCC* are associated with diverse psychiatric disorders (Grant et al., 2012; Manitt et al., 2013; Dunn et al., 2016; Okbay et al., 2016; Yan et al., 2016; Torres-Berrío et al., 2017; Ward et al., 2017; Zeng et al., 2017; Leday et al., 2018; Smeland et al., 2018; Wray et al., 2018), the second main objective of my thesis was to determine whether *DCC* haploinsufficiency in humans affects

mesocorticolimbic connectivity and whether these alterations associate with changes in dopamine-mediated behaviors.

1.2 Mirror movements

Mirror movements can occur in children but they do not normally persist beyond age 10 (Rasmussen, 1993). These age-linked and quite subtle movements are potentially explained by low levels of interhemispheric inhibition resulting from incomplete maturation of the corpus callosum (Mayston et al., 1999). Mirror movements that persist into adulthood are more rare, and can be a consequence of neurological and developmental disorders including Klippel-Feil syndrome (Gunderson and Solitare, 1968; Farmer et al., 1990), Kallmann syndrome (Krams et al., 1997; Mayston et al., 1997; Krams et al., 1999), agenesis of the corpus callosum (Lepage et al., 2012), and Parkinson's disease (Espay et al., 2005; Cincotta et al., 2006; Li et al., 2007). Adult mirror movements occurring in the absence of obvious neurological disorders have been reported also, and some early reports hinted at the unusual neural regulation that they reflected. For example, when a patient with lifelong mirror movements experienced a hemiplegia inducing stroke, voluntary movements in his paralyzed right hand became impossible yet this same hand continued to exhibit mirror movements (Haerer and Currier, 1966). Since the patient's daughter and granddaughter also had mirror movements, they were evidently of familial origin (Haerer and Currier, 1966).

Other instances of familial mirror movements occurring in the absence of frank neurological disorders have been reported. Typically these rare families exhibit a pattern of autosomal dominant inheritance with incomplete penetrance, although recessive inheritance and sporadic cases have been identified (Srour et al., 2009; Depienne et al., 2012; Ahmed et al., 2014; Méneret et al., 2014; Marsh et al., 2017). A 1967 review, summarizing articles published

between 1891 and 1966, identified congenital mirror movements in 14 families (59 affected individuals, twice as many males as females) (Regli et al., 1967). Since then, numerous additional cases and families have been identified, including the Quebec family of the present investigations (Srour et al., 2009), as well as families in Iran (Sharafaddinzadeh et al., 2008), Pakistan (Ahmed et al., 2014), France, Italy, Germany (Depienne et al., 2011; Depienne et al., 2012), North Africa, Australia (Marsh et al., 2017), and Mexico (Jamuar et al., 2017).

Mirror movements are primarily observed in the hands and fingers and, less frequently, in muscles of the feet, toes, and face. Mirror movements may be complete or fractionated compared to the voluntary movements, such as mirroring a subset of the muscles or having smaller amplitudes (Franz et al., 2015). The degree to which mirror movements are disruptive to daily functioning varies across cases but generally they are not incapacitating. However, since those with mirror movements cannot perform asymmetric movements, they may experience difficulties climbing ladders or ropes, running, sewing, shoe tying, typing, playing musical instruments, and crawl (but not breast stroke) swimming (Haerer and Currier, 1966; Regli et al., 1967; Cohen et al., 1991).

Within the Quebec family, the following characteristics were identified during their initial assessment. The penetrance of mirror movements is higher among males, the movements are not dependent on handedness, and all affected individuals present them in the forearms, hands, and fingers, while a subset exhibit mirror movements in the feet and toes. Commonly affected tasks include writing, tapping, and typing. Half of those with mirror movements report the capacity to partially suppress mirror movements. Generally, the mirror movements are not experienced as disabling, although some individuals report social difficulties stemming from self-consciousness of their condition (Srour et al., 2009).

1.3 Neurophysiology of congenital mirror movements

Voluntary fine motor movements, particularly of the muscles of the distal extremities, are subserved by the corticospinal tract. Of the axons composing this tract, 40% project from the motor cortex, via the internal capsule and cerebral peduncle, to the medullary pyramids. The fibers then cross the midline at the pyramidal decussation, and, finally, terminate in the motor neurons of the ventral horn of the spinal cord (Kandel et al., 2012) (Figure 1). In primates, 87% of the corticospinal axons decussate at the medullary pyramids, and, among those that do not, the majority cross the midline at the level of the spinal cord while a small proportion remain ipsilateral (Rosenzweig et al., 2009). Similarly, in rats, 96-98% of corticospinal axons innervate the contralateral spinal cord (Rouiller et al., 1991). In humans, neuroimaging studies have demonstrated that unilateral hand movements are primarily associated with increased activations in the contralateral hemisphere (primary motor cortex, supplementary motor area, premotor cortex, and basal ganglia), while the cerebellum is primarily activated in the ipsilateral hemisphere (Shibasaki et al., 1993; Turner et al., 1998).

The ability to perform exclusively unilateral movements (something that people with mirror movements cannot do) is normally regulated by inhibitory interhemispheric pathways of the corpus callosum (Beaulé et al., 2012). This interhemispheric inhibition can be assessed using transcranial magnetic stimulation (TMS) of the motor cortices and electromyographic (EMG) recordings of muscles in the hands. In healthy individuals, if TMS is applied to the motor cortex in one hemisphere immediately prior to stimulating the contralateral one, then the EMG activity following the test stimulus will be inhibited (Ferbert et al., 1992). In further support of

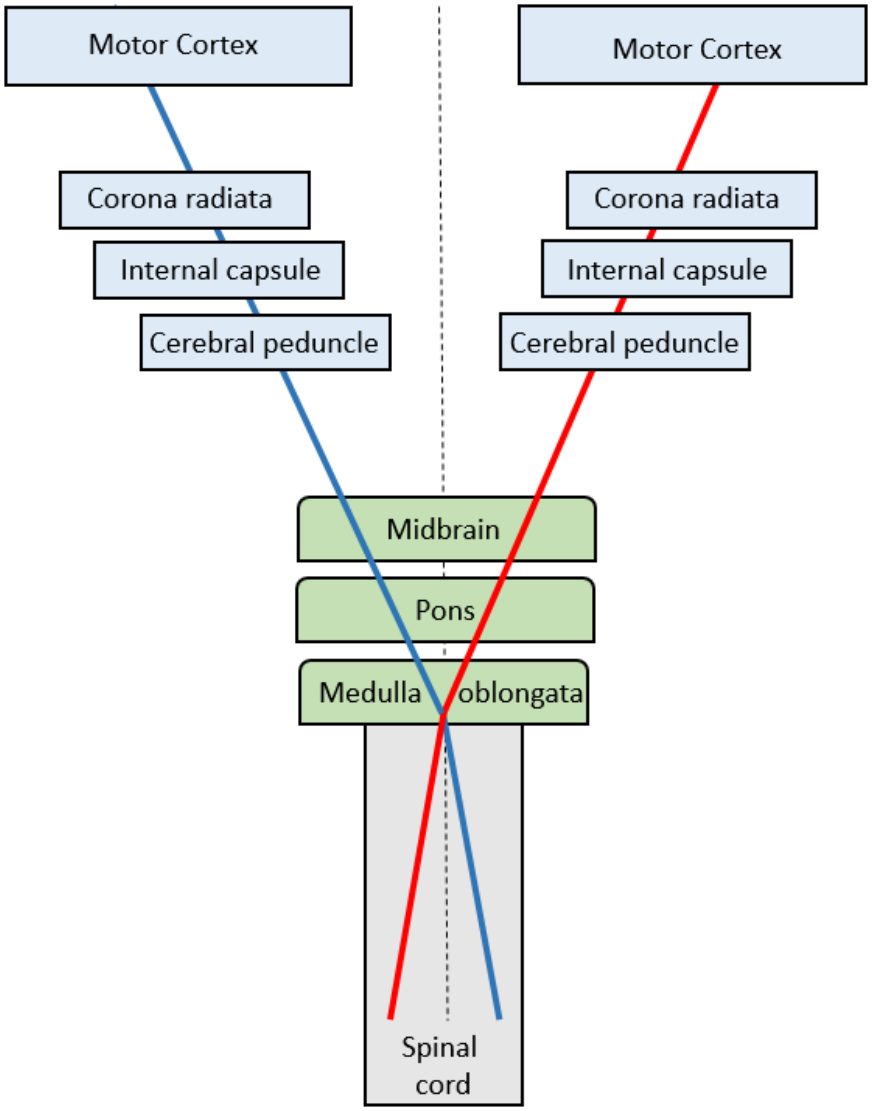

Figure 1. Recreated and adapted with permission from Jaspers et al. (2016). Diagram depicting trajectory of descending corticospinal tracts (red and blue) from the motor cortex to the spinal cord, decussating at the medullary pyramids in the medulla oblongata.

interhemispheric inhibition in motor pathways in healthy individuals, unilateral hand movements are associated with increased activations of the contralateral motor cortex and decreased activations in the ipsilateral motor cortex, assessed using functional magnetic resonance imaging (fMRI) (Newton et al., 2005).

1.3.1 Ipsilateral corticospinal tract

In individuals with mirror movements, EMG recordings of the voluntary and mirroring muscles indicate that the onset times, durations, and magnitudes of responses are highly correlated (Forget et al., 1986). These observations raised the possibility that, in addition to reduced interhemispheric inhibition, people with mirror movements also have more ipsilateral corticospinal tracts. TMS provides one strategy to investigate this possibility.

The first TMS study, conducted in a single individual, found that direct stimulation of the primary motor cortex elicited bilateral EMG responses in the abductor pollicis brevis and abductor digiti minimi muscles, which occurred effectively simultaneously (within 0.1-0.7 ms) (Konagaya et al., 1990). Strikingly, the ipsilateral EMG responses were of a greater amplitude than the contralateral EMG responses, suggesting an ipsilateral corticospinal tract with greater connectivity than the contralateral corticospinal tract (Konagaya et al., 1990). A subsequent TMS study of three individuals with mirror movements found that EMG onset times were delayed by 1-4 ms in the ipsilateral, compared to the contralateral, hand muscles (Capaday et al., 1991). These responses are still temporally close. Indeed, TMS-induced physiological mirror movements in normal children occur after a delay of 12-200 ms (Reitz and Müller, 1998). As further evidence that abnormal corticospinal tract decussation underlies mirror movements, bilateral hypertrophy of the corticospinal tract was identified in Kallmann syndrome patients with mirror movements (Krams et al., 1999).

1.3.2 Bilateral motor representations

Cohen et al., (1991), like Capaday et al., (1991), also reported TMS-EMG evidence of an ipsilateral corticospinal tract in two mirror movement participants. Moreover, Cohen and colleagues also found evidence that voluntary ipsilateral movements elicited bilateral premovement potentials. Intriguingly, these premovement potentials originated only in the hemisphere contralateral to the voluntary movement, and after 10 ms were observed in both hemispheres, suggesting a spread of the motor activation to the ipsilateral "mirroring" hemisphere (Cohen et al., 1991). The authors also found evidence of bilateral blood flow increases in motor cortices induced by unilateral movements, as measured with positron emission tomography (PET). This effect, however, was only observed in one of the two mirror movement participants. This mirror movement participant demonstrated an ipsilateral to contralateral motor cortex activation ratio of 1.09, markedly greater than the ratios observed in the control subjects (mean: 0.11, range: -0.27 to 0.24) (Cohen et al., 1991). The other mirror movement participant was excluded due to a failure of unilateral movements to reliably induce blood flow increases to the contralateral motor cortex (Cohen et al., 1991). Despite the shortcomings, these findings provided the first demonstration that mirror movements are associated with bilateral motor representations, suggesting abnormalities in callosal interhemispheric pathways.

In contrast to the observations reported by Cohen et al., (1991), a subsequent PET study with two mirror movement participants performing unilateral voluntary movements identified sensorimotor blood flow increases only in the contralateral cortex (Kanouchi et al., 1997). Moreover, in a third PET study, mirror movement participants exhibited bilateral motor representations, but similar ipsilateral motor cortex activations were produced by passive

movements alone (Krams et al., 1997). This raised the possibility that the ipsilateral motor cortex activations might not be contributing to the expression of mirror movements but, instead, might be explained by sensory feedback from the ipsilateral "mirroring" hand (Krams et al., 1997). These observations noted, the low spatial resolution of PET, rendering localization of the motor hand area challenging, might have contributed to the discrepant findings.

fMRI offers superior anatomical and temporal resolution (1-1.5 mm, 3-5 sec) compared to PET (4 mm, 45 sec) (Volkow et al., 1997). The first fMRI study of individuals with mirror movement found bilateral activations in the hand area during unilateral voluntary finger movements, with the ipsilateral hand area activations in the same location but of a smaller magnitude compared to the contralateral hand area (Leinsinger et al., 1997). However, as proposed by Krams et al. (1997), the ipsilateral activations are potentially explained by sensory feedback from the mirroring hand.

The above foundational studies leave some key questions open but provide evidence that individuals with mirror movements exhibit a functional ipsilateral corticospinal tract, as demonstrated by nearly simultaneous ipsilateral motor evoked potentials in the hand induced by unilateral TMS (Capaday et al., 1991; Cohen et al., 1991; Kanouchi et al., 1997; Cincotta et al., 2002). The reduced crossing of corticospinal projections may consequently innervate ipsilateral muscles, and functionally produce movements that mirror the activity of the contralateral muscles. Additionally, despite the caveats noted above, individuals with mirror movements exhibit more bilateral motor cortex activations during unilateral movements (Cohen et al., 1991; Krams et al., 1997; Leinsinger et al., 1997; Cincotta et al., 2002), which may be a consequence of decreased transcallosal inhibitory pathways (Hübers et al., 2008).

1.3.3 Mirror movement genes

In addition to *DCC* (Srour et al., 2010), two other genes have been implicated in mirror movements, *RAD51* (Depienne et al., 2012) and *DNAL4* (Ahmed et al., 2014). Some of the mirror movement features appear to be common across the genetic etiologies, while others differ. The best-studied of these are *RAD51* mutation carriers, and they have been the focus of at least one multimodal neuroimaging investigation. These individuals exhibit evidence of ipsilateral corticospinal tracts, bilateral motor representations during unilateral movements, and reduced interhemispheric inhibition (Gallea et al., 2013). Each of these alterations is hypothesized to occur in *DCC* mutation carriers. This noted, there are some motor differences in the gene defined populations. Whereas *RAD51* mutation carriers exhibit full mirror movements, such that the mirroring hand completely mirrors the intended hand, *DCC* mutation carriers exhibit "fractionated" mirror movements, such that the mirroring hand movements are more fragmented and saccadic (Franz et al., 2015). In both groups, though, some *DCC* and *RAD51* mutation carriers who do not display visually-evident mirror movements do exhibit subtler mirror movements that have been detected using accelerometer gloves (Franz et al., 2015).

1.4 Axon guidance

During neurodevelopment, the navigation of axons towards their targets is directed by extracellular axon guidance cues, which attract or repel growing axons by inducing molecular changes in their growth cones (Dickson, 2002). Growth cones are versatile structures with actin-based finger-like extensions (filopodia) and protruding sheets (lamellipodia) in their peripheral domains and microtubules in their central domains. Growth cones elongate, retract, or turn based on the dynamics of cytoskeletal proteins, including actin filaments and microtubules. These effects of guidance cues are accomplished by inducing alterations in the relative rates of

polymerization and depolymerization in actin filaments as well as changes in microtubule stabilization (Kalil and Dent, 2005; Dent et al., 2011). These processes play a critical role in organizing brain connectivity, and the human brain comprises up to 180,000 km of myelinated axons (Drachman, 2005). Remarkably, this staggering complexity of the nervous system is organized by comparatively few guidance cue families, including the netrins, slits, semaphorins, and ephrins (Dickson, 2002).

1.4.1 DCC is an axon guidance molecule receptor for Netrin-1

DCC is a transmembrane receptor for the laminin-related extracellular molecule, Netrin-1 (Keino-Masu et al., 1996). The name, deleted in colorectal cancer, is based on DCC's initial discovery as a potential tumor suppressor gene, due to the loss of heterozygosity identified in human colorectal cancers (Duman-Scheel, 2012). Since the 1990s, the role of DCC as a tumor suppressor gene has been the subject of ongoing debate, with some evidence in non-human animals implicating DCC in tumor suppression (Duman-Scheel, 2012).

DCC is a member of the large immunoglobulin superfamily, and its extracellular domains are composed of four immunoglobulin domains, in addition to six fibronectin type III repeats (Hedrick et al., 1994) (Figure 2). The fourth, fifth, and sixth fibronectin type III repeats constitute the binding sites for Netrin-1 (Finci et al., 2014; Xu et al., 2014). In humans, the *DCC* gene is located on chromosome 18 and comprises 29 exons (Cho et al., 1994). While attractive effects of Netrin-1 are mediated by DCC alone, repulsive actions are mediated by DCC/uncoordinated 5 homologues (UNC5H) receptor complexes (Keino-Masu et al., 1996; Manitt and Kennedy, 2002; Barallobre et al., 2005; Finci et al., 2014). The role of DCC in axon guidance is evolutionarily conserved, with homologous proteins and functions in *C. elegans* (Chan et al., 1996), *Drosophila* (Kolodziej et al., 1996), and *Xenopus* (de la Torre et al., 1997).

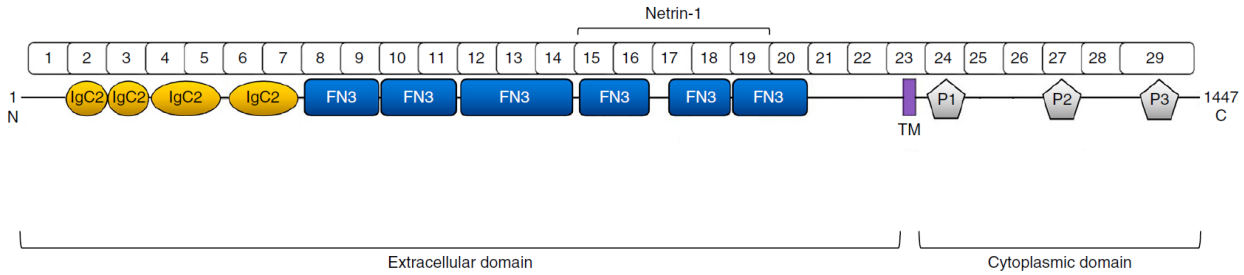

Figure 2. Adapted with permission from Springer Nature Customer Service Centre GmbH: Springer Nature © (Marsh et al., 2017). Structure of the human *DCC* gene, comprising 29 exons and depicting protein domains. **IgC2**: immunoglobulin-like type C2 domain; **FN3**: fibronectin type III–like domain; **TM**: transmembrane domain; **P1–3**: proline-rich conserved motifs. Netrin-binding site comprises the 4th, 5th, and 6th FN3.

Other Netrin-1 receptors that interact with DCC in axon guidance include Down's syndrome Cell Adhesion Molecule (DSCAM) (Ly et al., 2008) and Neogenin (Mawdsley et al., 2004; De Vries and Cooper, 2008).

In the developing neural tube, DCC is expressed by commissural axons that are attracted to Netrin-1 (Kennedy et al., 1994; Keino-Masu et al., 1996; Livesey, 1999). Across development, DCC is highly expressed throughout the nervous system (Gad *et al*, 1997; Harter *et al*, 2010; Livesey and Hunt, 1997). Brain regions expressing DCC include the commissural pathways: the corpus callosum, hippocampal commissure, and anterior commissure (Shu et al., 2000). DCC and Netrin-1 are also expressed in dopamine cell bodies and terminal regions (Osborne et al., 2005; Manitt et al., 2010; Manitt et al., 2011), and this includes the substantia nigra, ventral tegmental area, striatum, cerebellum, hippocampus, and cerebral cortex (Gad et al., 1997; Livesey and Hunt, 1997; Osborne et al., 2005; Grant et al., 2007; Harter et al., 2010; Manitt et al., 2010; Reyes et al., 2013).

1.4.2 Commissural and corticospinal tracts in DCC mutant mice

Dcc homozygous mice with targeted deletions of exon 3 do not survive beyond 24 hours. However, examination of their brains post-mortem identified profound perturbations in commissural pathway development, including absences of the corpus callosum and hippocampal commissure (Fazeli et al., 1997; Finger et al., 2002), and Probst bundles (*i.e.,* longitudinal white matter fibers that fail to cross the midline) (Fazeli et al., 1997). A separate strain of *Dcc* homozygous mice survives to adulthood carrying a spontaneous mutation that deletes exon 29 (Finger et al., 2002). These mutant mice are named “kanga” because they exhibit a symmetric hopping gait (Finger et al., 2002), a parallel to the mirror movements observed in humans

carrying a *DCC* mutation. Consistently, there are failures of corticospinal tract crossing in *Dcc* homozygous "kanga" mice (Finger et al., 2002).

1.4.3 Human DCC mutations and mirror movements

In the Quebec family, mirror movements are due to an abnormal skipping of exon 6 leading to a premature stop codon that encodes a truncated DCC protein that fails to bind to Netrin-1 (Srour et al., 2010). Bolstering support for this association, Srour and colleagues (Srour et al., 2010) also identified a *DCC* frameshift mutation (a guanine insertion into exon 3) in an Iranian family with congenital mirror movements. More recently, both heterozygous (Marsh et al., 2017) and homozygous (Jamuar et al., 2017) *DCC* mutations in humans were reported to underlie partial and complete agenesis of the corpus callosum, features that are also seen in *DCC* homozygous mice (Fazeli et al., 1997; Finger et al., 2002). Moreover, *DCC* mutation carriers in some families lack a hippocampal commissure (Jamuar et al., 2017; Marsh et al., 2017), a feature again seen in *Dcc* homozygous mice (Fazeli et al., 1997; Finger et al., 2002). In addition to these neurobiological alterations, the human *DCC* homozygous mutation carriers exhibit scoliosis, horizontal gaze palsy, and intellectual disability (Jamuar et al., 2017). In comparison, the IQ of *DCC* heterozygous mutation carriers identified by Marsh and colleagues ranged from normal to borderline intellectual impairment (Marsh et al., 2017).

To calculate the penetrance of these *DCC* mutation-related features, Marsh et al. (2017) analyzed data from their own study (9 families) and previous reports (Srour et al., 2009; Srour et al., 2010; Depienne et al., 2011; Méneret et al., 2014; Franz et al., 2015), and determined that, among 88 *DCC* mutation carriers, mirror movements and agenesis of the corpus callosum were seen in 42% and 26%, respectively. Mirror movements were more common in males and agenesis of the corpus callosum was more common in females, as observed in the Quebec

family, suggesting a role for gonadal hormones. The location of the mutation appears to be critical. Among the *DCC* missense mutations, all 8 were associated with agenesis of the corpus callosum, while two were additionally associated with mirror movements. Moreover, five of these missense mutations occurred in the Netrin-1 binding regions, the fourth, fifth, and sixth fibronectin type III-like domains (Marsh et al., 2017). In comparison, among the two *DCC* mutations resulting in a truncated DCC protein, both were associated with mirror movements and callosal agenesis, and these occurred in the immunoglobulin-like type C2 domain (Marsh et al., 2017). Modelling of the DCC/Netrin-1 interactions predicted that the mutations of *DCC* in the Netrin-1 binding regions would induce the greatest disturbances to the ligand's binding, as well as DCC's dimerization and axon guidance (Marsh et al., 2017). Interestingly, Marsh et al. (2017) reported tentative evidence that testosterone administration increases *DCC* expression, while acknowledging that other genetic and environmental factors must be implicated as well. Indeed, testosterone levels alone do not explain why callosal agenesis cases are more prevalent among females and mirror movements are more prevalent among males.

Using TMS and diffusion tensor imaging tractography, it was demonstrated that *DCC* haploinsufficient humans exhibit increased ipsilateral corticospinal projections (Marsh et al., 2017; Welniarz et al., 2017). Whole-brain diffusion tensor imaging investigation of one *DCC* homozygous individual confirmed the absence of commissural fibers as well as the presence of Probst bundles adjacent to the lateral ventricles (Jamuar et al., 2017). Broad reductions in non-commissural fibers were also identified, particularly in the anterior-posterior orientation; those that remained were markedly disordered and characterized by strikingly diminished axonal integrity, as assessed with fractional anisotropy (Jamuar et al., 2017).

Strikingly, it was recently discovered that, in four out of ten *DCC* mutation carriers with

mirror movements, painful sensations on one side of the body were induced by noxious mechanical stimulation of the contralateral side of the body (da Silva et al., 2018). These bilateral somatosensory sensations in *DCC* mutation carrier humans are congruent with the increased ipsilateral spinothalamic connectivity and somatosensory representations observed in mice with *Dcc* selectively knocked out in the spinal cord (da Silva et al., 2018).

Finally, mutations in *DCC* and *Netrin-1* have recently been identified in patients with Kallmann syndrome, which is often associated with mirror movements (Bouilly et al., 2018).

1.5 Mesocorticolimbic system

The mesocorticolimbic dopamine system comprises two main ascending pathways arising from the ventral tegmental area (VTA) in the upper brainstem: (i) the mesolimbic pathway that primarily innervates the nucleus accumbens (NAcc), in addition to the olfactory tubercle, septum, hippocampus, and amygdala, and (ii) the mesocortical pathway that projects most densely to the prefrontal, cingulate, and perirhinal cortices (Arias-Carrión et al., 2010) (Figure 3). In comparison, the nigrostriatal dopaminergic pathway projects from the VTA adjacent substantia nigra pars compacta (SNc) to the dorsal striatum (Arias-Carrión et al., 2010). This mesolimbic and nigrostriatal dopamine distinction is readily dissociable in rodents, but is more complex in primates, such that mesocorticolimbic dopamine fibers project from both the VTA and SNc (Düzel et al., 2009). Compared to rodents, the primate cortical dopamine projections are also more widespread, innervating the entire cortical mantle, albeit more so to anterior than posterior regions (Lewis et al., 2001; Taber et al., 2012).

1.5.1 Personality traits

In humans, variability in mesocorticolimbic dopamine function is implicated as a contributing factor to differences in personality traits and susceptibility to a wide range of

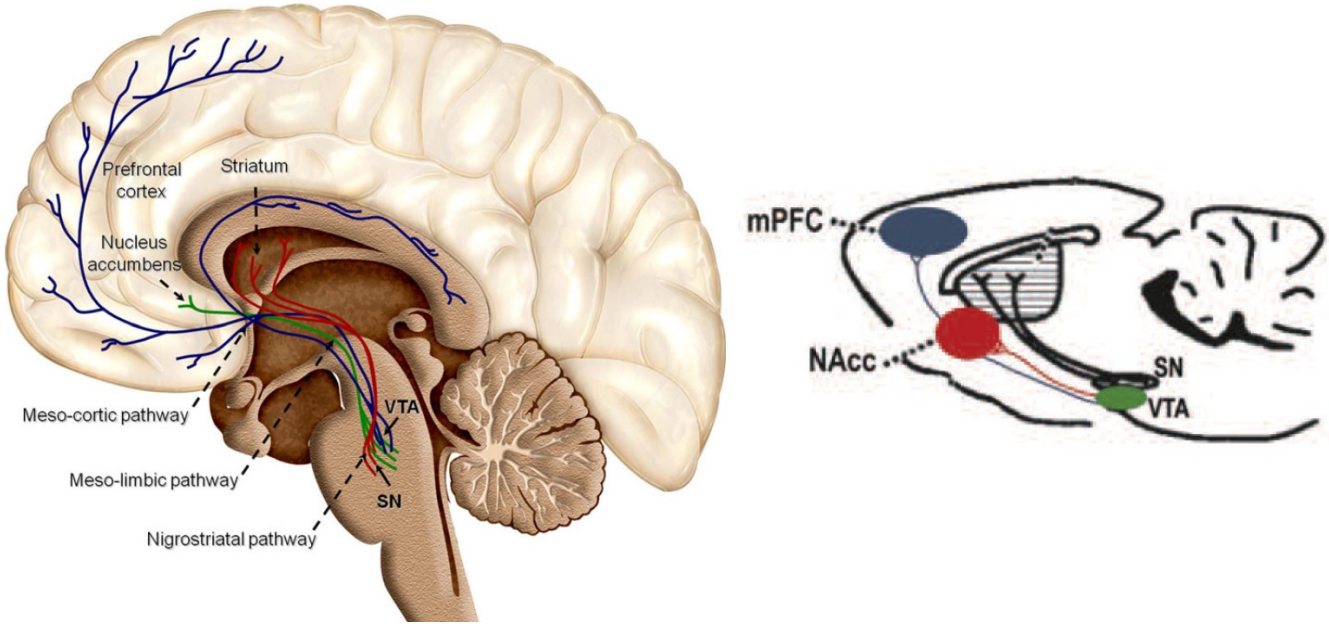

Figure 3. Human (left) and mouse (right) mesocorticolimbic systems, adapted with permission from Arias-Carrión et al. (2010) and Flores (2011). **mPFC**: medial prefrontal cortex; **NAcc**: nucleus accumbens; **SN:** substantia nigra; **VTA:** ventral tegmental area.

psychiatric disorders (Hutchison et al., 1999; Yasuno et al., 2001; Chau et al., 2004; Whitton et al., 2015; Leyton, 2017). For instance, in PET imaging studies individual differences in amphetamine-induced dopamine release in the ventral striatum are positively associated with novelty seeking (Leyton et al., 2002) and impulsivity related traits (Buckholtz et al., 2010). These findings were not unanticipated. In laboratory rodents, it has been reported that the degree of exploration of novel environments correlates positively with cell firing rates of midbrain dopamine cells (Marinelli and White, 2000) and the magnitude of stimulant-induced dopamine release in the NAcc (Hooks et al., 1991). These associations are thought to reflect dopamine's influence on the salience of emotionally and motivationally relevant stimuli (Leyton, 2010). For example, in people with Parkinson's disease on *vs.* off L-DOPA (high *vs.* low dopamine state), the high dopamine state is associated with increased sensitivity to reward and decreased sensitivity to punishment; the opposite pattern is observed when patients are in a low dopamine state (Frank et al., 2004).

1.5.2 Psychiatric disorders

Many psychiatric disorders appear to reflect, in part, alterations to the organization of mesocorticolimbic circuitry, as evidenced by alterations in the functional connectivity in these pathways in people with schizophrenia (Horga et al., 2016), psychostimulant addiction (Gu et al., 2010; Konova et al., 2013; Kohno et al., 2014; Lu et al., 2014), and depression (Harrison et al., 2009; Furman et al., 2011; Felger et al., 2016). Alterations to the mesocorticolimbic system are also implicated in an influential animal model of substance use disorders whereby repeated drug use induces sensitization of mesolimbic dopamine pathways, such that the drug-induced behavioral and dopamine responses progressively increase over time; since there are individual

differences in the magnitude of sensitization that animals develop, those that exhibit little sensitization might be less susceptible to excessive drug intake (Kalivas and Stewart, 1991; Vezina, 2004; Robinson and Berridge, 2008). Preliminary studies raise the possibility that multiple features of this model are relevant in humans too (Leyton & Vezina 2014; Leyton 2017).

1.6 The role of DCC in mesocorticolimbic circuitry

DCC receptors play a critical role in the development of the mesocorticolimbic dopamine system. Adult *Dcc* or *Netrin-1* haploinsufficient mice show alterations in mesocorticolimbic development, function, and associated behaviors (Grant et al., 2007; Flores, 2011; Auger et al., 2013; Kim et al., 2013; Pokinko et al., 2015; Hoops and Flores, 2017). This includes reduced sensitivity to the rewarding properties of stimulant drugs. For example, *Dcc* haploinsufficient mice exhibit a decreased ability of amphetamine paired cues to acquire incentive value as measured by reduced conditioned place preferences to the drug (Grant et al., 2007; Kim et al., 2013). Whereas cocaine administration increases intracranial self-stimulation behaviors in wild type mice, this effect is blunted in *Dcc* haploinsufficient mice (Reynolds et al., 2016). Upon repeated amphetamine administration, *Dcc* haploinsufficient mice fail to develop behavioral sensitization (Flores et al., 2005).

Adult *Dcc* haploinsufficient mice also exhibit disturbances in the function and connectivity of mesocorticolimbic dopamine pathways (Flores, 2011; Hoops and Flores, 2017). In the medial prefrontal cortex (mPFC), adult *Dcc* haploinsufficient mice exhibit increased baseline and amphetamine-induced dopamine release, relative to controls (Grant et al., 2007) whereas in the NAcc, they exhibit blunted amphetamine-induced dopamine release (Grant et al., 2007). *Dcc* haploinsufficient mice or those with conditional *Dcc* haploinsufficiency in dopamine

neurons exhibit increased dopamine fiber innervation to the mPFC (Manitt et al., 2011; Reynolds et al., 2015; Reynolds et al., 2018) and decreased dopamine innervation to the NAcc (Reynolds et al., 2018). In the pyramidal neurons of layer V of the mPFC, a site that is densely innervated by dopamine axons, the dopamine connectivity changes lead to structural and functional modifications including reductions in dendritic spine density and dendritic arborisation, and reduced excitability (Grant et al., 2007; Manitt et al., 2011; Manitt et al., 2013). In comparison, the effects in the NAcc might result from the reduced dopamine innervation to this region (Reynolds et al., 2018), and, secondly, from the increased dopamine transmission in the mPFC since converging evidence indicates that dopamine activity in the mPFC inhibits dopamine activity in the NAcc (Carr and Sesack, 2000; Ventura et al., 2004; Pokinko et al., 2015).

The above *Dcc* mutation-induced dopamine-related effects are age-dependent. The effects are observed in adult *Dcc* haploinsufficient mice but not in post-weanlings or adolescent mice (Grant et al., 2009). The emergence of the *Dcc* haploinsufficient phenotype in adulthood might reflect alterations in DCC and UNC5H levels across development. In developing embryos and pre-adolescent mice, DCC levels are high and UNC5H levels are relatively low (Manitt et al., 2010). In comparison, between adolescence and adulthood, DCC levels decrease and UNC5H levels increase, such that the ratio of DCC to UNC5H shifts from predominantly DCC to predominantly UNC5H (Manitt et al., 2010). This developmental shift in Netrin-1 receptors coincides with the marked increase of mesocortical dopamine fibers to the mPFC in adulthood, relative to adolescence (Hoops and Flores, 2017). Indeed, it has recently been demonstrated that dopamine axons continue to grow to the prefrontal cortex during adolescence, a developmental process that is mediated by DCC (Reynolds et al., 2018).

1.6.1 DCC and psychiatric disorders

Like the age-dependent effects of *Dcc* haploinsufficiency, many psychiatric disorders begin during adolescence (Paus et al., 2008). Recently, genetic and postmortem studies have linked DCC with psychiatric disorders, particularly those that are thought to reflect to varying degrees alterations in mesocorticolimbic system function, as discussed below.

1.6.2 Schizophrenia

Two studies have linked polymorphisms in the *DCC* gene with schizophrenia. Genetic variation in *DCC* was investigated in a case-control sample comprising 556 unrelated schizophrenic patients and 208 healthy controls. A single nucleotide polymorphism (SNP) (rs2270954) in *DCC* was found to be associated with schizophrenia. The authors postulated that this SNP, in the 3' untranslated region containing regulatory sequences, may lead to a reduction of translation efficacy and stability among schizophrenia patients, and consequently, increased translation of DCC mRNA (Grant et al., 2012).

The above finding was bolstered by a more recent study of 454 schizophrenia patients and 486 healthy controls that associated another *DCC* SNP (rs2229080) with schizophrenia (Yan et al., 2016). The authors found evidence that rs2229080 may induce a protein structural change and alter splicing regulation, and postulated that this might change the mesocorticolimbic dopamine circuitry and ultimately lead to schizophrenia (Yan et al., 2016).

1.6.3 Depression

There is increasing evidence that alterations in genetic variants and expression of *DCC* affect susceptibility to mood dysregulation and suicide. Two studies have shown that depressed suicide completers exhibit elevated *DCC* mRNA expression in the prefrontal cortex (Manitt et

al., 2013; Torres-Berrío et al., 2017). Furthermore, a SNP (rs4542757) in an intron of *DCC* has been associated with depressive symptoms in a genome wide association study (GWAS) which comprised 3,138 Hispanic/Latina women (Dunn et al., 2016). Although this effect did not achieve genome-wide significance and was not identified in a replication sample, the GWAS study was likely underpowered (Dunn et al., 2016). Consistent with this assertion, a larger GWAS study (n = 161,460) identified an association between depressive symptoms and a SNP (rs62100776) in *DCC* (Okbay et al., 2016). Moreover, two independent GWAS samples (n= 6455, n= 18,759) identified associations between major depressive disorder and the Netrin-1 signaling pathway, comprising SNPs from multiple genes involved in Netrin-1 signaling, including *DCC* (Zeng et al., 2017). Furthermore, a genome-wide investigation of differential gene expression identified 165 differentially expressed genes in major depressive disorder, including overexpression of *DCC* (Leday et al., 2018). Most recently, a GWAS meta-analysis of 135,458 individuals with major depression and 344,901 controls identified 44 genomic loci significantly associated with depression, including *DCC* (rs11663393) (Wray et al., 2018).

The above associations might reflect an effect on mood instability, a clinical feature common to numerous psychiatric disorders (Broome et al., 2015). In a GWAS study of 60,443 controls and 53,525 mood instability cases, genome-wide significance was detected for four independent genetic loci, including *DCC* (rs8084280) (Ward et al., 2017). Moreover, genetic correlations, which assess the degree of shared heritability between phenotypes, were identified between mood instability and three psychiatric conditions: major depressive disorder, schizophrenia, and anxiety disorder (Ward et al., 2017).

1.7 Objectives and hypotheses

As discussed here in chapter 1, the identification of the four generational Quebec family (n= 36), 20 of whom have a *DCC* mutation, has permitted investigation of the effects of DCC mutations on both the motor system and the mesocorticolimbic system, in living human brain. This presented an exceedingly rare opportunity to expand our knowledge of an axon guidance cue considered critical to the formation of commissural, corticospinal, and mesocorticolimbic pathways. These studies were also expected to help illuminate mechanisms mediating the lateralization of neural pathways. Finally, by investigating potential alterations in mesocorticolimbic pathway connectivity, structure, function, and associated behaviors, this work might also have implications for our understanding of a wide range of neuropsychiatric disorders.

Chapter 2 constitutes the first manuscript of the dissertation, and it presents multimodal neuroimaging and genetic investigations of the motor systems of *DCC* mutation carriers with and without mirror movements. A first objective was to determine, for the first time, the movement-induced activations, resting state functional connectivity, and interhemispheric inhibition of the motor system in *DCC* mutation carriers. Moreover, we aimed to identify neurobiological factors that might account for the partial penetrance of mirror movements in *DCC* mutation carriers. Finally, we sought to characterize the neurophysiology of the motor system in *DCC* mutation carriers without mirror movements. Overall, it was hypothesized that *DCC* mutation carriers with mirror movements would exhibit greater "mirroring" motor representations, reduced interhemispheric inhibition, altered motor system functional connectivity, alterations in callosal fiber integrity, and reduced *DCC* mRNA expression. *DCC* mutation carriers without mirror movements might exhibit only some of these effects.

Chapter three, the second manuscript of the dissertation, presents investigations of the mesocorticolimbic system in *DCC* mutation carriers. The following objectives and hypotheses were based on predictions from the anatomical, functional, and behavioral phenotypes of adult *Dcc* haploinsufficient mice (Flores, 2011; Hoops and Flores, 2017). For the first time, we sought to measure anatomical and functional connectivity in mesocorticolimbic circuitry in human *DCC* mutation carriers. It was predicted that *DCC* mutation carriers would exhibit alterations in mesocorticolimbic connectivity. It was hypothesized that *DCC* haploinsufficient humans would exhibit behavioral and personality traits consistent with diminished striatal dopamine transmission, including reductions in psychoactive substance use. Additionally, using automated volumetric MRI analyses, we tested whether there are striatal or cortical morphometric differences in *DCC* haploinsufficient humans and mice, allowing assessment of the translatability of these effects. Finally, we tested mice during adolescence and adulthood, allowing us to ask whether hypothesized volumetric effects precede or parallel the previously reported modifications observed in the mesocorticolimbic pathways of adult, but not adolescent, *Dcc* haploinsufficient mice.

Neural Function in *DCC* Mutation Carriers with and without Mirror Movements

Running head: *DCC* Mutation Carriers and Mirror Movements

*Daniel E. Vosberg PhD[1,2], *Vincent Beaulé PhD[5], Angélica Torres-Berrío PhD[2,4,8], Danielle Cooke BSc[6], Amanda Chalupa MSc[1], Natalia Jaworska PhD[1,7], Sylvia ML Cox PhD[1], Kevin Larcher MEng[3], Yu Zhang PhD[3], Dominique Allard BScN[1], France Durand MSc[1], Alain Dagher MD[2,3], Chawki Benkelfat MD CSPQ DERBH[1,2,3], Myriam Srour MD PhD[3], Donatella Tampieri MD[3], Roberta La Piana MD[3], Ridha Joober MD PhD[1,2,4], Franco Lepore PhD[5], Guy Rouleau MD PhD[3], Alvaro Pascual-Leone MD PhD[6], Michael Fox MD PhD[6], Cecilia Flores PhD[1,2,4], Marco Leyton PhD[1,2,3†], Hugo Théoret PhD[5†]

*shared first co-authorship.

Affiliations:
[1]Department of Psychiatry, McGill University, Montreal, QC, Canada. [2]Integrated Program in Neuroscience (IPN), McGill University, Montreal, QC, Canada. [3]Neurology and Neurosurgery, McGill University, Montreal, QC, Canada. [4]Douglas Mental Health University Institute, Montreal, QC, Canada. [5]Psychology, Université de Montréal, Montreal, QC, Canada, [6]Beth Israel Deaconess Medical Center, Harvard Medical School, Massachusetts, USA, [7]Institute of Mental Health Research, affiliated with the University of Ottawa, Ontario, Canada, [8]ATB current affiliation: Fishberg Department of Neuroscience and Friedman Brain Institute (EJN), Icahn School of Medicine at Mount Sinai, New York, NY, USA.

†Corresponding authors:

Marco Leyton, PhD
McGill University
Irving Ludmer Building
Montreal, QC, Canada, H3A 1A1
marco.leyton@mcgill.ca

Hugo Théoret, PhD
Université de Montréal
Pavillon Marie-Victorin
Montreal, QC, Canada, H2V 2S9
hugo.theoret@umontreal.ca

Word counts:	Character counts:	Figure/table counts:
Abstract: 219	Title: 74	Figures: 6
Introduction: 332	Running head: 42	Tables: 2
Discussion: 573		
Manuscript main text: **4186**		

ABSTRACT

Objective: Recently identified mutations of the axon guidance molecule receptor gene, *DCC,* present an opportunity to investigate, in living human brain, mechanisms affecting neural connectivity and the basis of mirror movements, involuntary contralateral responses that mirror voluntary unilateral actions. We hypothesized that haploinsufficient $DCC^{+/-}$ mutation carriers with mirror movements would exhibit decreased *DCC* mRNA expression, a functional ipsilateral corticospinal tract, greater "mirroring" motor representations, and reduced interhemispheric inhibition. $DCC^{+/-}$ mutation carriers without mirror movements might exhibit some of these features.

Methods: The participants (n=52) included 13 $DCC^{+/-}$ mutation carriers with mirror movements, 7 $DCC^{+/-}$ mutation carriers without mirror movements, 13 relatives without the mutation or mirror movements, and 19 unrelated healthy volunteers. The multimodal approach comprised quantitative real time polymerase chain reaction, transcranial magnetic stimulation (TMS), functional magnetic resonance imaging (fMRI) under resting and task conditions, and measures of white matter integrity.

Results: Mirror movements were associated with reduced *DCC* mRNA expression, increased ipsilateral TMS-induced motor evoked potentials, increased fMRI responses in the "mirroring" M1 and cerebellum, and markedly reduced interhemispheric inhibition. The $DCC^{+/-}$ mutation, irrespective of mirror movements, was associated with reduced functional connectivity and white matter integrity.

Interpretation: Diverse connectivity abnormalities were identified in mutation carriers with and without mirror movements, but corticospinal effects and decreased peripheral *DCC* mRNA

appeared driven by the mirror movement phenotype.

INTRODUCTION

The axon guidance molecule receptor, DCC (deleted in colorectal cancer), plays a critical role in directing normal decussation of corticospinal tract (CST) and commissural pathways. In homozygous *DCC* mutant mice, the ensuing failure of axonal interhemispheric crossing is associated with a lack of asymmetric movements[1]. Similar to the murine motor phenotype, humans with *DCC* mutations exhibit mirror movements (MM); that is, voluntary actions on one side of the body elicit simultaneous involuntary movements on the contralateral side[2].

The human *DCC* mutation related MM are substantially more pronounced than the smaller mirror movements that are commonly exhibited by young children and then, at around age 10, disappear following maturation of the corpus callosum and the development of normal interhemispheric inhibition[3]. Also unlike healthy children, adults with severe congenital MM exhibit evidence of a pronounced ipsilateral CST[4-8], and, among the recently identified *DCC* mutation carriers, some have agenesis of the corpus callosum, MM, both phenotypes, or neither phenotype[8-10].

A number of important features in *DCC* mutation carriers remain unknown. It is unknown whether they exhibit abnormal motor cortex activations, motor system connectivity, or interhemispheric function. The neurophysiological phenotype of *DCC* mutation carriers without MM is unknown. There is currently no explanation to account for the partial penetrance of MM among mutation carriers.

To map in detail the neurocircuitry of *DCC* mutation related MM, we have completed multimodal neuroimaging in 33 members of a large, four-generational Quebec family with a *DCC* frameshift mutation (NM_005215.3, c.1140+1G>A). This mutation results from abnormal skipping of exon 6, leading to a premature stop codon that encodes a truncated DCC protein that

fails to bind to its ligand, netrin[2]. Our *a priori* predictions were that, relative to controls, *DCC* mutation carriers with MM would exhibit an increased functional ipsilateral CST, increased "mirroring" motor representations, reduced interhemispheric inhibition, alterations in motor and interhemispheric anatomical and functional connectivity, and decreased *DCC* mRNA expression. Finally, we sought to determine the effects of the *DCC* mutation, potentially distinct from the effects of MMs.

METHODS

Participants. Fifty-two volunteers participated in the study (Table 1; Figure 1). This included 13 *DCC* haploinsufficient individuals with MM ($DCC^{+/-}$/MM+), 7 *DCC* haploinsufficient individuals without MM ($DCC^{+/-}$/MM-), and 13 relatives with neither the mutation nor MM ($DCC^{+/+}$/MM-); 19 unrelated healthy volunteers (UHV) were tested to control for *DCC* familial features unrelated to the mutation. Participant safety screening procedures were completed prior to magnetic resonance imaging (MRI) and transcranial magnetic stimulation (TMS). All participants gave written informed consent, and the protocol was carried out in accordance with the Declaration of Helsinki and approved by the relevant research ethics committees.

Genetics. Participants who had not been genotyped previously[2] were characterized for *DCC* variants. Genotyping was unavailable for one UHV, who only completed the MRI, and excluding this individual did not alter the findings. Coding exons and the exon-intron boundaries of *DCC* were screened for mutations based on sequence (NM_005215) (UCSC March 2006 Assembly HG 18). Primers were the same as used previously[2]. PCR products were sequenced on the ABI 3700 sequencer at the Genome Quebec Centre for Innovation according to the manufacturer's recommended protocol (Applied Biosystems). Sequences were aligned and analyzed using SeqMan 4.03 (DNAStar, WI, USA) and Mutation Surveyor v.3.1 (SoftGenetics, PA, USA).

Mirror movements (MM). Prior to testing, two self-adhesive electrodes were placed on the first dorsal interosseous (FDI) muscle bilaterally and a ground electrode was positioned on the right wrist. The electromyographic (EMG) signal was amplified using a Powerlab 4/30 system (ADInstruments, Colorado Springs, Colorado, USA), filtered with a band pass of 20-1000Hz and digitized at a sampling rate of 4KHz. First, seated participants were asked to relax their arms with their palms facing upward, supported by their legs. They were instructed to respond to an

auditory signal by pressing, then releasing, a small stress ball three times with one hand while the other hand was at rest. This protocol was performed for both hands and repeated five times. To assess more subtle MM, a protocol known to generate physiological mirror movements (pMM) in healthy participants was performed[3]. Participants were instructed to maintain a tonic contraction with one hand (using the minimal strength needed to hold a pencil without dropping it). Meanwhile, participants were required to respond to an auditory signal with their other hand by performing a voluntary phasic pinch contraction. This was performed 20 times for both hands. Physiological MM were defined as a significant increase in the background EMG activity of the hand maintaining the tonic contraction, starting at the moment of the phasic contraction and lasting 100ms, compared to 1000ms of background activity prior to the phasic contraction. Data were expressed as the ratio of EMG activity in the tonically contracting hand during phasic contraction of the contralateral hand over background activity preceding phasic contraction. The data from both hemispheres were averaged.

Single-pulse TMS. TMS was delivered through an 8-cm figure-of-eight coil connected to a Magstim 200 stimulator (Magstim, Whitland, UK) with a monophasic current waveform in a posterior-anterior orientation. The coil was positioned flat on the scalp at an angle of 45 degree from the midline. Single pulse stimulation was performed over the hand area of M1 at the optimal position (hot spot) eliciting MEPs of maximal amplitude in the contralateral FDI muscle. The hot spot was marked on the scalp with a pen to ensure stable coil positioning throughout the experiment. Stimulation intensity was adjusted to elicit contralateral MEPs of 1mV amplitude. MEPs were recorded using Scope v4.0 software (ADInstruments). The EMG signal was filtered with a bandwidth of 20–1000 Hz and digitized at a sampling rate of 4 kHz. Single pulse stimulation was performed over the hand area of M1 while participants were at rest with eyes

open, ten times for each hemisphere and MEPs were recorded bilaterally in the FDI muscle to confirm the presence or absence of mirror MEPs in all participants. Peak-to-peak amplitudes of contralateral and ipsilateral MEP were measured and averaged off-line. Relative amplitudes of ipsilateral and contralateral MEPs were expressed as an ipsilateral coefficient (ipsilateral MEP amplitude/contralateral MEP amplitude). MEP traces were monitored online to ensure that no muscle activity in the 100 ms window prior to TMS was present. Trials with pre-stimulus activity were discarded and repeated, and were less than 1% of all trials. The data from both hemispheres were averaged. Contralateral and ipsilateral TMS-induced MEP latencies were also measured, from TMS pulse to MEP onset.

Double-coil TMS. Interhemispheric inhibition (IHI) was measured using a protocol described by Ferbert and collaborators (1992) using two 50 mm custom-made coils connected to two Magstim 200 stimulators (Magstim, Whitland, UK)[11]. Each coil was placed over their respective M1 hot spot over the right and left hemispheres. The intensity of each TMS pulse was adjusted to elicit MEPs of approximately 1 mV contralaterally. A test stimulus was preceded by a conditioning stimulus applied 40ms earlier. IHI was measured for left-to-right and right-to-left directions of inhibition. IHI was expressed as the ratio of double stimulation MEPs over single-pulse MEPs. The data for both directions were averaged.

MRI parameters. Participants underwent an anatomical, diffusion weighted, resting-state functional, and two identical task functional MRI acquisitions in a scanning session using a 3T Siemens (Erlangen, Germany) Magnetom Trio MRI scanner (32 channel head coil). The high-resolution, T1-weighted anatomical acquisition parameters were as follows: TI/TR/TE=900/2300/2.98 msec; flip angle=9 degrees; slice thickness=1.0 mm (1 mm isotropic voxel size), with a field of view (FOV) of 256 × 256 mm^2, and duration of 9 min, 50 sec.

Participants underwent diffusion tensor imaging (DTI) using a single-shot spin-echo echo-planar pulse sequence with multi-directional diffusion weighting (MDDW; TR/TE = 12000/89 ms; 90 contiguous axial slices with an isotropic 2-mm resolution, FOV=256 × 256 mm^2, matrix size=128 × 128 with partial Fourier reconstructed to 6/8). Diffusion weighting was distributed evenly on the unit hemisphere using 64 non-collinear gradients and a b-value of 1000. One additional volume with no diffusion weighting (i.e. b-value=0) was acquired in the beginning of the acquisition. The task fMRI acquisition parameters were as follows: TR/TE=1500/30 msec; flip angle=90 degrees; slice thickness=4.0 mm (4 mm isotropic voxel size), slices=28, FOV=256 × 256 mm^2 and duration of 6 minutes, 08 sec. The resting state fMRI acquisition parameters were as follows: TR/TE=2000/30 msec; flip angle=90 degrees; slice thickness=4.0 mm (4 mm isotropic voxel size), slices=38, FOV=256 × 256 mm^2, and duration of 6 minutes, 08 sec.

Resting state functional connectivity MRI (rs-fcMRI). Rs-fcMRI data were processed as described previously[12, 13] including slice-acquisition-dependent time shifts, head motion correction, atlas registration, spatial smoothing (6 mm FWHM), low-pass temporal filtering (f < 0.08 Hz), and removal of confounding variables by linear regression including head-motion, the whole-brain (global) signal, and signals from the ventricles and white matter. A metric of overall movement was also computed for use as a covariate by computing the root mean square of the rotation, translation, and displacement of the brain relative to the time point before it, then averaging across all time points[14]. *A priori* ROIs (6 mm radius spheres) were generated in the left and right primary motor cortex (M1, MNI coordinates: -41, -20, 62 and 41, -20, 62) based on a prior fMRI study of hand movements[15]. *A priori* ROIs were also generated in the left and right cerebellum (MNI coordinates: -20, -52, -24 and 17, -52, -24), based on prior functional connectivity with left and right M1[15]. Rs-fcMRI between motor ROIs (one comparison), between

motor and cerebellar ROIs (4 comparisons), and between motor ROIs and all other brain voxels were computed[12]. For statistical comparisons, correlation coefficients (r values) from each subject were converted to a normal distribution using Fisher's r to z transform. For the fMRI 2nd level analyses, a full factorial using the same design described below in the *Statistics* section with the addition of total movement during the MRI as a covariate was run in SPM12. Since generalized estimating equations is not possible with SPM, family was instead entered as a fixed factor.

Task fMRI. fMRI analyses were conducted using Statistical Parametric Mapping (SPM) 12 software (Wellcome Department London). fMRI images were slice-time corrected, realigned, co-registered to the T1 image, segmented, normalized to standardized MNI space, and spatially smoothed with an 8 mm FWHM Gaussian kernel. For each participant, a general linear model (GLM) was generated in SPM per task, consisting of the following conditions: a) motor activity and rest; b) somatosensory stimulation and rest, which were convolved with the hemodynamic response function. For group analyses, single-subject contrast images were entered into a random effect model. Block design motor and somatosensory fMRI tasks comprised 18 sec of activity (motor: opening and closing right index finger and thumb; somatosensory: tactile stimulation on distal phalanx of right index finger) followed by 18 sec of rest, for a total of 10 blocks per condition. The somatosensory stimulation was conducted using circular domes (25 mm diameter), fabricated from solid plastic with deep rectangular grooves cut into the surface (3 mm equidistant grooves and bars; JVP Domes, Stoelting Co.). The left arm, hand, and fingers were restrained throughout. For the motor task, as with the rs-fMRI analysis, *a priori* ROIs (6 mm radius spheres) were generated in the left and right M1 (MNI coordinates: -41, -20, 62 and 41, -20, 62), as well as the left and right cerebellum (MNI coordinates: -20, -52, -24 and 17, -52, -24).

For the somatosensory task, *a priori* ROIs (6 mm radius spheres) were generated in the left and right somatosensory cortex (MNI coordinates: -42, -35, 65 and 42, -35, 65). Additionally, a single-blind investigator manually segmented the hand knob region of M1 using the McConnell Brain Imaging Centre (BIC) MINC tool, Display[16]. Following quality control, verifying the co-registration of each participant's T1 image, "default" left hand knob ROI, and right hand-induced motor task functional activation, two participants were excluded. Finally, mean beta-weights were extracted from ROIs using MarsBar 0.44. As for the rs-fcMRI data, a full factorial using the same design described below in the *Statistics* section was run in SPM12 for the fMRI 2nd level analyses, and family was entered as a fixed factor since generalized estimating equations is not possible with SPM.

Diffusion weighted imaging (DWI) of corpus callosum (CC). Images were denoised using NLMEANS denoising[17] as implemented in Dipy[18]. Magnetic field inhomogeneities were corrected using the N4 correction from Ants[19]. A brain mask was extracted using BET from the FSL toolkit[20, 21], which was used in conjunction with the FSL Eddy tool to correct for motion, eddy currents, and susceptibility artefacts[20, 22]. The T1 images were also denoised using NLMEANS, field inhomogeneities were corrected (N4 correction), and a brain mask was extracted (BET). The DWI datasets were then upsampled to 1×1×1 resolution, and tensor based diffusion metrics were computed using Dipy. Fiber orientation distribution functions (ODFs) were estimated using a fixed response function, set to correspond to a pure myelinated axon response (15, 4, 4 × 10^{-4} mm^2/second). The T1 image was registered to the upsampled DWI using ANTS. A white matter mask was segmented from the registered T1 using ANTS and was used for deterministic and probabilistic local tracking (as defined by [23]), which was run using 5 seeds per voxel of the WM mask, only keeping streamlines reaching the gray matter. Step size

was 0.5mm. Following generation of the whole brain tractogram, bundles composing the CC were automatically extracted using a modified version of the RecoBundles algorithm. In this algorithm, the whole brain tractogram was first registered to the atlas[25], and bundles were individually extracted based on centroids and distances to the atlas[26]. The atlas comprises 20 major WM bundles, presegmented on 4 different healthy subjects from the HCP dataset. Those segmentations were validated by 2 neuroanatomists for consistency to generally accepted anatomical definitions, and were used as references for the segmentation process. Subparts of the CC were segmented from the reference subject into 7 subparts as previously defined[27]. Fractional anisotropy (FA), mean diffusivity (MD), radial diffusivity (RD) and axial diffusivity (AD) values were extracted for each CC segment.

Lymphoblastoid cell line (LCL) growth, RNA extraction, and quantitative real time PCR (qRT-PCR). *DCC* mRNA expression was measured by performing RNA extraction followed by qRT-PCR, as previously described[28], using LCLs extracted from blood collected from the participants. LCLs established by transformation with Epstein-Barr virus were grown using standard protocols[29]. Total RNA was isolated from the lymphoblastoid cell lines with the miRNeasy Micro Kit protocol (Qiagen, Toronto, ON, Canada). All RNA samples were determined to have 260/280 and 260/230 values ≥1.8, using the Nanodrop 1000 system (Thermo Scientific, Toronto, ON, Canada). Reverse transcription for DCC mRNA (2mg) was performed using the High-Capacity cDNA Reverse Transcription Kit (Applied Biosystems, ON, Canada). Real time PCR using TaqMan probes (Thermo Fisher, ON, Canada) was carried out with an Applied Biosystems QuantStudio™ 6-Flex Real Time PCR system. Data for *DCC* mRNA expression were analyzed by using the Absolute Quantitation (AQ) standard curve method. Real time PCR was run in technical triplicates. The LCL sample (n=37) included 10 $DCC^{+/-}$/MM+, 6

DCC$^{+/-}$/MM-, 11 *DCC*$^{+/+}$/MM-, and 10 UHV. This included 4 previously-genotyped individuals (2 *DCC*$^{+/-}$/MM- and 2 *DCC*$^{+/+}$/MM-) who did not participate in the present neuroimaging study. Four outliers were removed, as identified by GraphPad Prism 7's ROUT test for definitive outliers (Q=0.1%).

Statistical analyses

Using SPSS20, ipsilateral EMG data, physiological MMs, ipsilateral/contralateral MEP coefficients, IHI, fiber integrity of the corpus callosum, fMRI motor responses, and *DCC* mRNA expression were each analyzed using generalized estimating equations (GEE), with an exchangeable working correlation matrix. These analyses coded for the two fixed factors of 1) the presence of MM and 2) the presence of the *DCC* mutation. In order to control for the correlations among family members, driven by shared genetics and environments, we defined clusters by the branches within the Quebec family, descending from the earliest generation. Moreover, each unrelated healthy volunteer comprised their own cluster. Additionally, age was used as a covariate due to previously-reported age-related effects of DCC[30-32] and of the motor system, as assessed with MRI and TMS[33-35]. For the EMG, ipsilateral/contralateral MEP coefficients, and physiological MM analyses, the data did not satisfy assumptions of normality and consequently, were log-transformed. Log transformations were not appropriate for the task fMRI or *DCC* mRNA data, due to negative values and the transformations rendering the data less Gaussian. However, sensitivity analyses and inspection of the residuals revealed that these data were approximately normal. The MD, RD, and AD of the corpus callosum values were highly non-normal, as indicated by normality tests and plots, and were unimproved by log transformations. Therefore, these data were not appropriate for GEE analyses and no significant

effects were detected following sensitivity analyses, comprising the removal of the most extreme outliers, identified using GraphPad Prism 7's ROUT test for definitive outliers (Q=0.1%).

RESULTS

TMS and Electromyography

GEE analyses revealed that increased EMG activity in the "mirroring" hand during voluntary unilateral contractions was associated with the presence of MM (β = 0.829, 95% CI [0.457, 1.201], p = 0.000013) but not with the *DCC* mutation (β = 0.156, 95% CI [-0.134, 0.446], p = 0.293). Similarly, increases in the ratio of ipsilateral/contralateral motor evoked potentials (MEPs) induced by unilateral single-pulse TMS of the primary motor cortex (M1) hand area were associated with MM (β = 1.666, 95% CI [1.498, 1.833], p < 0.00001) but, again, not the *DCC* mutation (β = -0.024, 95% CI [-0.290, 0.243], p = 0.862).

The ipsilateral MEPs detected among the $DCC^{+/-}$/MM+ participants occurred in 100% of trials. There was no effect of MM on the size of contralateral MEPs ($F_{(1,40)}$=0.0001; p=0.99). Among the $DCC^{+/-}$/MM+ participants, the amplitudes of ipsilateral MEPs, relative to contralateral MEPs, were smaller in 7 participants and larger in 5. Three participants presented ipsilateral MEPs that were more than 5 times larger than their contralateral counterpart. Ipsilateral (M=23.80, SD=3.05) and contralateral (M=23.50, SD=2.79) MEP latencies were nearly identical in the $DCC^{+/-}$/MM+ group and not significantly different ($F_{(1,11)}$=2.2; p=0.16), suggesting that the ipsilateral MEPs resulted from fast-conducting, ipsilateral CST projections (Figure 2).

Increased pMM were associated with MM (β = 0.437, 95% CI [0.402, 0.472], p < 0.00001). Again, these effects were uniquely associated with MM, as there were no significant effects of the *DCC* mutation on pMM (β = -0.007, 95% CI [-0.044, 0.031], p = 0.735). Finally, reductions in interhemispheric inhibition, indicated by increased responses following double-coil

TMS, were associated with MM (β = 0.531, 95% CI [0.337, 0.724], p < 0.00001). There were no significant effects of the *DCC* mutation on IHI (β = -0.028, 95% CI [-0.291, 0.235], p = 0.833).

Resting State and Task fMRI

Functional connectivity was evaluated between our *a priori* ROIs (Figure 3). Between the right M1 and left M1, reduced functional connectivity was associated with the *DCC* mutation (β = -0.259, 95% CI [-0.517, 0.000], p = 0.0497). Moreover, between the right M1 and left cerebellum, decreased connectivity was associated with the *DCC* mutation (β = -0.245, 95% CI [-0.436, -0.054], p = 0.012) and increased connectivity was associated with MM (β = 0.245, 95% CI [0.062, 0.428], p = 0.009). See Table 2 for all pairwise connectivity values. A whole-brain voxelwise search found no significant abnormalities (after FWE correction) in right M1 or left M1 connectivity.

Consistent with the reduction in interhemispheric inhibition, increases in "mirroring" fMRI motor responses were associated with the presence of MM. Right-hand induced, right sphere-based M1 activations were associated with MM (β = 0.498, 95% CI [0.073, 0.922], p = 0.0215) and not the *DCC* mutation (β = -0.174, 95% CI [-0.446, 0.099], p = 0.211) (Figure 4A). Similarly, in the right manually segmented hand area, increased right-hand induced activations were associated with MM (β = 0.462, 95% CI [0.101, 0.822], p = 0.012), and not with the *DCC* mutation (β = -0.138, 95% CI [-0.356, 0.079], p = 0.212) (Figure 4B). Moreover, in the left cerebellum, increased right-hand induced activations were associated with MM (β = 0.398, 95% CI [0.107, 0.689], p = 0.007), while decreased activations were associated with the *DCC* mutation (β = -0.185, 95% CI [-0.366, -0.004], p = 0.045) (Figure 4C). Small-volume corrected voxelwise analysis revealed a similar pattern of effects, whereby increased activation was associated with the presence of MM in the right M1 (t= 3.36, p_{FWE}=0.009) and left cerebellum

(t=3.62, p_{FWE}=0.005). Although these findings did not survive a whole-brain correction, the peak activation sites and largest clusters across the whole brain (p<0.001) were in the right motor cortex (t=4.21, MNI coordinates: 38, -16, 40) and left cerebellum (t=4.07, MNI coordinates: -26, -52, -16) (Figure 4D). As exploratory analyses, there were no significant effects identified in the analyses of the "default" left M1, left hand area, or right cerebellum (all p≥0.20) or for the somatosensory task (all p≥0.07).

DTI and Corpus Callosum

Subtle reductions in FA were associated with the *DCC* mutation in the anterior midbody (β = -0.023, 95% CI [-0.042, -0.003], p = 0.022), posterior midbody (β = -0.021, 95% CI [-0.036, -0.005], p = 0.0078), isthmus (β = -0.017, 95% CI [-0.033, 0.000], p = 0.048), and splenium (β = -0.016, 95% CI [-0.029, -0.002], p = 0.021). Following sensitivity analyses of non-normally distributed AD, MD, and RD data, no significant effects were identified in these measures. Partial agenesis of the corpus callosum with an absent rostrum was observed in one female $DCC^{+/-}$/MM- participant, as evaluated by a board-certified neuroradiologist (Figure 5).

DCC mRNA Expression

Quantitative real time PCR using RNA extracted from LCLs identified a significant reduction in *DCC* mRNA expression associated with the presence of MM (β = -1.056, 95% CI [-1.660, -0.451], p = 0.00062). There was no significant effect of the *DCC* mutation alone (β = 0.265, 95% CI [-0.164, 0.694], p = 0.226) (Figure 6).

DISCUSSION

The present study demonstrates that *DCC*$^{+/-}$/MM+ participants exhibit diverse functional and anatomical connectivity alterations, including increased "mirroring" activations in motor regions and reduced interhemispheric inhibition. Ipsilateral CSTs among the *DCC*$^{+/-}$/MM+ individuals are strongly suggested by the similar latencies between TMS-induced ipsilateral and contralateral MEPs. Strikingly, for the first time, we show distinct alterations of the motor system among *DCC*$^{+/-}$ mutation carriers, independently of MM. We also provide a possible mechanism underlying the partial penetrance of MM, as a reduction in peripheral *DCC* mRNA expression was only associated with the presence of MM and not the *DCC* mutation.

Contrary to what has been observed in *RAD51*$^{+/-}$/MM+ individuals[7], where mirror MEPs were elicited in no more than one third of TMS trials using 1.2 RMT intensity, mirror MEPs were induced in 100% of trials among *DCC*$^{+/-}$/MM+ participants using a similar stimulation intensity at rest (1mV MEP)[36], consistent with recent reports[10]. Therefore, it appears that downregulating DCC, compared to RAD51, has a larger impact on the development and excitability of the ipsilateral CST. While DCC's role in guiding commissural and corticospinal axons has been characterized *in vitro* and *in vivo*[1, 10, 37, 38], RAD51 is less well understood but is expressed at the pyramidal decussation[39]. Further elucidation of the molecular mechanisms is needed to explain phenotypic differences in CST between *DCC* and *RAD51* mutation carriers.

Previous studies have indicated greater "mirroring" motor representations among individuals with MM[6, 7, 40], but our study restrained the mirroring arm, hand, and fingers, minimizing the possibility that the motor activation is simply an artifact of the movement in the mirroring hand. Instead, it appears that the reduced interhemispheric inhibition results in increased "mirroring" motor representations. Our findings strongly suggest that unilateral motor

control of the hand relies on selective corticospinal wiring between the motor cortex and contralateral hand, as well as on normal interhemispheric communication.

A previous report indicated that some *DCC* and *RAD51* mutation carriers without visually-apparent MM nonetheless exhibited subtle MM[41]. In comparison, we did not detect any evidence of increased pMM in $DCC^{+/-}$/MM- individuals. However, we did identify evidence of reduced functional connectivity and white matter integrity associated with the $DCC^{+/-}$ mutation (independent of mirror movements), suggesting a neurophysiologically altered motor system in individuals with an abnormal *DCC* gene.

Although only some $DCC^{+/-}$ carriers exhibit MM, both MM+ and MM- $DCC^{+/-}$ groups exhibit alterations in corpus callosum tract architectures, including one $DCC^{+/-}$/MM- individual with partial agenesis of the corpus callosum. Thus, whereas decreased lateralization of the CST and movement-induced motor representations depend upon the presence of MM, callosal abnormalities depend upon the presence of the $DCC^{+/-}$ mutation. Similarly, Marsh et al. (2017)[8] observed independent expression of MM and callosal agenesis among $DCC^{+/-}$ individuals. These differential effects of the *DCC* mutation might reflect individual differences in the regionally specific expression of DCC; for example, suppression of DCC within CST neurons is not sufficient to disrupt CST crossing but selective inhibition of DCC within commissural neurons is sufficient to disrupt callosal decussation[10]. More generally, phenotypic differences between the two $DCC^{+/-}$ groups may be explained by more extensive and pervasive brain regional decreases in *DCC* expression, as suggested by the observation here that *DCC* mRNA reduction was associated with MM but not the $DCC^{+/-}$ mutation. Together, by identifying distinct phenotypes among *DCC* mutation carriers with and without MM, these findings affirm the critical role that DCC plays in the organization and function of commissural and CST fibers in humans.

Acknowledgments

This work was supported by funding from the Canadian Institutes for Health Research (CIHR, MOP-258547) and the National Institute on Drug Abuse (NIDA, R01DA037911).

We would like to acknowledge Dr. Jose Correa, director of the McGill University Statistical Counselling Service, and Irina Pokhvisneva, for their guidance on the statistical analyses. We are also grateful to Dr. Patricia Pelufo Silveira for her feedback on the statistical design. Finally, we would like to thank Dr. Jurgen Germann and Dr. Jorge Armony for providing advice and instructions on the fMRI analyses.

Author contributions

1) Conception and design of the study: AD, CB, MS, RJ, FL, GR, AP-L, MF, CF, ML, HT
2) Acquisition and analysis of data: DEV, VB, AT-B, DC, AC, NJ, SC, KL, DA, FD, YZ, DT, RL-P
3) Drafting a significant portion of the manuscript or figures: DEV, VB, AT-B, CF, ML, HT

Potential conflicts of interest

We have no conflicts of interest to declare.

REFERENCES

1. Finger JH, Bronson RT, Harris B, Johnson K, Przyborski SA, Ackerman SL. The netrin 1 receptors Unc5h3 and Dcc are necessary at multiple choice points for the guidance of corticospinal tract axons. The Journal of neuroscience. 2002;22(23):10346-56.
2. Srour M, Rivière J-B, Pham JM, et al. Mutations in DCC cause congenital mirror movements. Science. 2010;328(5978):592-.
3. Mayston MJ, Harrison LM, Stephens JA. A neurophysiological study of mirror movements in adults and children. Annals of neurology. 1999;45(5):583-94.
4. Capaday C, Forget R, Fraser R, Lamarre Y. Evidence for a contribution of the motor cortex to the long-latency stretch reflex of the human thumb. The Journal of physiology. 1991;440(1):243-55.
5. Cincotta M, Borgheresi A, Boffi P, et al. Bilateral motor cortex output with intended unimanual contraction in congenital mirror movements. Neurology. 2002;58(8):1290-3.
6. Cohen L, Meer J, Tarkka I, et al. Congenital mirror movements: abnormal organization of motor pathways in two patients. Brain. 1991 1991-02-01 00:00:00;114(1):381-403.
7. Gallea C, Popa T, Hubsch C, et al. RAD51 deficiency disrupts the corticospinal lateralization of motor control. Brain. 2013;136(11):3333-46.
8. Marsh AP, Heron D, Edwards TJ, et al. Mutations in DCC cause isolated agenesis of the corpus callosum with incomplete penetrance. Nature Genetics. 2017;49(4):511-4.
9. Jamuar SS, Schmitz-Abe K, D'Gama AM, et al. Biallelic mutations in human DCC cause developmental split-brain syndrome. Nature Genetics. 2017;49(4):606-12.
10. Welniarz Q, Morel M-P, Pourchet O, et al. Non cell-autonomous role of DCC in the guidance of the corticospinal tract at the midline. Scientific Reports. 2017;7(1):410.
11. Ferbert A, Priori A, Rothwell J, Day B, Colebatch J, Marsden C. Interhemispheric inhibition of the human motor cortex. The Journal of physiology. 1992;453(1):525-46.
12. Fox MD, Snyder AZ, Vincent JL, Corbetta M, Van Essen DC, Raichle ME. The human brain is intrinsically organized into dynamic, anticorrelated functional networks. Proceedings of the National Academy of Sciences of the United States of America. 2005;102(27):9673-8.
13. Van Dijk KR, Hedden T, Venkataraman A, Evans KC, Lazar SW, Buckner RL. Intrinsic functional connectivity as a tool for human connectomics: theory, properties, and optimization. Journal of neurophysiology. 2010;103(1):297-321.
14. Fox MD, Greicius M. Clinical applications of resting state functional connectivity. Frontiers in systems neuroscience. 2010;4.
15. Buckner RL, Krienen FM, Castellanos A, Diaz JC, Yeo BTT. The organization of the human cerebellum estimated by intrinsic functional connectivity. Journal of Neurophysiology. 2011;106(5):2322-45.
16. Yousry T, Schmid U, Alkadhi H, et al. Localization of the motor hand area to a knob on the precentral gyrus. Brain. 1997;120(Pt 1):141-57.
17. Coupé P, Yger P, Prima S, Hellier P, Kervrann C, Barillot C. An optimized blockwise nonlocal means denoising filter for 3-D magnetic resonance images. IEEE transactions on medical imaging. 2008;27(4):425-41.
18. Garyfallidis E, Brett M, Amirbekian B, et al. Dipy, a library for the analysis of diffusion MRI data. Frontiers in neuroinformatics. 2014;8.
19. Tustison NJ, Avants BB, Cook PA, et al. N4ITK: improved N3 bias correction. IEEE transactions on medical imaging. 2010;29(6):1310-20.

20. Jenkinson M, Beckmann CF, Behrens TE, Woolrich MW, Smith SM. Fsl. Neuroimage. 2012;62(2):782-90.
21. Smith SM. Fast robust automated brain extraction. Human brain mapping. 2002;17(3):143-55.
22. Andersson JL, Sotiropoulos SN. An integrated approach to correction for off-resonance effects and subject movement in diffusion MR imaging. Neuroimage. 2016;125:1063-78.
23. Descoteaux M, Deriche R, Knosche TR, Anwander A. Deterministic and probabilistic tractography based on complex fibre orientation distributions. IEEE transactions on medical imaging. 2009;28(2):269-86.
24. Presseau C, Jodoin P-M, Houde J-C, Descoteaux M. A new compression format for fiber tracking datasets. NeuroImage. 2015;109:73-83.
25. Garyfallidis E, Ocegueda O, Wassermann D, Descoteaux M. Robust and efficient linear registration of white-matter fascicles in the space of streamlines. NeuroImage. 2015;117:124-40.
26. Garyfallidis E, Côté M-A, Hau J, et al., editors. Recognition of bundles in healthy and severely diseased brains. . Proceeding of: International Society of Magnetic Resonance in Medicine (ISMRM); 2015; Toronto, Canada.
27. Witelson SF. Hand and sex differences in the isthmus and genu of the human corpus callosum: a postmortem morphological study. Brain. 1989;112(3):799-835.
28. Torres-Berrío A, Lopez JP, Bagot RC, et al. DCC confers susceptibility to depression-like behaviors in humans and mice and is regulated by miR-218. Biological psychiatry. 2017;81(4):306-15.
29. Anderson MA, Gusella JF. Use of cyclosporin A in establishing Epstein-Barr virus-transformed human lymphoblastoid cell lines. In Vitro Cellular & Developmental Biology-Plant. 1984;20(11):856-8.
30. Hibar DP, Stein JL, Renteria ME, et al. Common genetic variants influence human subcortical brain structures. Nature. 2015;520(7546):224-9.
31. Hoops D, Flores C. Making Dopamine Connections in Adolescence. Trends in Neurosciences. 2017;40(12):709-19.
32. Flores C. Role of netrin-1 in the organization and function of the mesocorticolimbic dopamine system. J Psychiatry Neurosci. 2011;36(5):296-310.
33. Betzel RF, Byrge L, He Y, Goñi J, Zuo X-N, Sporns O. Changes in structural and functional connectivity among resting-state networks across the human lifespan. Neuroimage. 2014;102:345-57.
34. Kochunov P, Williamson DE, Lancaster J, et al. Fractional anisotropy of water diffusion in cerebral white matter across the lifespan. Neurobiology of Aging. 2012 2012/01/01/;33(1):9-20.
35. Bhandari A, Radhu N, Farzan F, et al. A meta-analysis of the effects of aging on motor cortex neurophysiology assessed by transcranial magnetic stimulation. Clinical Neurophysiology. 2016 2016/08/01/;127(8):2834-45.
36. Goldsworthy MR, Vallence A-M, Hodyl NA, Semmler JG, Pitcher JB, Ridding MC. Probing changes in corticospinal excitability following theta burst stimulation of the human primary motor cortex. Clinical Neurophysiology. 2016 2016/01/01/;127(1):740-7.
37. Fazeli A, Dickinson SL, Hermiston ML, et al. Phenotype of mice lacking functional Deleted in colorectal cancer (Dcc) gene. Nature. 1997;386(6627):796.
38. Keino-Masu K, Masu M, Hinck L, et al. Deleted in Colorectal Cancer (DCC) encodes a netrin receptor. Cell. 1996;87(2):175-85.

39. Depienne C, Bouteiller D, Méneret A, et al. RAD51 haploinsufficiency causes congenital mirror movements in humans. The American Journal of Human Genetics. 2012;90(2):301-7.
40. Leinsinger GL, Heiss DT, Jassoy AG, Pfluger T, Hahn K, Danek A. Persistent mirror movements: functional MR imaging of the hand motor cortex. Radiology. 1997;203(2):545-52.
41. Franz EA, Chiaroni-Clarke R, Woodrow S, et al. Congenital mirror movements: phenotypes associated with DCC and RAD51 mutations. Journal of the neurological sciences. 2015;351(1):140-5.

Group	*DCC*$^{+/-}$/MM+	*DCC*$^{+/-}$/MM-	*DCC*$^{+/+}$/MM-	UHV	Statistical test (4 groups)
N_{Total}	13	7	13	19	
N_{MRI}	11	7	12	19	
$N_{task\text{-}fMRI}$	11	7	12	18	
$N_{rs\text{-}fcMRI}$	10	7	12	14	
N_{TMS}	12	7	12	14	
Age (Mean ± SD)	44.4±16.9	49.6±14.9	37.9±13.2	41.4±16.3	$F_{(3.48)}$= 0.96, p=0.42
Sex (M:F)	9:4	2:5	5:8	10:9	$\chi^2_{(3)}$= 3.95, p=0.27
Handedness	11 right, 2 left	5 right, 2 left	10 right, 3 left	19 right	$\chi^2_{(3)}$= 5.40, p=0.15

Table 1: Participant Characteristics. *DCC*$^{+/-}$/MM+: mutation carriers with mirror movements; *DCC*$^{+/-}$/MM-: mutation carriers without mirror movements; *DCC*$^{+/+}$/MM-: relatives without the mutation or mirror movements; UHV: unrelated healthy volunteers.

	Right M1 to Left Cerebellum	Right M1 to Right Cerebellum	Right M1 to Left M1	Left M1 to Left Cerebellum	Left M1 to Right Cerebellum
DCC$^{+/-}$/MM+	0.098	-0.110	0.707	0.075	0.062
DCC$^{+/-}$/MM-	-0.087	-0.208	0.514	-0.037	-0.030
DCC$^{+/+}$/MM-	0.173	-0.102	0.759	0.061	0.019
UHV	0.014	-0.052	0.818	-0.124	0.024

Table 2: Pairwise Connectivity Values. Average Fisher-Z score values between *a priori* regions of interest for *DCC*$^{+/-}$/MM+, *DCC*$^{+/-}$/MM-, *DCC*$^{+/+}$/MM-, and UHV.

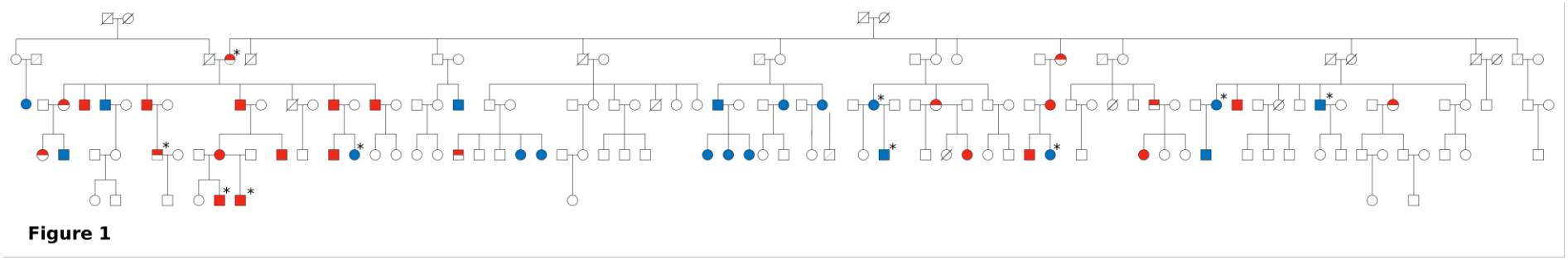

Figure 1. Pedigree of Quebec family. Full red indicates *DCC*$^{+/-}$/MM+; half red indicates *DCC*$^{+/-}$/MM-, blue indicates *DCC*$^{+/+}$/MM-relatives, white designates those who did not undergo genetic testing. Asterisks (*) indicate previously genotyped individuals who did not participate in the present study. Crossed lines designate deceased. Squares and circles are males and females, respectively.

Figure 2

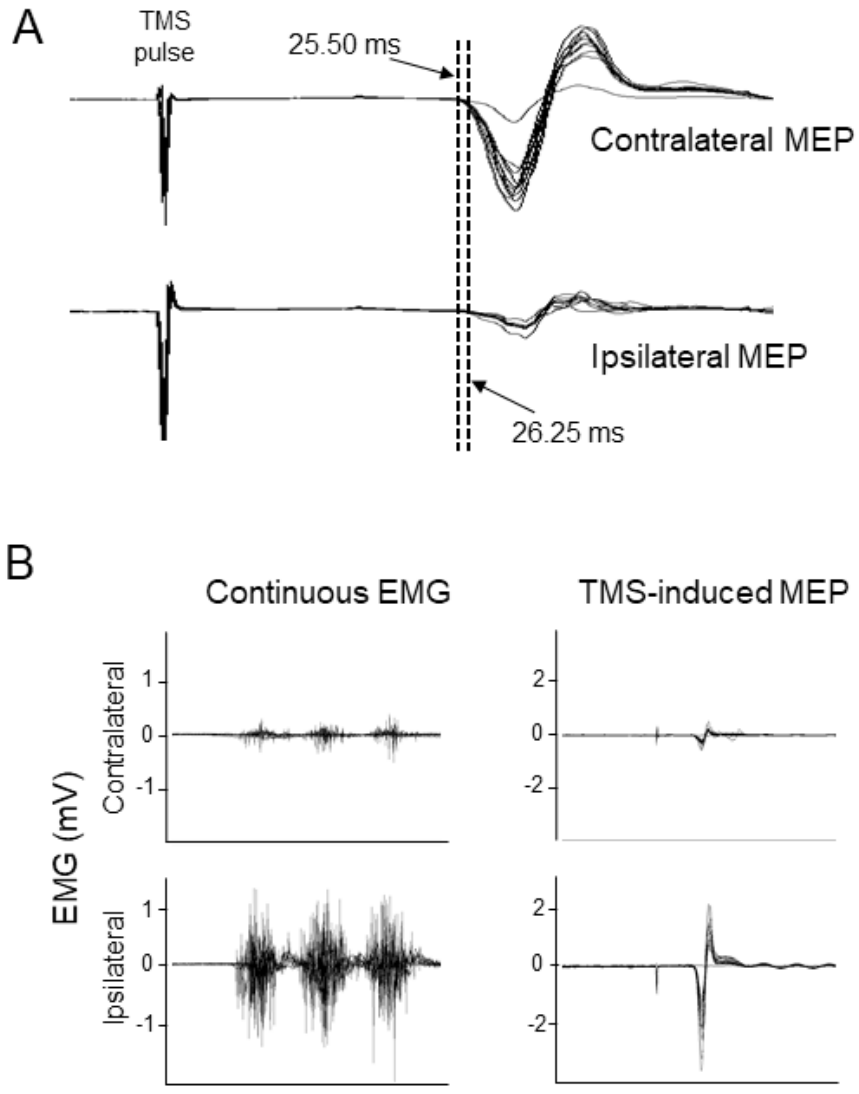

Figure 2. TMS/EMG. (A) Raw EMG traces of TMS-induced MEPs in a *DCC*$^{+/-}$/MM+ individual with larger MEPs in the hand contralateral to stimulation. Dashed lines indicate the onset of TMS-induced MEPs. **(B)** Raw EMG traces of TMS-induced MEPs and continuous EMG in a *DCC*$^{+/-}$/MM+ individual with larger MEPs in the hand ipsilateral to stimulation.

Figure 3

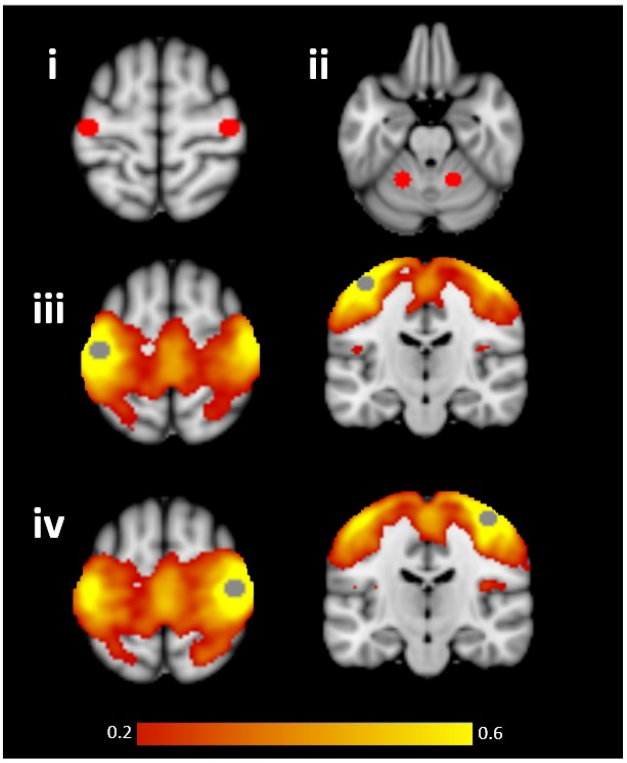

Figure 3. rs-fcMRI. *A priori* regions of interest in the left and right somatomotor cortex (i) and the left and right cerebellum (ii). Functional connectivity with the left somatomotor cortex (iii) and right somatomotor cortex (iv) is shown averaged across all participants.

Figure 4

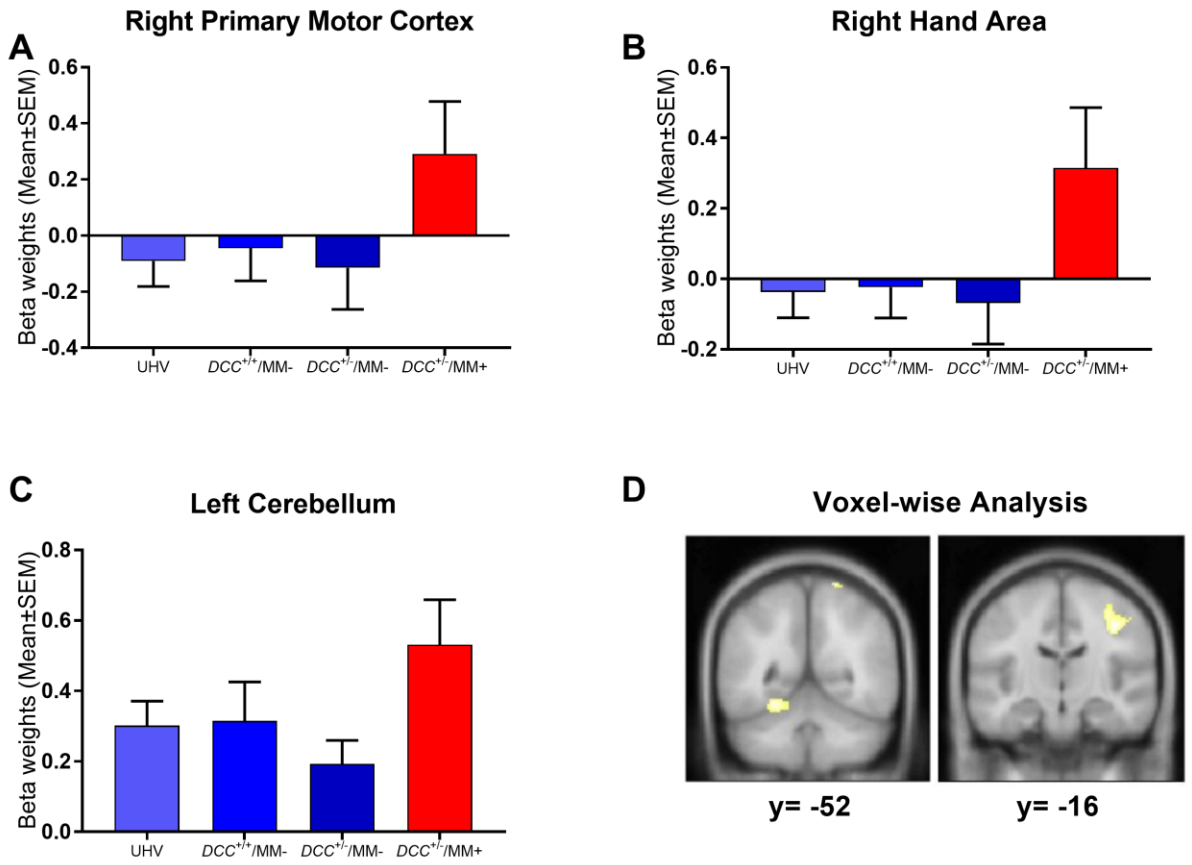

Figure 4. Task fMRI. Increased right-hand-induced activations associated with the presence of mirror movements in the ipsilateral **(A)** right M1 and **(B)** right M1 hand area, and in the contralateral **(C)** left cerebellum. **(D)** Peak activation sites in whole-brain voxel-wise analysis ($p<0.001$) in left cerebellum and right M1. Raw data are plotted.

Figure 5

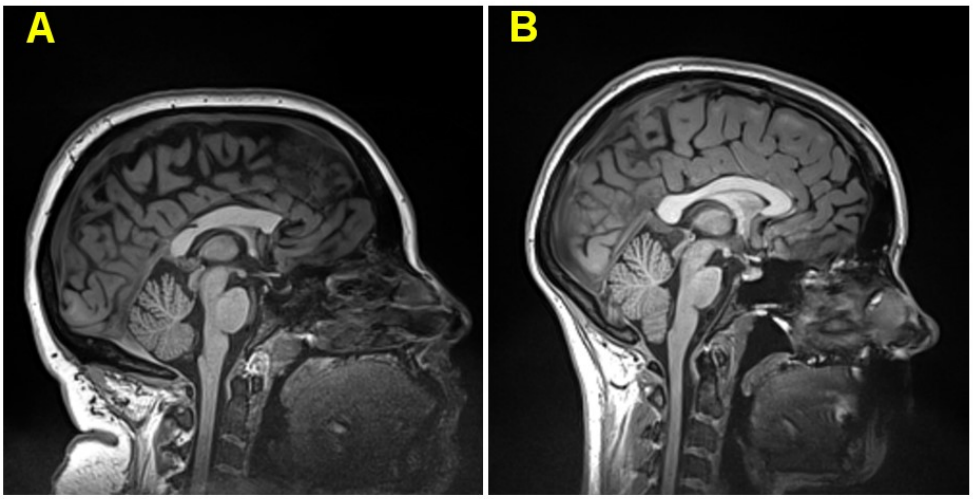

Figure 5. **Partial agenesis of the corpus callosum.** (**A**) Partial agenesis of the corpus callosum in female individual with a *DCC* mutation and without mirror movements, revealing absence of the rostrum. (**B**) Female UHV without a *DCC* mutation or mirror movements, for comparison.

Figure 6

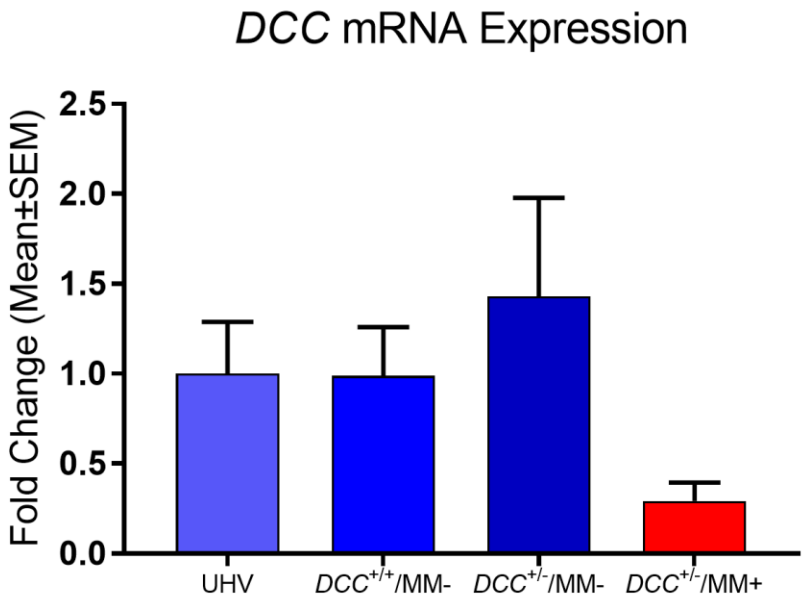

Figure 6. *DCC* mRNA. Decreased *DCC* mRNA (Quantity Mean: *DCC*/GAPDH) fold change, originating from both the functioning and mutated allele, is associated with the presence of mirror movements and not the *DCC* mutation. Raw data are plotted.

Connecting Statement between Manuscripts

The second chapter of the dissertation identified structural and functional neurophysiological alterations of the motor system among human *DCC* mutation carriers. The third chapter of the dissertation sought to determine whether *DCC* mutation carriers exhibit alterations to systems outside of the motor system, particularly the mesocorticolimbic pathways. This was the first study of mesocorticolimbic connectivity, volumes, and associated behavioral traits in humans with a *DCC* mutation, with hypotheses based on the findings of studies of *Dcc* haploinsufficient mice. Moreover, we sought to characterize the translatability of DCC-related effects in the mesocorticolimbic system by conducting volumetric studies of this system across species.

Mesocorticolimbic Connectivity and Volumetric Alterations in *DCC* Mutation Carriers

*Daniel E. Vosberg BSc[1,3], *Yu Zhang PhD[2], Aurore Menegaux MSc[4,7,8], Amanda Chalupa MSc[1], Colleen Manitt PhD[4], Simone Zehntner PhD[6], Conrad Eng MSc[4], Kristina DeDuck MSc[2], Dominique Allard BScN[1], France Durand MSc[1], Alain Dagher MD[2,3], Chawki Benkelfat MD CSPQ DERBH[1,2,3], Myriam Srour MD PhD[2], Ridha Joober MD PhD[1,3,4], Franco Lepore PhD[5], Guy Rouleau MD PhD[2], Hugo Théoret PhD[5], Barry J. Bedell MD PhD[2], Cecilia Flores PhD[1,2,3,4], Marco Leyton PhD[1,2,3]

*shared first co-authorship.

Affiliations

[1]Department of Psychiatry, McGill University, Montreal, Quebec, Canada. [2]Neurology and Neurosurgery, McGill University, Montreal, Quebec, Canada. [3]Integrated Program in Neuroscience (IPN), McGill University, Montreal, Quebec, Canada. [4]Douglas Mental Health University Institute, Montreal, QC, Canada. [5]Psychology, Université de Montréal, Montreal, Quebec, Canada. [6]Biospective Inc., Montreal, QC, Canada. Current affiliations for AM: [7]Department of Psychology, General and Experimental Psychology, Ludwig-Maximilians-Universität München, Leopoldstrasse 13, 80802 Munich, Germany; [8]Graduate School of Systemic Neurosciences GSN, Ludwig-Maximilians-Universität München, Biocenter, Großhaderner Strasse 2, 82152 Munich, Germany

Corresponding authors:

Marco Leyton, PhD
Irving Ludmer Psychiatry Building
Institute 1033 Pine Avenue West
Montreal, Quebec, Canada, H3A 1A1
marco.leyton@mcgill.ca

Cecilia Flores, PhD
Douglas Mental Health University
6875 Boulevard LaSalle,
Montreal, Quebec, Canada, H4H 1R3
cecilia.flores@mcgill.ca

Conflict of interest: The authors declare no competing financial interests.

Acknowledgments

This work was supported by funding from the Canadian Institutes for Health Research to ML (CIHR, MOP-119543) and the National Institute on Drug Abuse to CF (NIDA, RO1DA037911). We would also like to acknowledge Jared Rowley and Dr. Pedro Rosa-Neto for their technical assistance.

Word counts**:**

Introduction: 553
Discussion: 1272
Abstract: 239

Pages: 26
Figures: 7
Tables: 2

ABSTRACT

The axon guidance cue receptor DCC (deleted in colorectal cancer) plays a critical role in the organization of mesocorticolimbic pathways in rodents. To investigate whether this occurs in humans, we measured (1) anatomical connectivity between the substantia nigra/ventral tegmental area (SN/VTA) and forebrain targets, (2) striatal and cortical volumes, and (3) putatively associated traits and behaviors. To assess translatability, morphometric data were also collected in *Dcc*-haploinsufficient mice.

The human volunteers were 20 $DCC^{+/-}$ mutation carriers, 16 $DCC^{+/+}$ relatives, and 20 $DCC^{+/+}$ unrelated healthy volunteers (UHVs; 28 females). The mice were 11 $Dcc^{+/-}$ and 16 wildtype C57BL/6J animals assessed during adolescence and adulthood.

Compared with both control groups, the human $DCC^{+/-}$ carriers exhibited: (1) reduced anatomical connectivity from the SN/VTA to the ventral striatum [$DCC^{+/+}$: p= 0.0005, *r(effect size)*= 0.60; UHV: p= 0.0029, *r*= 0.48] and ventral medial prefrontal cortex [$DCC^{+/+}$: p= 0.0031, *r*= 0.53; UHV: p= 0.034, *r*= 0.35]; (2) lower novelty seeking scores ($DCC^{+/+}$: p= 0.034, *d*= 0.82; UHV: p= 0.019, *d*= 0.84); and (3) reduced striatal volume ($DCC^{+/+}$: p= 0.0009, *d*= 1.37; UHV: p= 0.0054, *d*= 0.93). Striatal volumetric reductions were also present in $Dcc^{+/-}$ mice, and these were seen during adolescence (p= 0.0058, *d*= 1.09) and adulthood (p= 0.003, *d*= 1.26).

Together these findings provide the first evidence in humans that an axon guidance gene is involved in the formation of mesocorticolimbic circuitry and related behavioral traits, providing mechanisms through which *DCC* mutations might affect susceptibility to diverse neuropsychiatric disorders.

SIGNIFICANCE STATEMENT

Opportunities to study the effects of axon guidance molecules on human brain development have been rare. Here, the identification of a large four-generational family that carries a mutation to the axon guidance molecule receptor gene, *DCC*, enabled us to demonstrate effects on mesocorticolimbic anatomical connectivity, striatal volumes, and personality traits. Reductions in striatal volumes were replicated in *DCC*-haploinsufficient mice. Together, these processes might influence mesocorticolimbic function and susceptibility to diverse neuropsychiatric disorders.

INTRODUCTION

What guides the alignment of mesocorticolimbic pathways in humans? The processes are poorly understood, but the axon guidance molecule receptor, DCC (deleted in colorectal cancer), might play an important role (Flores, 2011; Hoops and Flores, 2017). DCC is expressed throughout most of the nervous system during embryonic development (Gad *et al*, 1997; Livesey and Hunt, 1997; Harter *et al*, 2010), and continues to be expressed in adulthood in some regions, including the substantia nigra/ventral tegmental area (SN/VTA), striatum, hippocampus, and cortex (Gad et al., 1997; Livesey and Hunt, 1997; Osborne et al., 2005; Grant et al., 2007; Harter et al., 2010; Manitt et al., 2010; Reyes et al., 2013).

Mice haploinsufficient for the *Dcc* gene develop diverse alterations to mesocorticolimbic anatomy and related behaviors during the adolescent expansion of mesocortical dopamine projections (Hoops and Flores, 2017). *Dcc* haploinsufficiency in dopamine neurons causes mesolimbic dopamine axons that would normally be retained in the striatum to continue to grow to the medial prefrontal cortex (mPFC) throughout adolescence (Reynolds et al., 2018). As a consequence, adult *Dcc*-haploinsufficient mice have increased mPFC dopamine innervation and dopamine release (Grant et al., 2007; Manitt et al., 2011; Pokinko et al., 2015). This is coupled with decreased spine density, dendritic arbor complexity, and excitability of mPFC layer V pyramidal neurons (Grant et al., 2007; Manitt et al., 2013). In the nucleus accumbens (NAcc), these same processes lead to reduced dopamine innervation and amphetamine-induced dopamine release (Flores et al., 2005; Grant et al., 2007; Pokinko et al., 2015; Reynolds et al., 2018). Behaviorally, adult *Dcc*-haploinsufficient mice exhibit blunted stimulant drug-induced responses, including reductions in locomotor activity, sensorimotor gating, conditioned place preference, and intracranial self-stimulation (Flores et al., 2005; Grant et al., 2007; Kim et al.,

2013; Reynolds et al., 2016).

In the present study, we tested whether *DCC*-haploinsufficient humans exhibit mesocorticolimbic connectivity alterations and associated behavioral traits as have been identified in *Dcc*-heterozygous mice. The sample comprised a large four generational Quebec family, half of whom are carriers for an autosomal dominant mutation which induces *DCC* haploinsufficiency (Srour et al., 2009, 2010). Within the family, a genome-wide linkage analysis identified a *DCC* frameshift mutation (NM_005215.3, c.1140+1G>A) resulting from abnormal skipping of exon 6. This leads to a premature stop codon encoding a truncated DCC protein that fails to bind to its ligand, Netrin-1 (Srour et al., 2010).

To investigate alterations potentially associated with DCC related susceptibility to psychiatric pathology, we tested whether *DCC*-haploinsufficient humans, compared with *DCC* wild-type family relatives and unrelated healthy volunteers (UHVs), exhibit (1) altered structural and functional connectivity between the midbrain and projection sites in the ventral striatum (VS) and mPFC, and (2) a behavioral phenotype consistent with low striatal dopamine transmission comprising diminished novelty-seeking and reward-sensitivity traits, decreased substance use, and increased punishment sensitivity (Leyton et al., 2002; Frank et al., 2004). Finally, using a translational cross-species magnetic resonance imaging (MRI) approach, we tested whether these effects might be associated with alterations in striatal and cortical brain volume. Automated morphometric analyses were conducted in the *DCC*-haploinsufficient human volunteers and *Dcc*-haploinsufficient C57BL/6 mice. The rodents were tested in both adolescence and adulthood to determine whether volumetric effects preceded or coincided with the previously demonstrated changes to dopamine neurons.

METHODS

Human participants and data acquisition

Fifty-six volunteers participated in the study (28 males; age: 42.4 ± 15.3 years, from 19-72 years old). Among them, 20 were *DCC* mutation carriers ($DCC^{+/-}$; 11 males, age: 46.3 ± 16.1, from 20-72), 16 were age-matched relatives without the *DCC* mutation ($DCC^{+/+}$; six males, 37.9±13.0, 22-63 years old), and 20 were UHVs (11 males, age: 42.2±15.4, 19-60 years old). Four participants were not interested in completing the neuroimaging procedures and 3 were physically unable to fit into the MRI scanner. Detailed information regarding the participants and the number who completed each task are provided in Table 1. A pedigree of the Quebec family is provided in Figure 1. Recruitment of family members was solely based on interest and safety. UHVs were all neurologically intact and free of current major psychiatric disorders including substance use disorders except for one who met criteria for a possible mild mood disorder; excluding this individual did not change the results. All provided written informed consent to the study protocol, which was approved by the local research ethics committee.

Genotyping

All participants underwent genotyping either at assessment for the present study or previously (Srour et al., 2010). Genotyping was unavailable for one UHV and excluding this individual did not alter the findings. Coding exons and the exon-intron boundaries of the *DCC* gene were screened for mutations based on the sequence (NM_005215; UCSC (University of California, Santa Cruz) March 2006 Assembly hg18). Primers were determined in a previous study of the family (Srour et al., 2010). PCR products were sequenced on the ABI 3700 Sequencer at the Genome Quebec Centre for Innovation according to the manufacturer's

recommended protocol (Applied Biosystems). Sequences were aligned and analyzed using SeqMan 4.03 (DNAStar, WI, USA) and Mutation Surveyor v.3.1 (SoftGenetics, PA, USA).

Personality and substance use measures

Participants completed questionnaires assessing novelty seeking and sensitivity to punishment and reward. Novelty-seeking traits were measured using Cloninger's 240-item Temperament and Character Inventory (TCI) (De Fruyt et al., 2000). Sensitivity to punishment and reward were measured with the Sensitivity to Punishment and Sensitivity to Reward Questionnaire (SPSRQ), a 48-item scale developed to assess temperamental correlates of Gray's hypothesized behavioral activation and inhibition systems (Caseras et al., 2003). In a structured interview, self-reported weekly current substance use (e.g., drinks, cannabis, and tobacco cigarettes, etc.), lifetime substance use, and age of onset were evaluated for alcohol, cigarettes, and cannabis. Other substances were measured but not evaluated statistically because the number of self-reported users was too low. These comprised amphetamine, cocaine, 3,4-methylenedioxymethamphetamine (MDMA), heroin, ketamine, gamma hydroxybutyrate (GHB), ephedrine, steroids, psilocybin, and lysergic acid diethylamide (LSD).

Human MRI

Participants underwent anatomical, diffusion weighted and resting-state functional MRI (rs-fMRI) acquisitions in a scanning session using a 3T Siemens Magnetom Trio MRI scanner (12 channel head coil). Forty-nine participants underwent diffusion tensor imaging (DTI) using a single-shot spin-echo echo-planar pulse sequence with multi-directional diffusion weighting [repetition time (TR) = 12 s, echo time (TE) = 89 ms; 90 contiguous axial slices with an isotropic 2 mm resolution, field of view (FOV) = 256 × 256 mm^2, matrix size = 128 × 128 with partial Fourier reconstructed to 6/8]. Diffusion weighting was distributed along 64 different directions

using a b-value of 1000 s/mm^2. One additional volume with no diffusion weighting (i.e. $b = 0$) was acquired in the beginning of the acquisition. Using a T1-weighted 3D magnetization-prepared rapid acquisition with gradient echo sequence [200 axial slices; inversion time (TI) = 0.9 s, TR = 2.3 s, TE = 2.98 ms, FOV = 256 × 256 mm^2, flip angle = 9°, final voxel resolution: 1 mm × 1 mm × 1 mm], a high-resolution anatomical scan was also acquired for each participant.

Immediately after the DTI, participants underwent the rs-fMRI acquisition. Forty-three participants completed resting-state scans, including 17 *DCC*$^{+/-}$, 12 *DCC*$^{+/+}$, and 14 UHV. All participants were instructed to rest with their eyes closed, relax their minds, and remain as motionless as possible during the scanning. A total of 180 volumes, each covering the entire brain including the cerebellum with 38 axial slices, were acquired using gradient-echo echo planar imaging sequence (TR = 2000 ms, TE = 30 ms, FOV = 256 × 256 mm^2, matrix, 64 × 64, slice thickness = 4 mm with no gaps, flip angle, 90°). Slices were acquired in a descending and interleaved manner.

Human voxel-based morphometry analysis

Anatomical scans were preprocessed in SPM8 (www.fil.ion.ucl.ac.uk/spm/software/spm8) using the DARTEL (Diffeomorphic Anatomic Registration through Exponentiated Lie) and VBM8 toolbox (http://dbm.neuro.uni-jena.de/vbm8/). First, the structural MRI images were segmented into gray matter (GM), white matter (WM), CSF, bone, and soft tissue. The DARTEL algorithm registered these tissue segmentations back and forth with the default templates based on the ICBM152 brain, and finally generated population-specific tissue templates. GM and WM density images of all subjects were subsequently nonlinearly registered onto the corresponding template. In VBM8, all registered tissue images were modulated using the Jacobian determinants derived from the spatial normalisation step and corrected for individual head size. The modulated

GM and WM tissue images were then smoothed with an 8-mm full-width at half-maximum (FWHM) Gaussian kernel.

The Harvard-Oxford subcortical atlas with a 25% threshold (Desikan et al., 2006) was used to define four *a priori* selected regions: the caudate, putamen, accumbens, and hippocampus. The ventral mPFC (vmPFC) and mPFC/anterior cingulate cortex (mPFC/ACC) were defined by drawing a 6 mm sphere around the coordinates (vmPFC: x = ±6, y = 45, z = -9; mPFC/ACC: x = ±18, y = 42, z =9; as explained below).

Human connectivity seed and target regions

A substantia nigra (SN) seed mask was generated from a 7T MRI atlas of the basal ganglia based on high-resolution MP2RAGE and FLASH (fast low-angle shot) scans (Keuken and Forstmann, 2015) available at https://www.nitrc.org/projects/atag. The entire region of SN (Figure 2A) was extracted from the probabilistic atlas with a threshold of 33% of the population (*i.e.,* ≥10 of 30 participants showing this nucleus) with an ~300 mm^3 volume in each hemisphere. Considering the low spatial resolution of our functional and diffusion data [4-mm isotropic for rs-fMRI and 2-mm for DTI], the seed might also cover part of the adjacent VTA. Here, we designated this seed region as SN/VTA.

Target regions comprised VS and vmPFC, defined by drawing a 6-mm sphere around the peak coordinates (VS: x=±12, y=15, z=-6; vmPFC: x=±6, y=45, z=-9), acquired from a recent fMRI meta-analysis of subjective value (Bartra et al., 2013) (Figure 2B, C). Other regions, including the hippocampus (x=±24, y=-9, z=-15) and the mPFC/ACC (x=±18, y=42, z=9), identified from the whole-brain functional connectivity analysis, were also included in the anatomical and functional connectivity analyses (Figure 2D-E).

Human diffusion weighted imaging preprocessing

The diffusion MR data were preprocessed using the FMRIB's Diffusion Toolbox [FMRIB (Oxford Centre for Functional MRI of the Brain) Software Library (FSL) version 5.0; http://fsl.fmrib.ox.ac.uk/fsl/fslwiki/FSL), including eddy current correction, calculation of the principal directions in diffusion tensors, and estimation of the probabilistic distribution of fiber orientations. Specifically, motion artifacts and eddy current distortions were corrected by using affine registration of diffusion-weighted images to the non-diffusion-weighted images (b = 0 s/mm^2). Then, a diffusion tensor model was fitted for each voxel to estimate the principal fiber directions and a fractional anisotropy (FA) and mean diffusivity (MD) map was calculated.

Next, the probabilistic distribution of fiber orientations was estimated using FSL's BEDPOSTX with a maximum of two fiber directions per voxel (Behrens et al., 2007). The skull-stripped T1-weighted image from each participant was then linearly registered into the diffusion space by using rigid-body alignment of the anatomical image to the FA image. This coregistered T1-weighted image was further nonlinearly registered to the ICBM152 brain template (http://www.bic.mni.mcgill.ca/ServicesAtlases/ICBM152NLin2009) using FNIRT (FMRIB's Nonlinear Image Registration Tool) from the FSL package. The reverse transformation was then obtained and used to nonlinearly register the seed region from MNI standard space to native diffusion space.

Human anatomical connectivity profile

We mapped the anatomical connectivity profile of SN/VTA by performing probabilistic tractography with 10,000 streamline fibers per voxel within the seed region using FSL's PROBTRACKX. The number of fibers passing through each target region represents the strength of connectivity between the seed and target region. The resulting connectivity maps were first

normalized by the size of seed region and total number of streamlines (*i.e.,* 10,000) to generate the relative tracing strength from the seed to the rest of the brain. The resulting individual tractograms were combined to generate a population map of the major fiber projections from SN/VTA. The relative connection probability from SN/VTA to each target area was then calculated by averaging the tractography values of the population fiber-tract maps.

In addition to the tractography analysis, we also investigated group differences in FA and MD in the whole-brain WM skeletons, including tracts between the SN/VTA and the target regions, using Tract-Based Spatial Statistics (TBSS) from FSL (Smith et al., 2006). Threshold-Free Cluster Enhancement was used to correct for multiple comparisons (Smith and Nichols, 2009). The mean FA and MD values within SN/VTA and other target areas were also calculated.

Human resting state functional connectivity preprocessing

The rs-fMRI datasets were preprocessed using the script revised based on the 1000 Functional Connectome Project (www.nitrc.org/projects/fcon_1000) (Biswal et al., 2010) using both FSL and AFNI (Automated Functional NeuroImaging; http://afni.nimh.nih.gov/afni). The preprocessing steps included: 1) discarding the first 10 volumes in each scan series for signal equilibration, 2) performing slice timing correction and motion correction, 3) removing the linear and quadratic trends, 4) band-pass temporal filtering (0.01 Hz < f < 0.08 Hz), 5) spatial smoothing using a 6-mm full-width at half-maximum (FWHM) Gaussian kernel, 6) performing nuisance signal regression (including WM, CSF, the global signal, and six motion parameters), and 7) resampling into Montreal Neurological Institute (MNI) space with the concatenated transformations, including rigid transformation from the mean functional volume to the individual anatomical volume via FLIRT (FMRIB's Linear Image Registration Tool) (Jenkinson and Smith, 2001) followed by spatial normalization of the individual anatomical volume to the

MNI152 brain template (3 mm isotropic resolution) using FNIRT (Andersson et al., 2007). Finally, a four-dimensional time-series dataset in standard MNI space with 3 mm isotropic resolution was obtained for each participant after preprocessing.

Human resting-state functional connectivity

The mean time-course of the seed SN/VTA was extracted individually to calculate the whole-brain functional connectivity using Pearson's correlation along with normalization by Fisher's z-transform. As a result, a z-score connectivity map was generated for each individual. To detect the effect of the *DCC* mutation on projections from the SN/VTA, a two-sample t-test in SPM was performed on these connectivity maps ($DCC^{+/-}$ *vs*. $DCC^{+/+}$) and additionally corrected for multiple comparisons using false discovery rate (FDR) corrected p=0.05 with cluster size ≥ 540 mm^3. The functional connectivity between SN/VTA and our predefined target areas (including VS and vmPFC) were also calculated using Pearson's correlation and transformed into z-scores.

Experimental design and statistical analyses of human data

Group differences in personality traits, substance use, GM volume, and connectivity measures were examined with χ^2 analyses and one-way ANOVAs followed by t-test planned comparisons, comparing each control group to the $DCC^{+/-}$ group using both MATLAB15b for Linux and Graphpad Prism 7 for Windows. For non-parametric data, Kruskal-Wallis followed by Mann-Whitney U tests were conducted, comparing each control group to the $DCC^{+/-}$ group. Effect sizes were computed, specifically Cohen's *d* for parametric pairwise comparisons and $r = \frac{Z}{\sqrt{N}}$ for non-parametric pairwise comparisons (Fritz et al., 2012).

To investigate associations between SN/VTA connectivity and personality traits, we performed Pearson and Spearman partial correlation analyses, as appropriate to the data, between

both functional and anatomical connectivity and novelty seeking, sensitivity to punishment, sensitivity to reward, and lifetime substance use. Age and gender were used as covariates of no interest. For Pearson correlation analyses, outliers were removed prior to calculating the correlation coefficients, which were identified based on robust regression weights (Rousseeuw and Hubert, 2011). Additionally, for lifetime substance use, log transformations were performed prior to the correlations due to a large non-linear range in the values. Participants who reported zero or one current or lifetime substance use were removed from these group and correlation analyses because these values skewed the distributions.

Dcc haploinsufficient mice

Male *Dcc*-haploinsufficient mice were originally obtained from Dr. Susan Ackerman. They were maintained on a C57BL/6J (BL/6) background and bred with female BL/6 mice from The Jackson Laboratory. Volumetric differences were characterized between male *Dcc*-haploinsufficient (n = 11) and wild-type (n = 16) mice during adolescence [postnatal day (P) 33±2], and, again, in the same animals, in adulthood (P75±15). Mice were kept on a 12h light/dark cycle with ad libitum access to food and water. They were weaned at P20 and housed with same-sex littermates. In *Dcc* haploinsufficient mice, the *Dcc* gene was inactivated using homologous recombination by the insertion of a neomycin resistance cassette into exon 3, which encodes most of the second Ig-like domain of the protein. The proper targeting of the gene and complete loss of DCC expression were validated by Southern and Western blot analyses, respectively (Fazeli et al., 1997). Mouse genotypes were verified by PCR amplification of genomic DNA at an annealing temperature of 54°C for 30 cycles with the primers DCC code (GGT CAT TGA GGT TCC TTT), DCC reverse (AAG ACG ACC ACA CGC GAC), and DCC Neo (TCC TCG TGC TTT ACG GTA TC). All experiments and procedures were performed in

accordance with the guidelines of the Canadian Council of Animal Care and the McGill University/Douglas Mental Health University Institute Animal Care Committee.

Mouse magnetic resonance imaging (MRI)

MRI acquisition

Magnetic resonance imaging (MRI) was performed using a 7 tesla Bruker Biospec 70/30 USR at the Douglas Brain Imaging Center (Montreal, Canada) using a transmit circularly polarized resonator and a dedicated mouse brain receive-only circularly polarized surface coil (Bruker Canada). Mice were immobilized in a prone position on a water-heated mat. Anaesthesia was induced with 5% isoflurane for 2 minutes, and maintained with 2% isoflurane for the duration of the experiment. Anatomical images of brains within skulls were acquired using the standard Bruker 3D-TrueFISP pulse sequence with the following parameters: TE = 2.6 ms, TR = 5.2 ms, number of excitations = 2, effective bandwidth = 50,000 Hz, FOV = 1.80 cm x 1.80 cm x 0.9 cm, matrix size = 128 x 128 x 64, final spatial resolution =141 um isotropic voxels. To reduce banding artifacts, eight radio frequency phase advance values were used: 180, 0, 90, 270, 45, 225, 135, and 315°, resulting in 16 averages overall. Final images were root mean square averages of these phase advances. The total scan time for each animal was <40 min.

Segmentation of regions of interest

The *a priori* selected regions of interest were four mesocorticolimbic terminal regions: the medial prefrontal cortex (mPFC), dorsal striatum, NAcc, and hippocampus (Figure 3A-C). Within the inner layers of the mPFC three regions were analyzed: the cingulate 1, the prelimbic, and the infralimbic cortices. An anatomical template was generated from the non-linear average of the 54 scans. A single rater performed manual segmentation of the structures of interest on the group template using the Display software package

(http://www.bic.mni.mcgill.ca/software/Display/Display.html; Montreal Neurological Institute, Montreal, Canada). Structures were delineated in the coronal orientation slice by slice while comparing the other two orientations and the adjacent slices to the Mouse Brain Atlas (Paxinos and Franklin, 2004). As the template was symmetric, tracings of the left hemisphere of the template brain were flipped to the right hemisphere. The third and lateral ventricles were segmented first to define the boundaries of the dorsal striatum and NAcc. After each structure was labeled, its boundaries were checked again and corrections were made in reference to all three orientations. The volumes of each structure were determined for every animal via fully automated, volume-based morphometry using the NIGHTWING software (Biospective).

Experimental design and statistical analyses of mouse data

Differences in volume were analysed using two-way ANOVAs with genotype and age as between- and within-group variables, respectively. Statistical analyses were performed using GraphPad Prism 7 for Windows.

RESULTS

Human participant characteristics

The groups were well matched for age, sex, and handedness (Table 1). As hypothesized, the novelty seeking data analysis yielded a main effect of group ($F_{2,43}$= 3.74, p= 0.032) reflecting decreased scores among $DCC^{+/-}$ participants, compared to the $DCC^{+/+}$ relatives (T_{43}=2.19, p= 0.034, *effect size(d)*= 0.82) and UHV (T_{43}=2.44, p= 0.019, *effect size(d)*= 0.84) (Figure 4A). Intriguingly, $DCC^{+/-}$ participants, compared to $DCC^{+/+}$ relatives, also reported significantly lower lifetime cigarette smoking (U= 17, p= 0.026, *effect size(r)*= 0.51) and trends for decreased current cigarette use (T_{11}= 1.87, p= 0.089, *effect size(d)*= 1.04) as well as a later age of onset for cigarette use (T_{21}= 2, p= 0.059, *effect size(d)*= 0.83) (Figure 4B-D). Tobacco use in the $DCC^{+/-}$ participants did not differ from the UHV (age of onset: T_{18}= 1.27, p= 0.22; current use: T_{7}= 0.98, p= 0.36; lifetime use: U= 48, p= 0.94), but this was not unexpected given that their stricter selection criteria included an absence of tobacco and other substance use problems (see *Human participants and data acquisition*). Indeed, compared to $DCC^{+/+}$ relatives, the UHV also exhibited significantly reduced lifetime use (U= 15, p= 0.046) and increased age of onset (T_{19}=2.77, p= 0.012) of cigarette smoking. There were no statistically significant group effects for sensitivity to punishment, sensitivity to reward, alcohol use, or cannabis use.

Human anatomical connectivity

Main effects of group were found for anatomical connectivity between the SN/VTA seed and its target regions, the VS ($\chi^2_{(2)}$= 13.46, p= 0.0012) and vmPFC ($\chi^2_{(2)}$= 8.72, p= 0.013) (Figure 5A-B). These effects reflected connectivity reductions in $DCC^{+/-}$ carriers compared to both control groups; *i.e.,* compared to $DCC^{+/+}$ (VS*: U*= 30, p= 0.0005, *effect size(r)*= 0.60; vmPFC: U= 40, p= 0.0031, *effect size(r)*= 0.53) and UHV (VS: U= 75, p= 0.0029, *effect size(r)*=

0.48; vmPFC: U= 101.5, p= 0.034, *effect size(r)*= 0.35). Exploratory analyses identified a negative correlation between SN/VTA-hippocampus anatomical connectivity and lifetime cannabis (rho= -0.44, p= 0.019) (Figure 5C), though this association was not predicted *a priori*.

A main effect of group was detected for FA in the hippocampus ($F_{(2, 46)}$= 3.66, p= 0.034), such that FA was reduced among $DCC^{+/-}$ carriers compared to $DCC^{+/+}$ relatives (T_{46}= 2.70, p=0.0096, *effect size(d)*= 1.02) but not compared to UHV (T_{46}= 1.32, p=0.19, *effect size(d)*= 0.46) (Figure 5D). In order to investigate whole brain group differences in FA and MD, TBSS was performed among $DCC^{+/-}$ carriers, $DCC^{+/+}$ relatives, and UHV. No significant group alterations in FA or MD skeletons were detected. Similarly, no significant group differences were detected in mean FA (all ps ≥ 0.16) or mean diffusivity (all ps ≥ 0.26) within the SN/VTA, ventral striatum, vmPFC, or mPFC/ACC.

Human functional connectivity

The functional connectivity analyses did not yield statistically significant main effects of group for the SN/VTA with the *a priori* target sites. However, exploratory whole brain analyses tentatively identified other group differences within the $DCC^{+/-}$ family (FDR corrected p<0.05, and cluster size ≥540 mm^3), including decreased functional connectivity from the SN/VTA seed to the left mPFC/ACC (T_{27}= 5.02, p_{FDR}= 0.014, *effect size(d):* 1.93, peak: x= -18, y= 42, z= 9) and increased functional connectivity from the SN/VTA to the left hippocampus (T_{27}= 4.74, p_{FDR}= 0.047, *effect size(d)*: 1.82, peak: x= -24, y= -9, z= -15) in $DCC^{+/-}$participants, compared to $DCC^{+/+}$ relatives (Table 2)**.**

Human morphometry

Main effects of group were detected in the putamen ($F_{(2, 46)}$= 7.35, p= 0.0017), reflecting reduced volume in $DCC^{+/-}$ carriers compared to both control groups ($DCC^{+/+}$: T_{46}= 3.54, p=

0.0009, *effect size(d)*= 1.37; UHV: T_{46}= 2.92, p= 0.0054, *effect size(d)*= 0.93) (Figure 6A). No significant volumetric alterations between groups were detected in the nucleus accumbens, caudate nucleus, or hippocampus (Figure 6B-D).

A significant main effect of group was also observed in the vmPFC ($F_{(2, 46)}$= 3.59, p= 0.036), with increased volume among $DCC^{+/-}$ carriers compared to UHV (T_{46}= 2.53, p= 0.015, *effect size(d)*= 0.94), but there were no differences between $DCC^{+/-}$ carriers and $DCC^{+/+}$ relatives (T_{46}= 0.36, p= 0.72, *effect size(d)*= 0.12) (Figure 6E). In comparison, a significant main effect of group was detected in the mPFC/ACC ($F_{(2, 46)}$= 4.87, p= 0.012), a region detected in the functional connectivity whole-brain analysis, with the $DCC^{+/-}$ carriers exhibiting significantly increased volume, compared to both $DCC^{+/+}$ relatives (T_{46}= 2.43, p= 0.019, *effect size(d)*= 1.10) and UHV (T_{46}= 2.85, p= 0.0065, *effect size(d)*= 0.88) (Figure 6F).

Mouse morphometry

The two-way ANOVA of NAcc volumes yielded main effects of genotype and age without a genotype x age interaction ($F_{(1,25)}$= 0.04, p= 0.85). Compared to wild-type mice, *Dcc* haploinsufficient mice exhibited reduced NAcc volumes ($F_{(1,25)}$= 12.66, p= 0.0015), and this was apparent both at adolescence (T_{50}= 2.88, p= 0.0058, *effect size(d)*= 1.09) and at adulthood (T_{50}= 3.09, p= 0.003, *effect size(d)*= 1.26). The main effect of age reflected increased NAcc volumes in adulthood, relative to adolescence, for both genotypes ($F_{(1,25)}$= 16.61, p= 0.0004) (Figure 7A). There was not a significant effect of genotype in dorsal striatum ($F_{(1,25)}$= 0.84, p= 0.37), but there was an effect of age ($F_{(1,25)}$= 46.77, p< 0.0001) reflecting increased volume in adulthood, relative to adolescence (Figure 7B).

As with the NAcc, a volumetric reduction in hippocampus was detected among *Dcc* haploinsufficient, relative to wild-type mice, as evidenced by a main effect of genotype ($F_{(1,25)}$=

6.77, p= 0.015), with significant effects at adolescence (T_{50}= 2.78, p= 0.0077, *effect size(d)*= 1.05) and adulthood (T_{50} = 2.17, p= 0.035, *effect size(d)*= 0.88). Hippocampal volumes also exhibited a main effect of age ($F_{(1,25)}$ = 21.55, p< 0.0001), whereby volumes were increased in adulthood, relative to adolescence, for both genotypes. The genotype x age interaction was not significant ($F_{(1,25)}$= 0.97, p= 0.33) (Figure 7C).

There were no statistically significant effects of genotype in the cingulate-1, prelimbic, or infralimbic regions of the mPFC. However, main effects of age were identified in cingulate-1 where volumes were reduced in adulthood, relative to adolescence, for both genotypes ($F_{(1,25)}$ = 28.56, p < 0.0001). Similar trends for effects of age were detected in the prelimbic ($F_{(1,25)}$= 3.69, p= 0.066) and infralimbic ($F_{(1,25)}$= 3.55, p= 0.071) cortices (Figures 7D-F).

DISCUSSION

The study's primary findings are that humans who are haploinsufficient for the axon guidance molecule receptor gene, *DCC,* exhibited decreased mesocorticolimbic anatomical connectivity, decreased striatal volume, lower novelty seeking personality trait scores, and, more tentatively, less use of at least one addictive substance, cigarettes. Volumetric reductions seen in striatum were paralleled by strikingly similar findings in *Dcc* haploinsufficient mice.

Alterations in human mesocorticolimbic connectivity

To our knowledge, the present study provides the first evidence that *DCC* haploinsufficient humans have decreased anatomical connectivity between the SN/VTA and forebrain projection sites. This finding is consistent with results from a recent DTI study of a single individual with homozygous $DCC^{-/-}$ mutations. That study identified broad disorganization and axon reduction, including a decrease in anterior-posterior fibers (Jamuar et al., 2017). Of greater relevance for the current study, the more extensive literature with DCC-deficient mice has identified direct evidence of mesocorticolimbic specific connectivity disturbances. During adolescence, DCC receptors in mesolimbic dopamine neurons promote their targeting in the NAcc, preventing them from growing ectopically to the mPFC (Manitt et al., 2011; Manitt et al., 2013; Reynolds et al., 2018). In conditional *Dcc* haploinsufficient mice, the mesolimbic dopamine neurons are rerouted to the cingulate 1 and prelimbic portions of the pregenual mPFC (Manitt et al., 2011; Reynolds et al., 2018), concomitantly reduced dopamine varicosities in the NAcc (Reynolds et al., 2018), and diminished amphetamine-induced NAcc dopamine release (Flores et al., 2005; Grant et al., 2007). The effects of *Dcc* haploinsufficiency on non-dopamine corticolimbic-midbrain connectivity have not been explored in detail.

Functional connectivity changes between the SN/VTA and its targets in the mPFC/ACC

and hippocampus were also identified when contrasting *DCC*$^{+/-}$ carriers and their *DCC*$^{+/+}$ relatives. However, these same alterations were not observed between *DCC*$^{+/-}$ carriers and UHV. This could reflect that the *DCC*$^{+/+}$ relatives constituted a better-matched control group with shared genetic and environmental features. Moreover, the selection criteria were stricter for UHV, compared to both family groups, with volunteers excluded on the basis of psychiatric disorders including substance use disorders. This noted, since the functional connectivity alterations in the *DCC*$^{+/-}$ carriers differed from one of the two control groups only, these particular results should be interpreted with caution.

Volumetric alterations

Striatal volumetric reductions were seen in *DCC* haploinsufficient humans and mice. These striatal effects occurred ventrally in mice and more dorsally in humans. The different locus of effect might plausibly be explained by anatomical and functional differences between the species. First, in rodents there is a clear dissociation between mesolimbic (VTA to ventral striatum) and nigrostriatal (SN to dorsal striatum) pathways (Düzel et al., 2009) whereas, in humans, mesolimbic pathways originate from both VTA and SN (Düzel et al., 2009). Second, the ventral striatum comprises the NAcc and olfactory tubercle in rodents, whereas in primates it also includes ventral aspects of the putamen and caudate nucleus (Haber et al., 1990; Holt et al., 1997). Finally, the dorsal striatum, comprising the unified caudate-putamen in rodents, exists as two structures in humans (caudate nucleus and putamen) separated by the internal capsule, a bundle of fibers richly expressing DCC (Shu et al., 2000).

The NAcc volumetric reductions identified in adolescent and adult *Dcc*$^{+/-}$ mice are interesting in light of the previously reported NAcc findings including reduced dopamine fiber innervation, blunted amphetamine-induced dopamine release, and disrupted amphetamine-

induced behaviors (Hoops and Flores, 2017). Since the striatal volumetric reductions are present in adolescence, they precede the dopamine pathway alterations observed in adult, and not adolescent, *Dcc*$^{+/-}$ mice (Hoops and Flores, 2017). Since the precise etiology of these volumetric effects is unknown, they may be driven by DCC-induced alterations to either dopaminergic or non-dopaminergic neurons. Moreover, developmental changes between adolescence and adulthood were identified: striatal and hippocampal volumes increased while mPFC volumes decreased, and these effects were independent of genotype.

The human putamen effect might not be restricted to rare *DCC* mutations. Indeed, a recent large genome-wide association study in the general population (n= 30,717) found that putamen volume was influenced by four genes, including a single nucleotide polymorphism (SNP) in an intronic locus of *DCC* (Hibar et al., 2015). To our knowledge, the consequence of this SNP on the expression or function of the DCC protein is unknown. In comparison, in the present *a priori* hypothesis guided study, knowing that the mutated allele results in non-functional DCC protein (Srour et al., 2010), we have strengthened the evidence for and identified the direction of this *DCC*-associated effect on human putamen.

Personality traits, substance use, and associations with mesocorticolimbic connectivity

The low novelty seeking trait scores and low tobacco use findings among *DCC*$^{+/-}$ humans are remarkably consistent with the phenotype of adult *Dcc*$^{+/-}$ mice, which exhibit blunted stimulant drug-induced behavioral responses and reduced intracranial self-stimulation reward (Grant et al., 2007; Yetnikoff et al., 2007; Flores, 2011; Kim et al., 2013; Reynolds et al., 2016). Novelty seeking scores in the *DCC*$^{+/-}$ mutation carriers were reduced as compared to both control groups, whereas cigarette use was reduced as compared to *DCC*$^{+/+}$ relatives only. Although the lack of differences in cigarette use between *DCC*$^{+/-}$ and UHV groups diminishes the robustness

of the finding, the result is not unanticipated given that problematic tobacco and other substance use were exclusion criteria for UHV. Finally, lifetime cannabis use was negatively correlated with anatomical connectivity between the SN/VTA and hippocampus. This finding was not hypothesized *a priori,* though it might have some bearing with respect to previously reported evidence of anatomical connectivity reductions in hippocampal pathways among long-term cannabis users (Zalesky et al., 2012).

Limitations

The present study should be considered in light of the following. First, there are general limitations of diffusion MRI tractography to infer fiber pathways, including indirect measurement of axonal orientations and the challenge of resolving crossing fibers (Jones et al., 2013; Jbabdi et al., 2015). However, the tractography maps from SN/VTA accord closely with tract tracing studies in macaques (Haber, 2014) with main projections to striatum, prefrontal and limbic areas. Second, functional and diffusion MRI cannot discern the direction or neurochemistry of axonal projections, but postmortem DCC mapping studies (Harter et al., 2010; Manitt et al., 2013; Reyes et al., 2013) and the growing animal literature (Osborne et al., 2005; Manitt et al., 2010; Flores, 2011; Hoops and Flores, 2017) suggest that dopamine neurons and their post-synaptic targets are likely prominent contributors. Third, our sample size is modest (20 *DCC* mutation carriers and 36 controls). This noted, the *a priori* hypotheses were guided by an in-depth animal literature (Flores, 2011; Hoops and Flores, 2017), the haploinsufficient *DCC* mutation is known to produce non-functional DCC protein (Srour et al., 2010), and the sample size is the largest DTI study of *DCC* mutation carriers reported to date. Previous studies evaluated corticospinal pathways in seven (Marsh et al., 2017) and two carriers in another (Welniarz et al., 2017). A third study evaluated whole-brain connectivity in one carrier (Jamuar

et al., 2017). Thus, though caution is warranted as with any novel observation, we propose that the clear *a priori* hypotheses, the carefully matched samples, and the general robustness of the core findings provide some confidence.

Conclusions

We have identified in humans for the first time the effects of a mutated axon guidance receptor gene on mesocorticolimbic connectivity, terminal region volumes, and mesocorticolimbic related behaviors. Strikingly, the striatal volume reductions were seen in both *DCC*-haploinsufficient humans and mice. Together these effects of *DCC* haploinsufficiency might have implications for understanding recently reported associations between genetic variations in this axon guidance receptor and neuropsychiatric disorders (Grant et al., 2012; Manitt et al., 2013; Dunn et al., 2016; Okbay et al., 2016; Yan et al., 2016; Leday et al., 2017; Torres-Berrío et al., 2017; Ward et al., 2017; Zeng et al., 2017).

REFERENCES

Andersson JL, Jenkinson M, Smith S (2007) Non-linear registration, aka Spatial normalisation FMRIB technical report TR07JA2. FMRIB Analysis Group of the University of Oxford 2.

Bartra O, McGuire JT, Kable JW (2013) The valuation system: a coordinate-based meta-analysis of BOLD fMRI experiments examining neural correlates of subjective value. Neuroimage 76:412-427.

Behrens TE, Berg HJ, Jbabdi S, Rushworth MF, Woolrich MW (2007) Probabilistic diffusion tractography with multiple fibre orientations: What can we gain? Neuroimage 34:144-155.

Biswal BB et al. (2010) Toward discovery science of human brain function. Proceedings of the National Academy of Sciences of the United States of America 107:4734-4739.

Caseras X, Avila C, Torrubia R (2003) The measurement of individual differences in behavioural inhibition and behavioural activation systems: a comparison of personality scales. Personality and individual differences 34:999-1013.

De Fruyt F, Van De Wiele L, Van Heeringen C (2000) Cloninger's psychobiological model of temperament and character and the five-factor model of personality. Personality and individual differences 29:441-452.

Desikan RS, Ségonne F, Fischl B, Quinn BT, Dickerson BC, Blacker D, Buckner RL, Dale AM, Maguire RP, Hyman BT (2006) An automated labeling system for subdividing the human cerebral cortex on MRI scans into gyral based regions of interest. Neuroimage 31:968-980.

Dunn EC, Wiste A, Radmanesh F, Almli LM, Gogarten SM, Sofer T, Faul JD, Kardia SL, Smith JA, Weir DR (2016) Genome-wide association study (GWAS) and genome-wide by environment interaction study (GWEIS) of depressive symptoms in African American and Hispanic/Latina women. Depression and anxiety 33:265-280.

Düzel E, Bunzeck N, Guitart-Masip M, Wittmann B, Schott BH, Tobler PN (2009) Functional imaging of the human dopaminergic midbrain. Trends in neurosciences 32:321-328.

Fazeli A, Dickinson SL, Hermiston ML, Tighe RV, Steen RG, Small CG, Stoeckli ET, Keino-Masu K, Masu M, Rayburn H (1997) Phenotype of mice lacking functional Deleted in colorectal cancer (Dcc) gene. Nature 386:796.

Flores C (2011) Role of netrin-1 in the organization and function of the mesocorticolimbic dopamine system. J Psychiatry Neurosci 36:296-310.

Flores C, Manitt C, Rodaros D, Thompson K, Rajabi H, Luk K, Tritsch N, Sadikot A, Stewart J, Kennedy T (2005) Netrin receptor deficient mice exhibit functional reorganization of dopaminergic systems and do not sensitize to amphetamine. Molecular psychiatry 10:606-612.

Frank MJ, Seeberger LC, O'reilly RC (2004) By carrot or by stick: cognitive reinforcement learning in parkinsonism. Science 306:1940-1943.

Fritz CO, Morris PE, Richler JJ (2012) Effect size estimates: current use, calculations, and interpretation. Journal of experimental psychology: General 141:2.

Gad JM, Keeling SL, Wilks AF, Tan S-S, Cooper HM (1997) The expression patterns of guidance receptors, DCC and Neogenin, are spatially and temporally distinct throughout mouse embryogenesis. Developmental biology 192:258-273.

Grant A, Fathalli F, Rouleau G, Joober R, Flores C (2012) Association between schizophrenia and genetic variation in DCC: A case–control study. Schizophrenia research 137:26-31.
Grant A, Hoops D, Labelle-Dumais C, Prévost M, Rajabi H, Kolb B, Stewart J, Arvanitogiannis A, Flores C (2007) Netrin-1 receptor-deficient mice show enhanced mesocortical dopamine transmission and blunted behavioural responses to amphetamine. European Journal of Neuroscience 26:3215-3228.
Haber S, Lynd E, Klein C, Groenewegen H (1990) Topographic organization of the ventral striatal efferent projections in the rhesus monkey: an anterograde tracing study. Journal of Comparative Neurology 293:282-298.
Haber SN (2014) The place of dopamine in the cortico-basal ganglia circuit. Neuroscience 282:248-257.
Harter P, Bunz B, Dietz K, Hoffmann K, Meyermann R, Mittelbronn M (2010) Spatio-temporal deleted in colorectal cancer (DCC) and netrin-1 expression in human foetal brain development. Neuropathology and applied neurobiology 36:623-635.
Hibar DP, Stein JL, Renteria ME, Arias-Vasquez A, Desrivières S, Jahanshad N, Toro R, Wittfeld K, Abramovic L, Andersson M (2015) Common genetic variants influence human subcortical brain structures. Nature 520:224-229.
Holt DJ, Graybiel AM, Saper CB (1997) Neurochemical architecture of the human striatum. Journal of Comparative Neurology 384:1-25.
Hoops D, Flores C (2017) Making Dopamine Connections in Adolescence. Trends in Neurosciences.
Jamuar SS, Schmitz-Abe K, D'Gama AM, Drottar M, Chan W-M, Peeva M, Servattalab S, Lam A-TN, Delgado MR, Clegg NJ (2017) Biallelic mutations in human DCC cause developmental split-brain syndrome. Nature Genetics.
Jbabdi S, Sotiropoulos SN, Haber SN, Van Essen DC, Behrens TE (2015) Measuring macroscopic brain connections in vivo. Nature neuroscience 18:1546-1555.
Jenkinson M, Smith S (2001) A global optimisation method for robust affine registration of brain images. Medical image analysis 5:143-156.
Jones DK, Knösche TR, Turner R (2013) White matter integrity, fiber count, and other fallacies: the do's and don'ts of diffusion MRI. Neuroimage 73:239-254.
Keuken MC, Forstmann BU (2015) A probabilistic atlas of the basal ganglia using 7 T MRI. Data in brief 4:577-582.
Kim JH, Lavan D, Chen N, Flores C, Cooper H, Lawrence AJ (2013) Netrin-1 receptor-deficient mice show age-specific impairment in drug-induced locomotor hyperactivity but still self-administer methamphetamine. Psychopharmacology 230:607-616.
Leday GG, Vértes PE, Richardson S, Greene JR, Regan T, Khan S, Henderson R, Freeman TC, Pariante CM, Harrison NA (2017) Replicable and coupled changes in innate and adaptive immune gene expression in two case-control studies of blood microarrays in major depressive disorder. Biological Psychiatry.
Leyton M, Boileau I, Benkelfat C, Diksic M, Baker G, Dagher A (2002) Amphetamine-induced increases in extracellular dopamine, drug wanting, and novelty seeking: a PET/[11C] raclopride study in healthy men. Neuropsychopharmacology 27:1027-1035.
Livesey F, Hunt S (1997) Netrin and netrin receptor expression in the embryonic mammalian nervous system suggests roles in retinal, striatal, nigral, and cerebellar development. Molecular and Cellular Neuroscience 8:417-429.

Manitt C, Labelle-Dumais C, Eng C, Grant A, Mimee A, Stroh T, Flores C (2010) Peri-pubertal emergence of UNC-5 homologue expression by dopamine neurons in rodents. PLoS One 5:e11463.
Manitt C, Mimee A, Eng C, Pokinko M, Stroh T, Cooper HM, Kolb B, Flores C (2011) The netrin receptor DCC is required in the pubertal organization of mesocortical dopamine circuitry. The Journal of Neuroscience 31:8381-8394.
Manitt C, Eng C, Pokinko M, Ryan R, Torres-Berrio A, Lopez J, Yogendran S, Daubaras M, Grant A, Schmidt E (2013) DCC orchestrates the development of the prefrontal cortex during adolescence and is altered in psychiatric patients. Translational psychiatry 3:e338.
Marsh AP, Heron D, Edwards TJ, Quartier A, Galea C, Nava C, Rastetter A, Moutard M-L, Anderson V, Bitoun P (2017) Mutations in DCC cause isolated agenesis of the corpus callosum with incomplete penetrance. Nature Genetics 49:511-514.
Okbay A, Baselmans BM, De Neve J-E, Turley P, Nivard MG, Fontana MA, Meddens SFW, Linnér RK, Rietveld CA, Derringer J (2016) Genetic variants associated with subjective well-being, depressive symptoms, and neuroticism identified through genome-wide analyses. Nature genetics 48:624-633.
Osborne P, Halliday G, Cooper H, Keast J (2005) Localization of immunoreactivity for deleted in colorectal cancer (DCC), the receptor for the guidance factor netrin-1, in ventral tier dopamine projection pathways in adult rodents. Neuroscience 131:671-681.
Paxinos G, Franklin KB (2004) The mouse brain in stereotaxic coordinates: Gulf Professional Publishing.
Pokinko M, Moquin L, Torres-Berrío A, Gratton A, Flores C (2015) Resilience to amphetamine in mouse models of netrin-1 haploinsufficiency: role of mesocortical dopamine. Psychopharmacology 232:3719-3729.
Reyes S, Fu Y, Double KL, Cottam V, Thompson LH, Kirik D, Paxinos G, Watson C, Cooper HM, Halliday GM (2013) Trophic factors differentiate dopamine neurons vulnerable to Parkinson's disease. Neurobiology of aging 34:873-886.
Reynolds LM, Gifuni AJ, McCrea ET, Shizgal P, Flores C (2016) dcc haploinsufficiency results in blunted sensitivity to cocaine enhancement of reward seeking. Behavioural brain research 298:27-31.
Reynolds LM, Pokinko M, Berrío AT, Cuesta S, Lambert LC, Pellitero EDC, Wodzinski M, Manitt C, Krimpenfort P, Kolb B (2017) DCC receptors drive prefrontal cortex maturation by determining dopamine axon targeting in adolescence. Biological Psychiatry.
Rousseeuw PJ, Hubert M (2011) Robust statistics for outlier detection. Wiley Interdisciplinary Reviews: Data Mining and Knowledge Discovery 1:73-79.
Shu T, Valentino KM, Seaman C, Cooper HM, Richards LJ (2000) Expression of the netrin-1 receptor, deleted in colorectal cancer (DCC), is largely confined to projecting neurons in the developing forebrain. Journal of Comparative Neurology 416:201-212.
Smith SM, Nichols TE (2009) Threshold-free cluster enhancement: addressing problems of smoothing, threshold dependence and localisation in cluster inference. Neuroimage 44:83-98.
Smith SM, Jenkinson M, Johansen-Berg H, Rueckert D, Nichols TE, Mackay CE, Watkins KE, Ciccarelli O, Cader MZ, Matthews PM (2006) Tract-based spatial statistics: voxelwise analysis of multi-subject diffusion data. Neuroimage 31:1487-1505.

Srour M, Philibert M, Dion M-H, Duquette A, Richer F, Rouleau G, Chouinard S (2009) Familial congenital mirror movements: report of a large 4-generation family. Neurology 73:729-731.
Srour M, Rivière J-B, Pham JM, Dubé M-P, Girard S, Morin S, Dion PA, Asselin G, Rochefort D, Hince P (2010) Mutations in DCC cause congenital mirror movements. Science 328:592-592.
Torres-Berrío A, Lopez JP, Bagot RC, Nouel D, Dal Bo G, Cuesta S, Zhu L, Manitt C, Eng C, Cooper HM (2017) DCC confers susceptibility to depression-like behaviors in humans and mice and is regulated by miR-218. Biological psychiatry 81:306-315.
Ward J, Strawbridge RJ, Bailey ME, Graham N, Ferguson A, Lyall DM, Cullen B, Pidgeon LM, Cavanagh J, Mackay DF (2017) Genome-wide analysis in UK Biobank identifies four loci associated with mood instability and genetic correlation with major depressive disorder, anxiety disorder and schizophrenia. Translational psychiatry 7:1264.
Welniarz Q, Morel M-P, Pourchet O, Gallea C, Lamy J-C, Cincotta M, Doulazmi M, Belle M, Méneret A, Trouillard O (2017) Non cell-autonomous role of DCC in the guidance of the corticospinal tract at the midline. Scientific Reports 7:410.
Yan P, Qiao X, Wu H, Yin F, Zhang J, Ji Y, Wei S, Lai J (2016) An Association Study Between Genetic Polymorphisms in Functional Regions of Five Genes and the Risk of Schizophrenia. Journal of Molecular Neuroscience 59:366-375.
Yetnikoff L, Labelle-Dumais C, Flores C (2007) Regulation of netrin-1 receptors by amphetamine in the adult brain. Neuroscience 150:764-773.
Zalesky A, Solowij N, Yücel M, Lubman DI, Takagi M, Harding IH, Lorenzetti V, Wang R, Searle K, Pantelis C (2012) Effect of long-term cannabis use on axonal fibre connectivity. Brain 135:2245-2255.
Zeng Y, Navarro P, Fernandez-Pujals AM, Hall LS, Clarke T-K, Thomson PA, Smith BH, Hocking LJ, Padmanabhan S, Hayward C (2017) A combined pathway and regional heritability analysis indicates NETRIN1 pathway is associated with major depressive disorder. Biological psychiatry 81:336-346.

	UHV	*DCC*$^{+/+}$ relatives	*DCC*$^{+/-}$	ANOVA or $\chi 2$ p-value
N (Total)	20	16	20	
N (MRI)	19	12	18	
Age (Mean±SD)	41.8±16.0	38.3±13.2	46.2±16.0	p= 0.31
Sex (M:F)	11:9	6:10	11:9	p= 0.50
Handedness	19 right, 1 left	11 right, 3 left, 2 ambidextrous	15 right, 4 left, 1 ambidextrous	p= 0.25
Sensitivity to Punishment (Mean±SD)	6.8±4.6 (n=19)	6.9±5.5 (n=14)	8.4±5.2 (n=19)	p= 0.59
Sensitivity to Reward (Mean±SD)	9.7±3.8 (n=20)	8.1±3.1 (n=14)	9.4±4.6 (n=19)	p= 0.48
Novelty Seeking (Mean±SD)	104.8±12.3* (n=15)	104.2±11.2* (n=13)	94.9±11.2 (n=18)	p= 0.03

Table 1: **Participant characteristics.** Sample sizes, demographic characteristics, and personality traits for *DCC*$^{+/-}$ mutation carriers, *DCC*$^{+/+}$ relatives, and UHV. Asterisks (*) indicate $p \leq 0.05$ compared to *DCC*$^{+/-}$ participants.

Contrasts	Hemisphere	Brain Region	*Cluster-size* (mm^3)	*T-score*	*p*-value FDR-corr.	*Cohen's D*	*x*	*y*	*z*
$DCC^{+/-}$ >	L/R	ITG	1188	5.55	0.014	2.14	45	-12	-39
$DCC^{+/+}$	L/R	SFG/MFG	1755	5.10	0.014	1.96	18	63	30
	L	Hippocampus	540	4.74	0.047	1.82	-24	-9	-15
$DCC^{+/-}$ <	L	mPFC/ACC	729	5.02	0.014	1.93	-18	42	9
$DCC^{+/+}$	L/R	SPL/IPL	972	4.75	0.047	1.83	21	-75	51
	R	PCG	567	4.69	0.047	1.81	3	-24	72

Table 2: **Whole-brain functional connectivity differences between $DCC^{+/-}$ carriers and $DCC^{+/+}$ relatives, using the SN/VTA seed.** ITG: inferior temporal gyrus; SFG/MFG: superior frontal gyrus/middle frontal gyrus; mPFC/ACC: medial prefrontal cortex/anterior cingulate cortex; SPL/IPL: superior parietal lobule/inferior parietal lobule; PCG: precentral gyrus. **$DCC^{+/-}$ > $DCC^{+/+}$** : increased connectivity among $DCC^{+/-}$, compared to $DCC^{+/+}$. **$DCC^{+/-}$ < $DCC^{+/+}$** : decreased connectivity among $DCC^{+/-}$, compared to $DCC^{+/+}$. p values are false discovery rate (FDR) corrected and cluster size ≥540 mm^3.

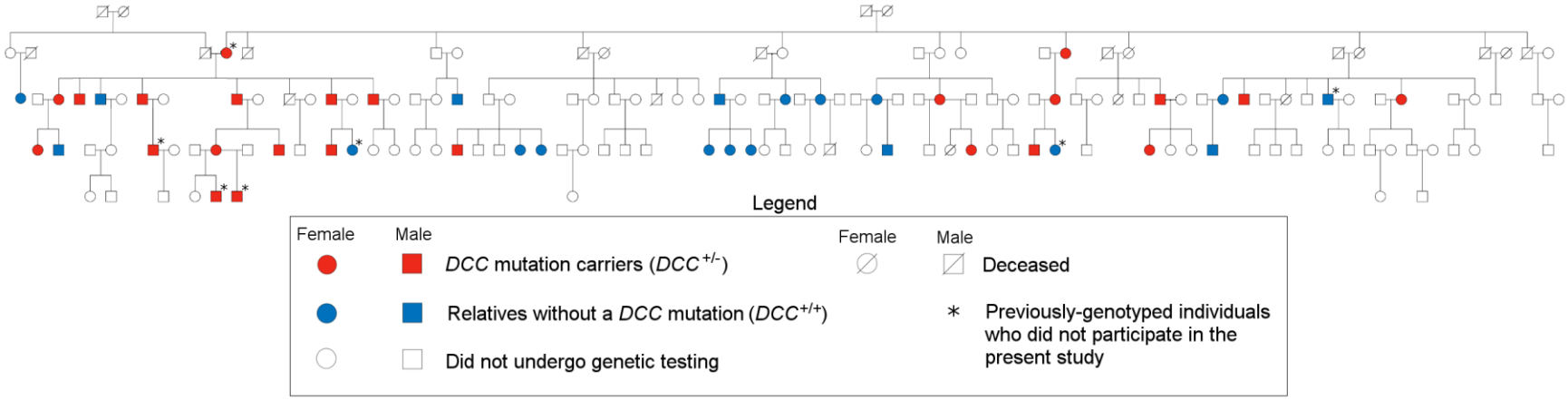

Figure 1. **Pedigree of the Quebec family.** Red indicates $DCC^{+/-}$; blue indicates $DCC^{+/+}$; white designates those who did not undergo genetic testing. Crossed lines designate deceased. Squares and circles are males and females, respectively. * indicates previously genotyped (Srour et al., 2010) individuals who did not participate in the present study.

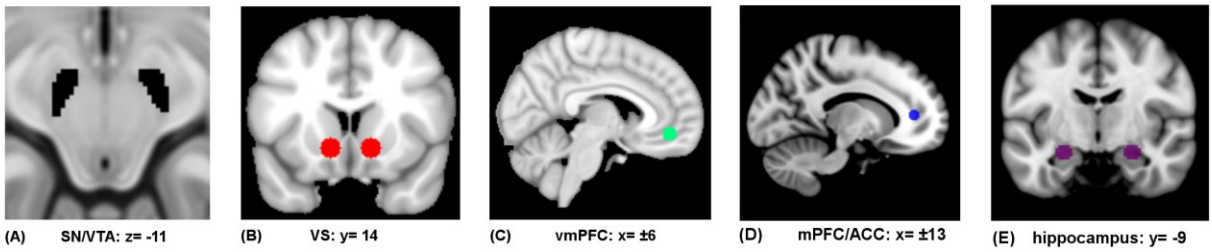

Figure 2. **Depiction of human regions of interest (ROIs): (A)** substantia nigra/ventral tegmental area (SN/VTA) (black), **(B)** ventral striatum (VS) (red), **(C)** ventral medial prefrontal cortex (vmPFC) (green), (D) medial prefrontal cortex/anterior cingulate cortex (mPFC/ACC) (blue), and **(E)** hippocampus (purple).

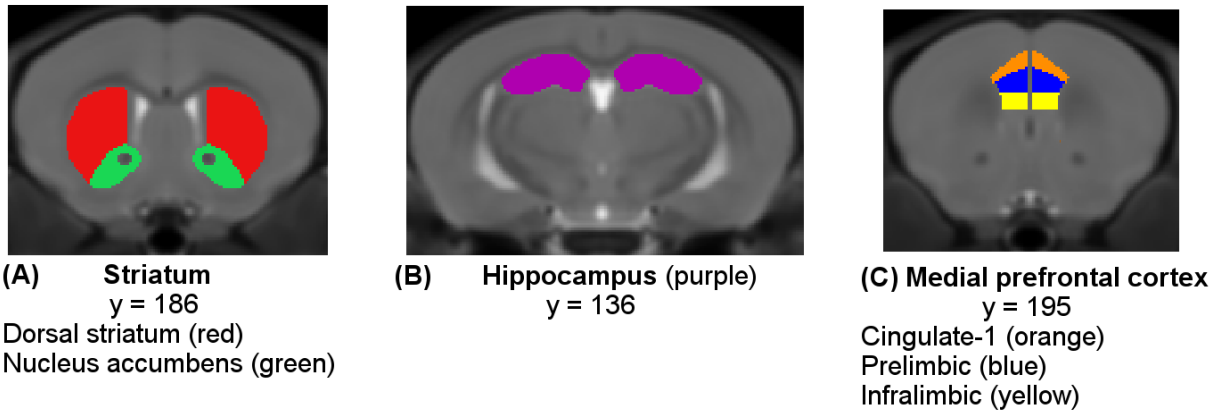

Figure 3. **Depiction of mouse regions of interest (ROIs): (A)** striatum including the nucleus accumbens (NAcc) (green) and dorsal striatum (red), **(B)** hippocampus (purple), **(C)** medial prefrontal cortex (mPFC) subregions comprising the cingulate-1 (orange), prelimbic (blue), and infralimbic (yellow).

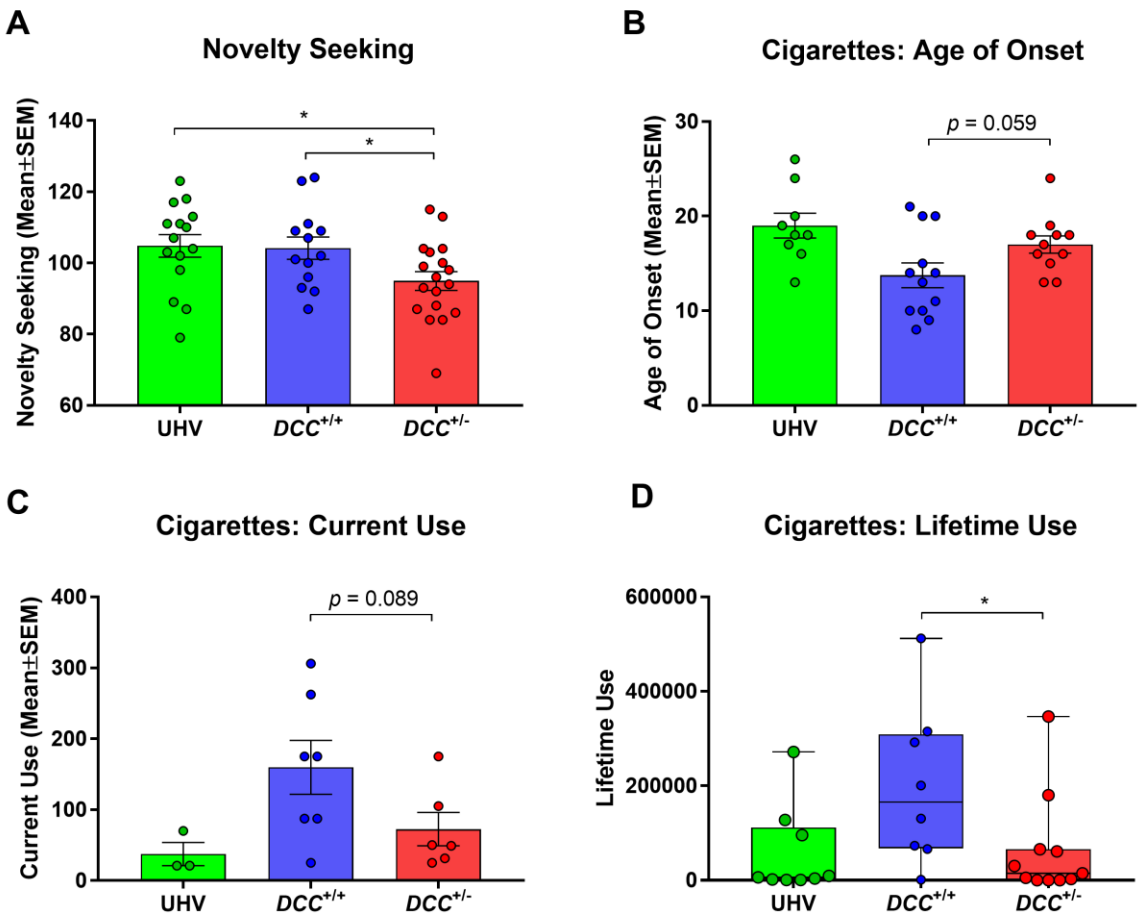

Figure 4. Personality traits and cigarette Use. Group differences in **(A)** novelty seeking, and three measures of cigarette smoking: **(B)** age of onset, **(C)** current weekly use, and **(D)** lifetime use. Because the UHV selection criteria were stricter, excluding on the basis of psychiatric disorders including tobacco and other substance use disorders, they were excluded from the cigarette analyses. * $p \leq 0.05$

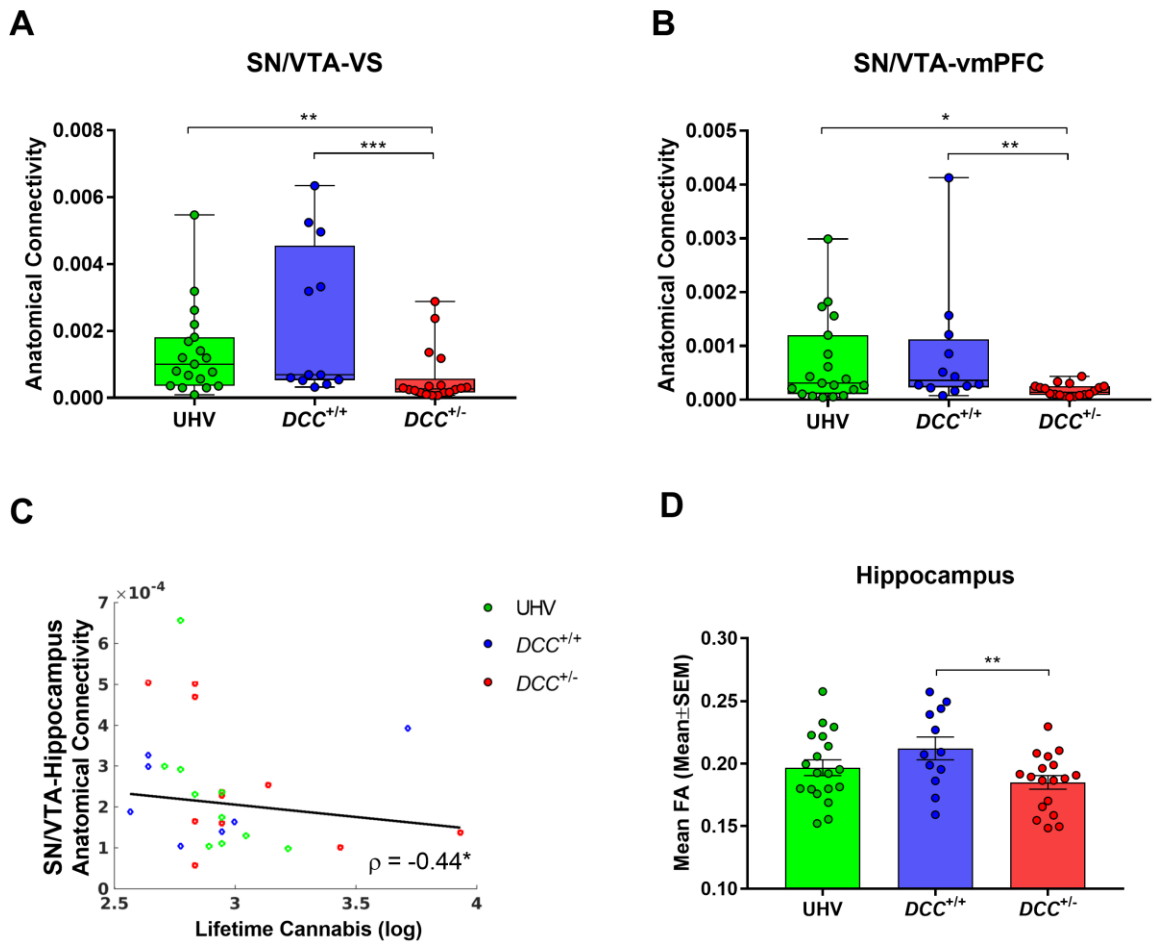

Figure 5. Diffusion tensor imaging (DTI). Group differences in anatomical connectivity with seed in SN/VTA and targets in **(A)** VS and **(B)** vmPFC. **(C)** SN/VTA-hippocampus anatomical connectivity is negatively correlated with lifetime cannabis use. **(D)** Mean fractional anisotropy (FA) in the hippocampus is reduced in *DCC*$^{+/-}$ carriers. Red circles are *DCC*$^{+/-}$, blue circles are *DCC*$^{+/+}$, and green circules are UHV. * $p \leq 0.05$, ** $p \leq 0.01$, *** $p \leq 0.001$

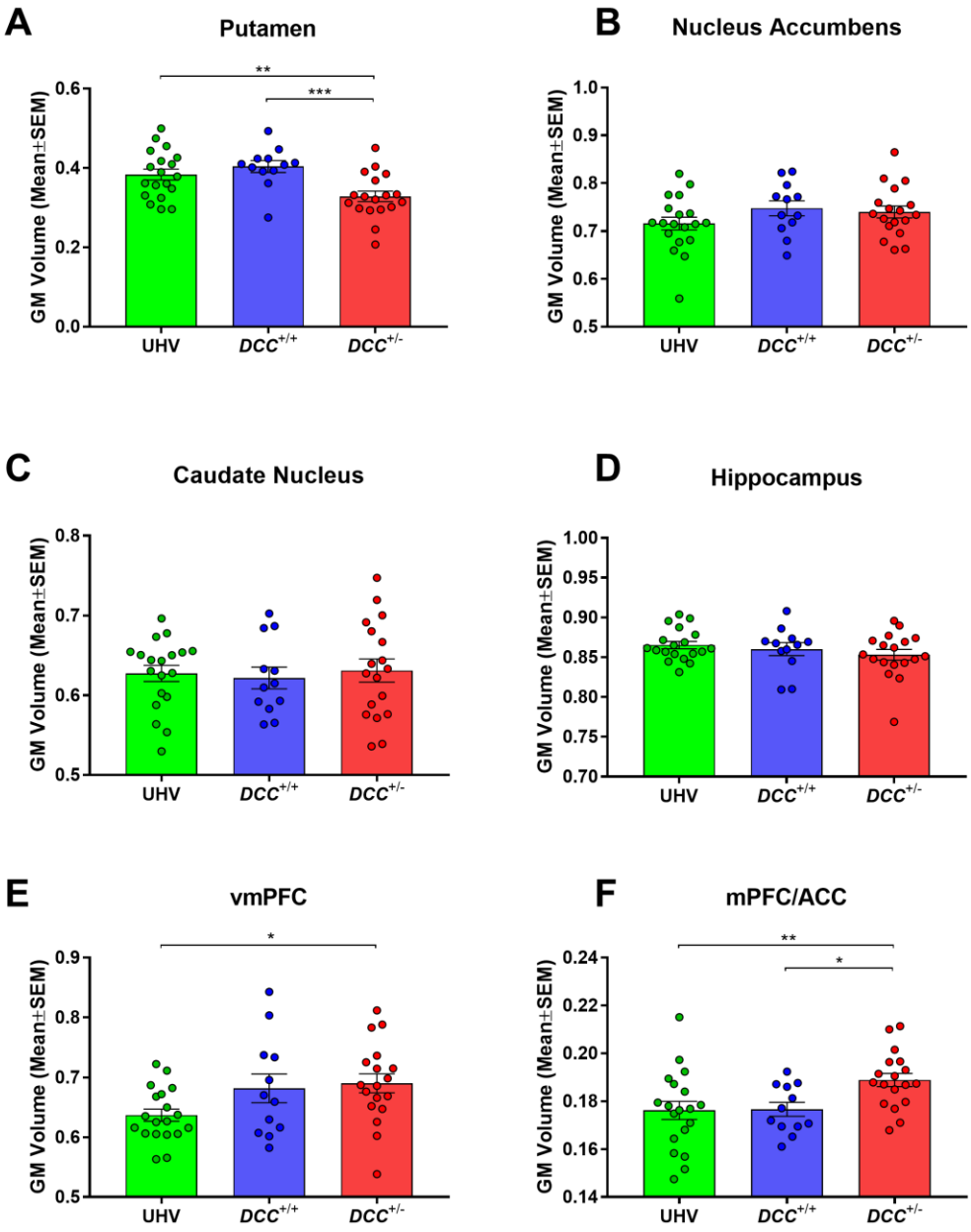

Figure 6. Human morphometry. Regional grey matter (GM) volume in *DCC*$^{+/-}$ carriers, *DCC*$^{+/+}$ relatives, and unrelated healthy volunteers (UHV). Targets identified in whole-brain voxel-based morphometry (VBM) and regions of interest comprised the **(A)** putamen, **(B)** nucleus accumbens, **(C)** caudate nucleus, **(D)** hippocampus, **(E)** ventromedial prefrontal cortex (vmPFC)**,** and **(F)** medial prefrontal cortex/anterior cingulate cortex (mPFC/ACC). * $p \leq 0.05$, ** $p \leq 0.01$, *** $p \leq 0.001$

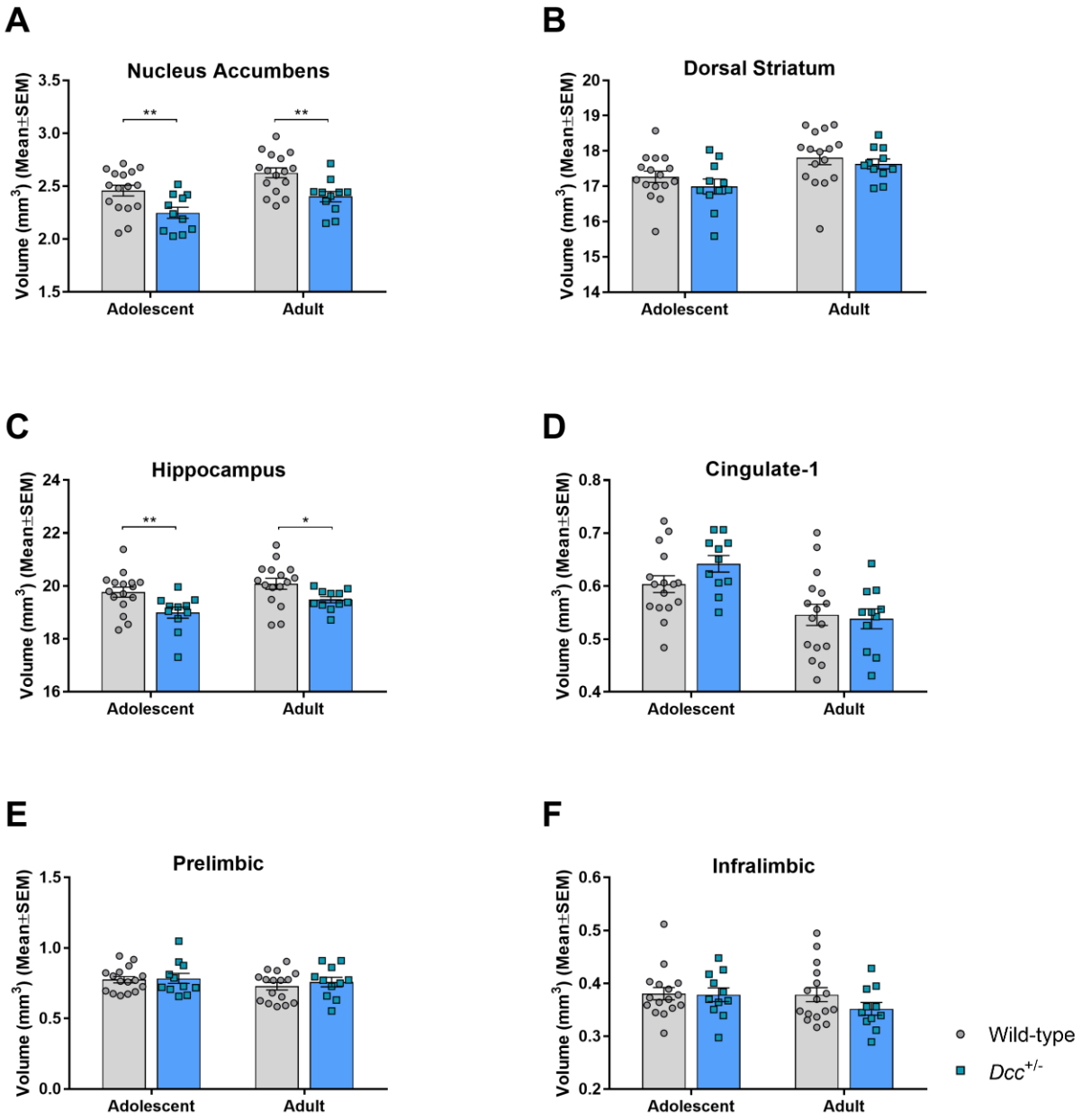

Figure 7. Mice morphometry. Regional brain volumes in *Dcc* haploinsufficient and wild-type mice, measured at adolescence and again, in the same animals, at adulthood. Regions of interest comprised the **(A)** nucleus accumbens (NAcc), **(B)** dorsal striatum, **(C)** hippocampus, and three subregions of the medial prefrontal cortex (mPFC): **(D)** cingulate-1, **(E)** prelimbic, and **(F)** infralimbic. * $p \leq 0.05$, ** $p \leq 0.01$

Chapter IV: General Discussion

The studies described in this dissertation investigated the effects of DCC on the structure, connectivity, function, and associated behaviors of the motor and mesocorticolimbic systems of the human brain. The first human *DCC* mutation was identified in the Quebec family (Srour et al., 2009; Srour et al., 2010) that has been the focus of the present neuroimaging, genetic expression, psychological, and behavioral investigations.

4.1 Summary of primary findings

In the motor system, mirror movements were associated with a dramatically increased ipsilateral corticospinal tract, increased "mirroring" motor representations, alterations in motor system functional connectivity, reduced interhemispheric inhibition, and reduced peripheral *DCC* mRNA expression. Intriguingly, both *DCC* mutation carrier subgroups, independently of mirror movements, exhibit a wide range of functional connectivity changes, in addition to reductions in corpus callosum fiber integrity. One female *DCC* mutation carrier without mirror movements exhibited partial agenesis of the corpus callosum.

The *DCC* haploinsufficient participants also exhibited multiple mesocorticolimbic alterations including strikingly reduced anatomical connectivity between the midbrain and projection sites in the ventral striatum and mPFC. These neurobiological changes were accompanied by reductions in novelty seeking traits and tobacco cigarette smoking. Applying a translational approach, both *DCC* haploinsufficient humans and mice exhibited reductions in striatal volumes. Indeed, the other findings too are in line with results from studies with transgenic *Dcc* haploinsufficient mice, which exhibit altered mesocorticolimbic connectivity, function, and related behaviors (Hoops and Flores, 2017). The present studies represent the first demonstration of these effects in humans.

4.2 Human *DCC* mRNA expression

Only mirror movements, and not the *DCC* mutation, was associated with decreased peripheral *DCC* mRNA expression, originating from both the mutated and normal alleles. These reductions might explain the partial penetrance of mirror movements. Nonetheless, neither the presence of mirror movements nor the level of peripheral *DCC* mRNA expression was related to corpus callosal white matter integrity, mesocorticolimbic anatomical connectivity, striatal or cortical volumes, tobacco cigarette smoking, or novelty seeking personality traits. In interpreting these findings, there are at least three factors worth considering. First, peripheral levels of *DCC* mRNA were measured, not brain levels. Secondly, whether reduced *DCC* mRNA levels translate into a similar reduction in functional protein remains to be established. Thirdly, *DCC* mRNA expression was measured at one time point only (adulthood), whereas *DCC* expression varies across the lifespan and is highest in the first two trimesters of embryological development (Kang et al., 2011; Hibar et al., 2015).

4.3 Mirror movements and agenesis of the corpus callosum in *DCC* mutation carriers

In the Quebec family, approximately half (20/36) of the participating family members carried a *DCC* mutation. Among the mutation carriers, approximately two-thirds (13/20) exhibited mirror movements. Moreover, 9 out of 13 of those *with* mirror movements were male, while only 2 out of 7 *DCC* mutation carriers *without* mirror movements were male. Furthermore, the only mutation carrier in the Quebec family with partial agenesis of the corpus callosum was female, and she did not express mirror movements. The increased prevalence of mirror movements among males and increased prevalence of corpus callosum agenesis among females in *DCC* mutation carriers is consistent with other reports (Marsh et al., 2017). As a possible explanation for these sex associated prevalence rates, Marsh et al. (2017) demonstrated dose-

dependent testosterone increases of *DCC* mRNA expression in neural stem cells. However, although the data appear positively skewed in 2 of the 3 groups, the authors used parametric statistics and assumed equality of variance between groups. It is unclear if non-parametric tests or data transformations to reduce positive skew would have produced the same results. Moreover, while Marsh et al. (2017) proposed that the increased agenesis of the corpus callosum among female *DCC* mutation carriers was due to decreased testosterone, resulting in diminished *DCC* expression, it begs the question of why mirror movements are more prevalent among males.

More broadly, the frequency of agenesis of the corpus callosum in the general population is 1 in 4000 (Paul et al., 2007), compared to 1 in 18 *DCC* mutation carriers in the present study who underwent an MRI. Although a single case must be treated cautiously, the finding is consistent with reports of agenesis of the corpus callosum in humans (Jamuar et al., 2017; Marsh et al., 2017) and mice (Fazeli et al., 1997; Finger et al., 2002) with *DCC* mutations. Additional, unknown genetic and environmental variables must be contributing to both callosal agenesis and mirror movements, due to the partial penetrance of these phenomena among *DCC* mutation carriers.

4.4 Neurophysiology of mirror movements

In the present investigations, unilateral TMS of the primary motor cortex induced ipsilateral movements in *DCC* mutation carriers with mirror movements in 100% of trials. The statistically simultaneous movements on the contralateral and ipsilateral sides suggest an ipsilateral corticospinal tract in *DCC* mutation carriers with mirror movements. The present findings are consistent with the extensive evidence that mirror movement individuals, across a range of precipitating causes, exhibit an ipsilateral corticospinal tract (Capaday et al., 1991;

Cohen et al., 1991; Kanouchi et al., 1997; Cincotta et al., 2002; Gallea et al., 2013). Moreover, evidence that *DCC* mutation carriers with mirror movements exhibit a functional and structural corticospinal tract has recently been reported as well (Marsh et al., 2017; Welniarz et al., 2017).

While the DTI data at the level of the pyramidal decussation in the present investigations were not of sufficient quality to assess the *structural* corticospinal tracts, other investigators have reported laterality coefficients by computing the difference between the number of crossed and uncrossed corticospinal fibers, relative to the total number of fibers (Marsh et al., 2017; Welniarz et al., 2017). Merging the results from these studies, a total of 8 control participants exhibited more crossed than uncrossed fibers, whereas 9 *DCC* mutation carriers with mirror movements exhibited more uncrossed than crossed fibers (Marsh et al., 2017; Welniarz et al., 2017). Some investigators have noted that this technique is likely to overestimate the number of uncrossed fibers, but the group comparisons remain informative since the overestimation applies equally to controls and to mutation carriers (Gallea et al., 2013). Our own data suggest that substantial individual variability is likely: approximately half of those with mirror movements exhibited greater TMS-induced contralateral MEPs, and half exhibited greater ipsilateral MEPs. Indeed, a subset of the latter individuals exhibited ipsilateral MEPs that were more than five times larger than the contralateral MEPs.

As predicted, *DCC* mutation carriers with mirror movements exhibited increased "mirroring" motor representations in the primary motor cortex and cerebellum. This is the first demonstration of these effects in *DCC* mutation carriers and the first report of greater "mirroring" cerebellar responses in those with mirror movements. In previous studies of people with mirror movements, there was evidence that passive hand movements can induce ipsilateral M1 representations similar to those observed during mirror movements (Krams et al., 1997).

These observations have raised the possibility that activations reflect sensory feedback from the unintended mirror movements rather than being the cause of the unintended movement. As a strategy to minimize this confound, in the present study each participant's arm, hand, and fingers contralateral to the voluntary movements was tightly restrained. Despite this, "mirroring" activations were still seen. When combined with the TMS-identified reductions of interhemispheric inhibition, the results are at least consistent with the proposition that mirror movements are the consequence of disinhibited unilateral activations of motor cortex.

4.4.1 Transcallosal inhibition

The corpus callosum, comprising 200-800 million fibers and interconnecting homologous cortical regions, mediates both inhibitory and excitatory signals between the cerebral hemispheres (Bloom and Hynd, 2005). In humans, the fibers of the corpus callosum begin to appear by 11-12 fetal weeks, forming a callosal commissural plate by 12-13 weeks, and exhibiting a shape similar to the adult corpus callosum by 18-20 weeks (Rakic and Yakovlev, 1968). The corpus callosum continues to expand throughout development until early adulthood, potentially reflecting continued myelination or increases in axonal size (Pujol et al., 1993; Keshavan et al., 2002). Transcallosal inhibition is absent or minimal in young children (Glocker et al., 1997; Heinen et al., 1998) and develops around age 10 (Müller et al., 1997), coinciding with the disappearance of the physiological mirror movements occasionally observed in children (Rasmussen, 1993). Consistently, in healthy adults lacking visually-apparent mirror movements, the magnitude of EMG-recorded physiological mirror movements is reduced when interhemispheric inhibition is increased (Hübers et al., 2008).

Human electrophysiological studies suggest that transcallosal inhibition is mediated by inputs to inhibitory interneurons in the primary motor cortex (Schnitzler et al., 1996). In rats,

cellular evidence indicates that the interhemispheric inhibition acts via dendritic $GABA_B$ receptors (Palmer et al., 2012). Moreover, by investigating patients with callosal lesions, it was found that the posterior third and anterior fourth segment of the corpus callosum mediate interhemispheric inhibition (Meyer et al., 1998).

The phenotype in individuals with mirror movements of reduced interhemispheric inhibition and increased ipsilateral M1 motor activations is observed in other neurological disorders. For instance, multiple sclerosis is characterized by axonal degeneration; affected individuals exhibit abnormal delays in interhemispheric inhibition, as assessed with TMS (Boroojerdi et al., 1998), and increased fMRI-measured activations in the hemisphere ipsilateral to voluntary movements, reflecting reduced inhibition of the ipsilateral motor cortex (Manson et al., 2006). Interestingly, experienced musicians, who demonstrate advanced bimanual motor coordination, exhibit reduced interhemispheric inhibition (Ridding et al., 2000) and less lateralized cortical motor outputs (Lin et al., 2002).

The motor systems of *DCC* mutation carriers *without* mirror movements had not been previously explored. In comparison to *DCC* mutation carriers with mirror movements, the *DCC* mutation alone was not associated with an ipsilateral corticospinal tract, reductions in interhemispheric inhibition, greater "mirroring" motor representations, or any evidence of increases in subtler, physiological mirror movements. However, *DCC* mutation carriers, regardless of mirror movement status, exhibited reductions in fractional anisotropy in regions of the corpus callosum that innervate motor and somatosensory areas. Fractional anisotropy alterations must be interpreted cautiously, since they could reflect changes in myelination, axonal diameter, or fiber density (Scholz et al., 2014). Nonetheless, a reduction in fiber density is plausible as reflected by the callosal agenesis in *DCC* mutation carriers (Fazeli et al., 1997;

Jamuar et al., 2017; Marsh et al., 2017) and DCC's established role in guiding commissural axons (Keino-Masu et al., 1996; Livesey and Hunt, 1997). Moreover, interhemispheric inhibition between motor hand areas is positively correlated with fractional anisotropy in hand motor fibers (Wahl et al., 2007). This is concordant with the present findings of reduced interhemispheric inhibition and fractional anisotropy in *DCC* mutation carriers with mirror movements. The absence of interhemispheric inhibition changes in mutation carriers without mirror movements might reflect compensatory changes that remain to be elucidated.

The differential effects observed here in callosal compared to corticospinal tracts might be explained by differences in DCC's function in these pathways (Welniarz et al., 2017). Surprisingly, in a mouse line bred to selectively delete DCC in the neocortex (including the corticospinal tract), there were no consequences on the crossing of the corticospinal tract, despite an absence of corticospinal tract crossing in *Dcc* "kanga" mice (Welniarz et al., 2017). This indicates that DCC expressed outside, rather than expressed within, the corticospinal tract, is critical for the development of this pathway. In contrast, DCC within commissural fibers is critical for the development of commissural pathways (Fazeli et al., 1997; Finger et al., 2002). Therefore, DCC's role in the formation of the corpus callosum might be more direct than its role in the corticospinal tract; the latter appears to be dependent upon additional factors. However, the partial penetrance of mirror movements and callosal agenesis remains unclear, and further elucidation of DCC's roles in corticospinal and callosal pathways is needed.

4.4.2 RAD51 mutation carriers with mirror movements

RAD51 plays an important role in the repair of DNA double-strand breaks (Kawabata et al., 2005). A *RAD51* mutation is also associated with mirror movements (Depienne et al., 2012). Compared to non-carriers, *RAD51* mutation carriers with mirror movements exhibit more

bilateral primary motor cortex representations, an ipsilateral corticospinal tract, and reduced interhemispheric inhibition (Gallea et al., 2013). As done here, Gallea et al., (2013) assessed interhemispheric inhibition using a relatively long interval of 40 ms between the conditioning stimulus and the test stimulus, in order to avoid confounding effects of the mirror movements. Moreover, the resting state functional connectivity between primary motor cortices was negatively correlated with the degree of interhemispheric inhibition (Gallea et al., 2013). While this does not establish causation, it suggests that abnormalities in interhemispheric inhibition may underlie bilateral motor cortex activations, thus contributing to the mirror movement phenotype. Whereas the *DCC* mutation carriers exhibited fractional anisotropy reductions in the motor and somatosensory regions of the corpus callosum, the *RAD51* mutation carriers with mirror movements exhibited increased fractional anisotropy in the hand area of the corpus callosum (Gallea et al., 2013). The increased fractional anisotropy in *RAD51* mutation carriers may represent a compensatory increase in white matter integrity, which nonetheless fails to restore normal interhemispheric inhibition or inhibit the mirror movements.

4.5 DCC and regional brain volume

4.5.1 Striatal volume

Using a translational neuroimaging approach, striatal volumetric reductions were identified in both *DCC* haploinsufficient humans and mice. Whereas the effect was specific to the putamen within the dorsal striatum in humans, the effect was localized to the NAcc of the ventral striatum in mice. The differential striatal effects are credibly explained by interspecies anatomical differences. The mesolimbic/nigrostriatal dissociation in rodents is less apparent in humans, such that fibers projecting to the ventral striatum originate from both the substantia nigra and ventral tegmental area (Düzel et al., 2009). Moreover, as distinct from rodent ventral

striatum, the primate ventral striatum includes ventral aspects of the putamen and caudate nucleus (Haber et al., 1990; Holt et al., 1997).

The reduced NAcc volumes among *Dcc* haploinsufficient mice is intriguing given the recent demonstration that these rodents exhibit diminished mesolimbic dopamine innervation (Reynolds et al., 2018). Moreover, *Dcc* haploinsufficient mice exhibit blunted amphetamine-induced dopamine release and reductions in reward-related behaviors known to depend on NAcc dopamine function (Grant et al., 2007; Flores, 2011; Pokinko et al., 2015; Hoops and Flores, 2017). Since volumetric reductions of the NAcc are already present in adolescence, they precede the alterations in dopamine connectivity and function observed only in adult *Dcc* haploinsufficient mice. It is unclear if the volumetric, connectivity, and behavioral phenotypes are causally related to one another, or whether they are each a separate consequence of the *Dcc* mutation. In the current study, mesocorticolimbic connectivity features and various behavioural features occurred in both groups of *DCC* haploinsufficient volunteers irrespective of whether they exhibited mirror movements. Further elucidation of the mechanisms underlying each of these phenotypes is needed to address this question.

The effect of reduced putamen volume among human *DCC* mutation carriers is highly consistent with a series of recent GWAS investigations. As part of the Enhancing Neuro Imaging Genetics through Meta-Analysis (ENIGMA) initiative, a GWAS of 30,717 participants investigated genetic variants associated with the volumes of seven subcortical structures (putamen, nucleus accumbens, caudate, pallidum, amygdala, thalamus, and hippocampus) (Hibar et al., 2015). Approximately half of the participants comprised the discovery sample and the other half comprised the replication sample. Genetic loci associated with putamen volume were identified in four genes: *KTN1*, *DCC*, *BCL2L1,* and *DLG2* in both the discovery and replication

cohorts. The locus identified in *DCC* (rs62097986) was in the intronic domain (Hibar et al., 2015). These GWAS findings parallel those of the present investigations, with alterations in *DCC* specifically associated with putamen volume, and not volume of the other subcortical structures. Hibar et al. (2015) computed heritability estimates, including data from 148 monozygotic and 202 dizygotic twin pairs, as well as additional siblings for a total of 1030 participants. Among the seven subcortical structures, the putamen had the highest heritability estimate (h^2= 0.89) while the heritability estimate of the nucleus accumbens was markedly lower (h^2= 0.49). Shared environmental effects were not found to significantly contribute to the goodness-of-fit of the model (Hibar et al., 2015).

Interestingly, by searching for "putamen volume" in the UK Biobank Brain Imaging Data browser (http://big.stats.ox.ac.uk/), comprising neuroimaging GWAS data from 9,707 participants (Elliott et al., 2017), a SNP (rs62098013; p= 1.6e-9) in *DCC* associated with bilateral putamen volume is detected.

Concurrent with these studies, an additional GWAS investigation identified that schizophrenia (n= 82,315) and putamen volume (n= 11,598) were both associated with an intronic locus of *DCC* (rs4632195) (Smeland et al., 2018). The risk allele for schizophrenia was associated with larger putamen volumes. Notably, by analyzing publicly available post-mortem tissue data, the authors reported that *DCC* mRNA expression was highest in the striatum, following the postnatal period. Earlier work had also identified larger putamen volumes among those with schizophrenia (Hokama et al., 1995; Okada et al., 2016). This is also consistent with genetic investigations that found associations between SNPs in *DCC* and schizophrenia (Grant et al., 2012; Yan et al., 2016). Furthermore, these authors predicted that schizophrenia was associated with increased *DCC* expression (Grant et al., 2012; Yan et al., 2016), which is

associated with increased putamen volumes (Hokama et al., 1995; Okada et al., 2016). Our findings of decreased putamen volumes among *DCC* haploinsufficient individuals, who have reduced functional DCC protein, supports this rapidly growing literature.

4.5.2 mPFC volume

Volumes of the mPFC were increased among *DCC* haploinsufficient humans, but not mice. While translational studies reveal similar functions between the primate and rodent PFC, the evidence for homologous anatomical subregions of the PFC between primates and rodents is weak (Brown and Bowman, 2002). Therefore, interspecies differences in anatomical complexity and organization of the PFC are likely contributing factors. Moreover, the mPFC volumetric finding has not been identified, to the author's knowledge, in human neuroimaging GWAS investigations. However, GWAS studies require conservative statistics given the large number of comparisons, and the effect of the *DCC* mutation on the volume of the cortex may be more pronounced than the effects of common population variants in the *DCC* gene. Therefore, caution is warranted given that the effect is not observed in GWAS studies or rodents, and efforts should be made to replicate the finding in similar human cohorts of *DCC* mutation carriers.

4.5.3 Hippocampal volume

Volumes of the hippocampus were decreased among *Dcc* haploinsufficient mice, but not humans. Although we do not have an explanation for this finding, the role of DCC in hippocampal development and function has been investigated at multiple levels of analysis. In rodents, using *in situ* hybridization, hippocampal areas CA1, CA2, and CA3 and dentate gyrus highly express *Dcc* mRNA (Livesey and Hunt, 1997; Volenec et al., 1997). Moreover, by assessing DCC protein using immunoreactivity, there is a signal in hippocampal neuronal cell bodies, although it is weak compared to the signal observed in dopamine neurons (Osborne et al.,

2005). Using subcellular fractionation and immunohistochemistry, DCC is detected in hippocampal synapses and dendritic spines (Horn et al., 2013). Moreover, selective deletion of DCC from neurons results in reduced dendritic spine lengths, impaired spatial and novel-object-recognition memory, and impaired long term potentiation (LTP) (Horn et al., 2013). DCC is implicated in hippocampal pathway development as well, such that the hippocampal commissure is absent in *Dcc* knockout mice (Fazeli et al., 1997; Finger et al., 2002) and humans with a *DCC* homozygous mutation (Jamuar et al., 2017). Moreover, both ipsilateral and contralateral hippocampal circuitry are altered in mice lacking Netrin-1 (Barallobre et al., 2000).

Although hippocampal volumetric effects were not detected among humans, increased functional connectivity between the SN/VTA and hippocampus was observed among *DCC* mutation carriers, compared to their relatives. Moreover, hippocampal white matter integrity reductions were observed among the human *DCC* mutation carriers, consistent with DCC's role in hippocampal circuitry (Barallobre et al., 2000).

4.5.4 DCC and apoptosis

The volumetric changes we report might be related to the evidence that in the absence of Netrin-1, DCC induces apoptosis by serving as a caspase substrate (Mehlen et al., 1998). Consistently, in Netrin-1 knockouts *in vivo*, apoptosis is increased in DCC-expressing cells during neurodevelopment (Llambi et al., 2001). Interestingly, *Dcc* homozygous knockout mice also exhibit increased cell death in the locus coeruleus (Shi et al., 2008) and retina (Shi et al., 2010), suggesting that DCC can also contribute to cell survival. Moreover, among adult *Dcc* haploinsufficient mice, there is a reduction of dopamine neurons in the VTA and SN (Flores et al., 2005). While consequences of human *DCC* mutations on apoptosis or cell survival have not

been directly demonstrated, this is a credible possibility given the role of DCC in these processes.

4.6 DCC and mesocorticolimbic connectivity

For the first time, altered mesocorticolimbic anatomical connectivity has been identified in *DCC* haploinsufficient humans. This is strikingly in line with studies revealing mesocorticolimbic connectivity alterations in *Dcc* mutant rodents (Hoops and Flores, 2017). Whereas mesolimbic connectivity is diminished in humans and mice with a *DCC* mutation, mesocortical connectivity is increased in mice and reduced in humans with a *DCC* mutation. Importantly, the rodent work specifically examined dopamine fibers in these pathways whereas the MRI methodologies employed in the present human work cannot discern the underlying neurochemistry in these pathways. Since mesocorticolimbic pathways contain dopamine, gamma-Aminobutyric acid (GABA) and glutamate axons (Morales and Pickel, 2012), the human anatomical connectivity findings are plausibly the result of alterations to both dopaminergic and non-dopaminergic axons.

In rodents, dopamine axons express relatively high DCC expression in the NAcc and only rarely express DCC in the mPFC (Manitt et al., 2011). Conversely, Netrin-1 expression is low in the NAcc but relatively high Netrin-1 in the mPFC (Manitt et al., 2011). Therefore, dopamine axons expressing high levels of DCC appear more attracted to regions with lower levels of Netrin-1, and vice-versa. In the case of *DCC* haploinsufficiency, since DCC expression is reduced, dopamine axons originating in the VTA express lower levels of DCC, therefore failing to remain in the NAcc and instead, continue to grow ectopically into the mPFC during adolescence (Hoops and Flores, 2017). With regard to the human *DCC* mutation carriers with reduced mesolimbic and mesocortical anatomical connectivity, it may be that fewer axons are

innervating the ventral striatum, and these fibers are projecting ectopically, but to a wider range of brain regions, compared to the rodents.

4.7 DCC, personality, and behaviors

The present investigations revealed that *DCC* haploinsufficient humans have a behavioral phenotype that is remarkably consistent with that of *Dcc* haploinsufficient mice. Adult *Dcc* haploinsufficient mice exhibit diminished sensitivity to stimulant drugs and fail to exhibit amphetamine-induced behavioral sensitization (Flores, 2011; Hoops and Flores, 2017). In comparison, there are no differences in conditioned place preference to morphine or ethanol between *Dcc* haploinsufficient mice and controls (Personal Communication; CF). As a potential parallel, the *DCC* haploinsufficient humans smoke less tobacco, but they do not use less alcohol or cannabis, consistent with the evidence in mice that DCC's effects are specific to stimulant drugs.

The present work also identified reduced novelty seeking among *DCC* haploinsufficient humans. Although this was the only personality trait to differ in the *DCC* mutation carriers, the result was not unanticipated. DCC-deficient mice, compared to controls, exhibit reduced impulsivity (Reynolds et al., 2018) and attend less to a novel object in the presence of a familiar object (Horn et al., 2013). Diminished novelty seeking is associated with reduced stimulant drug-induced dopamine release in the ventral striatum of humans (Leyton et al., 2002) and rodents (Hooks et al., 1991). These findings are in accordance with the blunted amphetamine-induced dopamine release in the NAcc of *Dcc* haploinsufficient mice (Grant et al., 2007).

4.8 Neuropsychiatric disorders

There is growing evidence of associations between genetic variants in *DCC* and psychiatric disorders including schizophrenia and depression (Grant et al., 2012; Manitt et al.,

2013; Dunn et al., 2016; Okbay et al., 2016; Yan et al., 2016; Torres-Berrío et al., 2017; Ward et al., 2017; Zeng et al., 2017; Leday et al., 2018; Smeland et al., 2018; Wray et al., 2018). The altered mesocorticolimbic connectivity in *DCC* mutation carriers is a potential explanation of these associations, given that mesocorticolimbic connectivity alterations are associated with schizophrenia (Horga et al., 2016) and depression (Harrison et al., 2009; Furman et al., 2011; Felger et al., 2016). Interestingly, whereas the human *DCC* mutation carriers exhibited increases in volumes of the prefrontal cortex and decreases in volumes of the putamen, patients with schizophrenia exhibit the converse: volumetric decreases in the prefrontal cortex (Breier et al., 1992; Ohtani et al., 2014; Pillai et al., 2015) and increases in the putamen (Hokama et al., 1995; Okada et al., 2016). In depression, there are numerous reports of decreases in putamen volume (Parashos et al.; Husain et al., 1991; Koolschijn et al., 2009; Pan et al., 2009; Arnone et al., 2012; Sachs-Ericsson et al., 2017) although some other groups have failed to replicate this finding (Lenze and Sheline, 1999; Schmaal et al., 2016). Moreover, several studies have identified volumetric reductions among depressed patients in the prefrontal cortex (Botteron et al.; Frodl et al.; Koolschijn et al., 2009; Schmaal et al., 2017).

Recently, a UK Biobank study (n= ~6400) found that SNPs in the Netrin-1 signalling pathway, conferring risk for major depression, were associated with altered white matter microstructure in thalamic radiations, namely lower fractional anisotropy and higher mean diffusivity (Barbu et al., 2018). This might reflect a role of Netrin-1 in the development of thalamocortical circuitry, which projects from the dorsal thalamus to the neocortex (Braisted et al., 2000). Important for the interpretation of the present findings of altered mesocorticolimbic connectivity, tractography studies indicate that the thalamus and striatum are highly interconnected (Draganski et al., 2008).

Moreover, given DCC's role in the development of the corpus callosum, it is notable that patients with schizophrenia exhibit reductions in the size and fractional anisotropy of the corpus callosum (Woodruff et al., 1995; Foong et al., 2000; Balevich et al., 2015; Grazioplene et al., 2017). Additionally, enlargement of the corpus callosum has been reported in depression (Wu et al., 1993), although one study only detected this effect in familial depression (Lacerda et al., 2005). Finally, some authors have reported that patients with depression exhibit reduced fractional anisotropy of the corpus callosum (Nobuhara et al., 2006; Kieseppä et al., 2010; Korgaonkar et al., 2011), although others did not find these effects (Brambilla et al., 2004; Bae et al., 2006), while one group found a trend-level effect ($p= 0.068$) and was plausibly underpowered (patients: $n= 31$; controls: $n= 15$) (Yang et al., 2007).

4.8.1 Brain lateralization

Investigations of *DCC* mutation carriers and mirror movements have provided a rare opportunity to investigate altered brain lateralization, whereby corticospinal tracts and motor representations were more bilateral and accompanied by reduced interhemispheric inhibition. Given *DCC*'s association with schizophrenia and depression, it is worth considering studies of altered brain lateralization in these disorders. Intriguingly, there is evidence that patients with schizophrenia exhibit reduced interhemispheric inhibition (Fitzgerald et al., 2002), reduced lateralization of the sensory motor cortex (Bertolino et al., 2004) and of language processing (Sommer et al., 2001), as well as altered lateralization of subcortical regional brain volumes (Okada et al., 2016). Moreover, verbal and non-verbal perceptual tasks identified evidence of abnormal brain lateralization among groups with various diagnostic subtypes of depression, compared to control participants (Bruder et al., 1989). Therefore, while further investigations are

certainly required, DCC's effect on brain lateralization might be important for the development of various psychopathologies.

4.8.2 Parkinson's disease

The present findings might have implications for understanding Parkinson's, a dopaminergic neurodegenerative disease that gives rise to both motor and neuropsychiatric symptoms. The motor features include tremor, rigidity, slowness of movement, and, in some cases, mirror movements (Espay et al., 2005; Cincotta et al., 2006; Li et al., 2007). In a study of asymmetric Parkinson's disease, nearly 90% of patients exhibited mirror movements in the less affected limb, when voluntary actions were performed with the more affected limb (Espay et al., 2005). Moreover, TMS investigations revealed that mirror movements among Parkinson's disease patients were associated with increased motor output from the ipsilateral motor cortex and reduced interhemispheric inhibition, but not with an ipsilateral corticospinal tract (Cincotta et al., 2006; Li et al., 2007). Common neuropsychiatric symptoms of Parkinson's disease, with respective prevalence rates among patients, include major depression (10-30%), hallucinations (40-50%), delusions (5-10%), apathy (17-70%), and anxiety disorders (30-40%) (Aarsland et al., 2009). Moreover, Parkinson's disease patients exhibit reductions in novelty seeking (Menza et al., 1993; Tomer and Aharon-Peretz, 2004). Novelty seeking in this patient population is negatively associated with dopamine D_2 receptor availability (Kaasinen et al., 2004). This is similar to the reduced novelty seeking observed here among the human *DCC* mutation carriers, who are predicted to exhibit blunted striatal dopamine release, based on the *Dcc* mutant rodent findings (Grant et al., 2007).

Due to the expression of DCC and Netrin-1 in nigral and striatal dopamine neurons, researchers have previously proposed that these guidance cues may have an important role in the

etiology of Parkinson's disease (Livesey and Hunt, 1997). Consistent with this, SNPs in *DCC* (rs17468382) are predictive of Parkinson's disease susceptibility (Lesnick et al., 2007). Other Netrin-1 receptor genes belonging to the *UNC5* family were also associated with these measures, in addition to being differentially expressed in the putamen and caudate nucleus (Lesnick et al., 2007). Finally, variability in *DCC* expression may confer vulnerability for Parkinson's disease by reducing putamen volume, a volumetric feature found among early and advanced Parkinson's patients (Geng et al., 2006).

4.9 Conclusions

The *in vivo* neuroimaging studies described here in human *DCC* mutation carriers have contributed two main findings. First and foremost, they have documented that an axon guidance receptor accounts for substantial variability in human brain neurodevelopment and wiring, including the guidance of callosal, corticospinal, and mesocorticolimbic pathways. Since mesocorticolimbic connectivity and striatal volumes are altered in psychiatric disorders, this work also potentially identifies neural mechanisms that underlie the association between variants in the *DCC* gene and neuropsychiatric disorders.

References: General Introduction and Discussion

Aarsland D, Marsh L, Schrag A (2009) Neuropsychiatric symptoms in Parkinson's disease. Movement Disorders 24:2175-2186.

Ahmed I, Mittal K, Sheikh TI, Vasli N, Rafiq MA, Mikhailov A, Ohadi M, Mahmood H, Rouleau GA, Bhatti A, Ayub M, Srour M, John P, Vincent JB (2014) Identification of a homozygous splice site mutation in the dynein axonemal light chain 4 gene on 22q13.1 in a large consanguineous family from Pakistan with congenital mirror movement disorder. Hum Genet 133:1419-1429.

Arias-Carrión O, Stamelou M, Murillo-Rodríguez E, Menéndez-González M, Pöppel E (2010) Dopaminergic reward system: a short integrative review. International archives of medicine 3:24.

Arnone D, McIntosh AM, Ebmeier KP, Munafò MR, Anderson IM (2012) Magnetic resonance imaging studies in unipolar depression: Systematic review and meta-regression analyses. European Neuropsychopharmacology 22:1-16.

Auger ML, Schmidt ER, Manitt C, Dal-Bo G, Pasterkamp RJ, Flores C (2013) unc5c haploinsufficient phenotype: striking similarities with the dcc haploinsufficiency model. The European journal of neuroscience 38:2853-2863.

Bae JN, MacFall JR, Krishnan KRR, Payne ME, Steffens DC, Taylor WD (2006) Dorsolateral prefrontal cortex and anterior cingulate cortex white matter alterations in late-life depression. Biological psychiatry 60:1356-1363.

Balevich EC, Haznedar MM, Wang E, Newmark RE, Bloom R, Schneiderman JS, Aronowitz J, Tang CY, Chu K-W, Byne W (2015) Corpus callosum size and diffusion tensor anisotropy in adolescents and adults with schizophrenia. Psychiatry Research: Neuroimaging 231:244-251.

Barallobre MJ, Pascual M, Del Rio JA, Soriano E (2005) The Netrin family of guidance factors: emphasis on Netrin-1 signalling. Brain research Brain research reviews 49:22-47.

Barallobre MJ, Del Rio JA, Alcantara S, Borrell V, Aguado F, Ruiz M, Carmona MA, Martin M, Fabre M, Yuste R, Tessier-Lavigne M, Soriano E (2000) Aberrant development of hippocampal circuits and altered neural activity in netrin 1-deficient mice. Development 127:4797-4810.

Barbu MC, Zeng Y, Shen X, Cox S, Clarke T, Gibson J, Adams MJ, Johnstone M, Haley CS, Lawrie SM (2018) Association of whole-genome and NETRIN1 signaling pathway-derived polygenic risk scores for Major Depressive Disorder and thalamic radiation white matter microstructure in UK Biobank. bioRxiv:282053.

Beaulé V, Tremblay S, Théoret H (2012) Interhemispheric control of unilateral movement. Neural plasticity 2012.

Bertolino A, Blasi G, Caforio G, Latorre V, De Candia M, Rubino V, Callicott JH, Mattay VS, Bellomo A, Scarabino T, Weinberger DR, Nardini M (2004) Functional lateralization of the sensorimotor cortex in patients with schizophrenia: effects of treatment with olanzapine. Biological Psychiatry 56:190-197.

Bloom JS, Hynd GW (2005) The role of the corpus callosum in interhemispheric transfer of information: excitation or inhibition? Neuropsychology review 15:59-71.

Boroojerdi B, Hungs M, Mull M, Töpper R, Noth J (1998) Interhemispheric inhibition in patients with multiple sclerosis. Electroencephalography and Clinical Neurophysiology/Electromyography and Motor Control 109:230-237.

Botteron KN, Raichle ME, Drevets WC, Heath AC, Todd RD Volumetric reduction in left subgenual prefrontal cortex in early onset depression. Biological Psychiatry 51:342-344.
Bouilly J et al. (2018) DCC/NTN1 complex mutations in patients with congenital hypogonadotropic hypogonadism impair GnRH neuron development. Human Molecular Genetics 27:359-372.
Braisted JE, Catalano SM, Stimac R, Kennedy TE, Tessier-Lavigne M, Shatz CJ, O'Leary DDM (2000) Netrin-1 Promotes Thalamic Axon Growth and Is Required for Proper Development of the Thalamocortical Projection. The Journal of Neuroscience 20:5792-5801.
Brambilla P, Nicoletti M, Sassi R, Mallinger A, Frank E, Keshavan M, Soares J (2004) Corpus callosum signal intensity in patients with bipolar and unipolar disorder. Journal of Neurology, Neurosurgery & Psychiatry 75:221-225.
Breier A, Buchanan RW, Elkashef A, Munson RC, Kirkpatrick B, Gellad F (1992) Brain morphology and schizophrenia: A magnetic resonance imaging study of limbic, prefrontal cortex, and caudate structures. Archives of General Psychiatry 49:921-926.
Broome MR, Saunders KEA, Harrison PJ, Marwaha S (2015) Mood instability: significance, definition and measurement. The British Journal of Psychiatry 207:283-285.
Brown VJ, Bowman EM (2002) Rodent models of prefrontal cortical function. Trends in neurosciences 25:340-343.
Bruder GE, Quitkin FM, Stewart JW, Martin C, Voglmaier MM, Harrison WM (1989) Cerebral laterality and depression: differences in perceptual asymmetry among diagnostic subtypes. Journal of abnormal psychology 98:177.
Buckholtz JW, Treadway MT, Cowan RL, Woodward ND, Li R, Ansari MS, Baldwin RM, Schwartzman AN, Shelby ES, Smith CE, Kessler RM, Zald DH (2010) Dopaminergic Network Differences in Human Impulsivity. Science 329:532-532.
Capaday C, Forget R, Fraser R, Lamarre Y (1991) Evidence for a contribution of the motor cortex to the long-latency stretch reflex of the human thumb. The Journal of Physiology 440:243-255.
Carr DB, Sesack SR (2000) Projections from the rat prefrontal cortex to the ventral tegmental area: target specificity in the synaptic associations with mesoaccumbens and mesocortical neurons. The Journal of neuroscience : the official journal of the Society for Neuroscience 20:3864-3873.
Chan S-Y, Zheng H, Su M-W, Wilk R, Killeen M, Hedgecock E, Culotti J (1996) UNC-40, a C. elegans homolog of DCC (Deleted in Colorectal Cancer), is required in motile cells responding to UNC-6 netrin cues. Cell 87:187-195.
Chau DT, Roth RM, Green AI (2004) The neural circuitry of reward and its relevance to psychiatric disorders. Current psychiatry reports 6:391-399.
Cho KR, Oliner JD, Simons JW, Hedrick L, Fearon ER, Preisinger AC, Hedge P, Silverman GA, Vogelstein B (1994) The DCC gene: structural analysis and mutations in colorectal carcinomas. Genomics 19:525-531.
Cincotta M, Borgheresi A, Boffi P, Vigliano P, Ragazzoni A, Zaccara G, Ziemann U (2002) Bilateral motor cortex output with intended unimanual contraction in congenital mirror movements. Neurology 58:1290-1293.
Cincotta M, Borgheresi A, Balestrieri F, Giovannelli F, Ragazzoni A, Vanni P, Benvenuti F, Zaccara G, Ziemann U (2006) Mechanisms underlying mirror movements in Parkinson's disease: a transcranial magnetic stimulation study. Movement disorders 21:1019-1025.

Cohen L, Meer J, Tarkka I, Bierner S, Leiderman D, Dubinsky R, Sanes J, Jabbari B, Branscum B, Hallett M (1991) Congenital mirror movements: abnormal organization of motor pathways in two patients. Brain 114:381-403.
da Silva RV, Johannssen HC, Wyss MT, Roome RB, Bourojeni FB, Stifani N, Marsh AP, Ryan MM, Lockhart PJ, Leventer RJ (2018) DCC Is Required for the Development of Nociceptive Topognosis in Mice and Humans. Cell reports 22:1105-1114.
de la Torre JR, Höpker VH, Ming G-l, Poo M-m, Tessier-Lavigne M, Hemmati-Brivanlou A, Holt CE (1997) Turning of retinal growth cones in a netrin-1 gradient mediated by the netrin receptor DCC. Neuron 19:1211-1224.
De Vries M, Cooper HM (2008) Emerging roles for neogenin and its ligands in CNS development. Journal of neurochemistry 106:1483-1492.
Dent EW, Gupton SL, Gertler FB (2011) The Growth Cone Cytoskeleton in Axon Outgrowth and Guidance. Cold Spring Harbor perspectives in biology 3:a001800.
Depienne C, Cincotta M, Billot S, Bouteiller D, Groppa S, Brochard V, Flamand C, Hubsch C, Meunier S, Giovannelli F (2011) A novel DCC mutation and genetic heterogeneity in congenital mirror movements. Neurology 76:260-264.
Depienne C, Bouteiller D, Méneret A, Billot S, Groppa S, Klebe S, Charbonnier-Beaupel F, Corvol J-C, Saraiva J-P, Brueggemann N (2012) RAD51 haploinsufficiency causes congenital mirror movements in humans. The American Journal of Human Genetics 90:301-307.
Dickson BJ (2002) Molecular mechanisms of axon guidance. Science 298:1959-1964.
Drachman DA (2005) Do we have brain to spare? Neurology 64:2004-2005.
Draganski B, Kherif F, Klöppel S, Cook PA, Alexander DC, Parker GJM, Deichmann R, Ashburner J, Frackowiak RSJ (2008) Evidence for Segregated and Integrative Connectivity Patterns in the Human Basal Ganglia. The Journal of Neuroscience 28:7143-7152.
Duman-Scheel M (2012) Deleted in Colorectal Cancer (DCC) Pathfinding: Axon Guidance Gene Finally Turned Tumor Suppressor. Current drug targets 13:1445-1453.
Dunn EC, Wiste A, Radmanesh F, Almli LM, Gogarten SM, Sofer T, Faul JD, Kardia SL, Smith JA, Weir DR (2016) Genome-wide association study (GWAS) and genome-wide by environment interaction study (GWEIS) of depressive symptoms in African American and Hispanic/Latina women. Depression and anxiety 33:265-280.
Düzel E, Bunzeck N, Guitart-Masip M, Wittmann B, Schott BH, Tobler PN (2009) Functional imaging of the human dopaminergic midbrain. Trends in neurosciences 32:321-328.
Elliott L, Sharp K, Alfaro-Almagro F, Douaud G, Miller K, Marchini J, Smith S (2017) The genetic basis of human brain structure and function: 1,262 genome-wide associations found from 3,144 GWAS of multimodal brain imaging phenotypes from 9,707 UK Biobank participants. bioRxiv.
Espay A, Li J, Johnston L, Chen R, Lang A (2005) Mirror movements in parkinsonism: evaluation of a new clinical sign. Journal of Neurology, Neurosurgery & Psychiatry 76:1355-1359.
Farmer S, Ingram D, Stephens J (1990) Mirror movements studied in a patient with Klippel-Feil syndrome. The Journal of physiology 428:467-484.
Fazeli A, Dickinson SL, Hermiston ML, Tighe RV, Steen RG, Small CG, Stoeckli ET, Keino-Masu K, Masu M, Rayburn H, Simons J, Bronson RT, Gordon JI, Tessier-Lavigne M,

Weinberg RA (1997) Phenotype of mice lacking functional Deleted in colorectal cancer (Dcc) gene. Nature 386:796-804.
Felger JC, Li Z, Haroon E, Woolwine BJ, Jung MY, Hu X, Miller AH (2016) Inflammation is associated with decreased functional connectivity within corticostriatal reward circuitry in depression. Molecular psychiatry 21:1358.
Ferbert A, Priori A, Rothwell J, Day B, Colebatch J, Marsden C (1992) Interhemispheric inhibition of the human motor cortex. The Journal of physiology 453:525-546.
Finci LI, Krüger N, Sun X, Zhang J, Chegkazi M, Wu Y, Schenk G, Mertens HDT, Svergun DI, Zhang Y, Wang J-h, Meijers R (2014) The crystal structure of netrin-1 in complex with DCC reveals the bi-functionality of netrin-1 as a guidance cue. Neuron 83:839-849.
Finger JH, Bronson RT, Harris B, Johnson K, Przyborski SA, Ackerman SL (2002) The netrin 1 receptors Unc5h3 and Dcc are necessary at multiple choice points for the guidance of corticospinal tract axons. Journal of Neuroscience 22:10346-10356.
Fitzgerald PB, Brown TL, Daskalakis ZJ, deCastella A, Kulkarni J (2002) A study of transcallosal inhibition in schizophrenia using transcranial magnetic stimulation. Schizophrenia Research 56:199-209.
Flores C (2011) Role of netrin-1 in the organization and function of the mesocorticolimbic dopamine system. J Psychiatry Neurosci 36:296-310.
Flores C, Manitt C, Rodaros D, Thompson KM, Rajabi H, Luk KC, Tritsch NX, Sadikot AF, Stewart J, Kennedy TE (2005) Netrin receptor deficient mice exhibit functional reorganization of dopaminergic systems and do not sensitize to amphetamine. Mol Psychiatry 10:606-612.
Foong J, Maier M, Clark C, Barker G, Miller D, Ron M (2000) Neuropathological abnormalities of the corpus callosum in schizophrenia: a diffusion tensor imaging study. Journal of Neurology, Neurosurgery & Psychiatry 68:242-244.
Forget R, Boghen D, Attig E, Lamarre Y (1986) Electromyographic studies of congenital mirror movements. Neurology 36:1316-1316.
Frank MJ, Seeberger LC, O'reilly RC (2004) By carrot or by stick: cognitive reinforcement learning in parkinsonism. Science 306:1940-1943.
Franz EA, Chiaroni-Clarke R, Woodrow S, Glendining KA, Jasoni CL, Robertson SP, Gardner RM, Markie D (2015) Congenital mirror movements: phenotypes associated with DCC and RAD51 mutations. Journal of the neurological sciences 351:140-145.
Frodl T, Reinhold E, Koutsouleris N, Reiser M, Meisenzahl EM Interaction of childhood stress with hippocampus and prefrontal cortex volume reduction in major depression. Journal of Psychiatric Research 44:799-807.
Furman DJ, Hamilton JP, Gotlib IH (2011) Frontostriatal functional connectivity in major depressive disorder. Biology of mood & anxiety disorders 1:11.
Gad JM, Keeling SL, Wilks AF, Tan S-S, Cooper HM (1997) The expression patterns of guidance receptors, DCC and Neogenin, are spatially and temporally distinct throughout mouse embryogenesis. Developmental biology 192:258-273.
Gallea C, Popa T, Hubsch C, Valabregue R, Brochard V, Kundu P, Schmitt B, Bardinet E, Bertasi E, Flamand-Roze C (2013) RAD51 deficiency disrupts the corticospinal lateralization of motor control. Brain:awt258.
Geng D-y, Li Y-X, Zee C-S (2006) Magnetic Resonance Imaging-Based Volumetric Analysis of Basal Ganglia Nuclei and Substantia Nigra in Patients with Parkinson's Disease. Neurosurgery 58:256-262.

Glocker FX, Heinen F, Fietzek U, Meyer B-U, Korinthenberg R, Lücking CH (1997) Focal transcranial magnetic stimulation: complete lack of transcallosal inhibition in children. Electroencephalography and Clinical Neurophysiology 1:64-65.
Grant A, Speed Z, Labelle-Dumais C, Flores C (2009) Post-pubertal emergence of a dopamine phenotype in netrin-1 receptor-deficient mice. The European journal of neuroscience 30:1318-1328.
Grant A, Fathalli F, Rouleau G, Joober R, Flores C (2012) Association between schizophrenia and genetic variation in DCC: A case–control study. Schizophrenia research 137:26-31.
Grant A, Hoops D, Labelle-Dumais C, Prévost M, Rajabi H, Kolb B, Stewart J, Arvanitogiannis A, Flores C (2007) Netrin-1 receptor-deficient mice show enhanced mesocortical dopamine transmission and blunted behavioural responses to amphetamine. European Journal of Neuroscience 26:3215-3228.
Grazioplene R, Bearden C, Subotnik K, Ventura J, Green MF, Nuechterlein K, Cannon T (2017) 85. Diffusion Imaging of White Matter Pathways in Schizophrenia: Are Illness-Linked Changes Progressive? Schizophrenia Bulletin 43:S47-S47.
Gu H, Salmeron BJ, Ross TJ, Geng X, Zhan W, Stein EA, Yang Y (2010) Mesocorticolimbic circuits are impaired in chronic cocaine users as demonstrated by resting-state functional connectivity. Neuroimage 53:593-601.
Gunderson H, Solitare GB (1968) Mirror movements in patients with the Klippel-Feil syndrome: neuropathologic observations. Archives of neurology 18:675-679.
Haber S, Lynd E, Klein C, Groenewegen H (1990) Topographic organization of the ventral striatal efferent projections in the rhesus monkey: an anterograde tracing study. Journal of Comparative Neurology 293:282-298.
Haerer AF, Currier RD (1966) Mirror movements. Neurology 16:757-757.
Harrison NA, Brydon L, Walker C, Gray MA, Steptoe A, Critchley HD (2009) Inflammation causes mood changes through alterations in subgenual cingulate activity and mesolimbic connectivity. Biological psychiatry 66:407-414.
Harter P, Bunz B, Dietz K, Hoffmann K, Meyermann R, Mittelbronn M (2010) Spatio-temporal deleted in colorectal cancer (DCC) and netrin-1 expression in human foetal brain development. Neuropathology and applied neurobiology 36:623-635.
Hedrick L, Cho KR, Fearon ER, Wu T-C, Kinzler KW, Vogelstein B (1994) The DCC gene product in cellular differentiation and colorectal tumorigenesis. Genes & development 8:1174-1183.
Heinen F, Glocker FX, Fietzek U, Meyer BU, Lücking CH, Korinthenberg R (1998) Absence of transcallosal inhibition following focal mangnetic stimulation in preschool children. Annals of neurology 43:608-612.
Hibar DP, Stein JL, Renteria ME, Arias-Vasquez A, Desrivières S, Jahanshad N, Toro R, Wittfeld K, Abramovic L, Andersson M (2015) Common genetic variants influence human subcortical brain structures. Nature 520:224-229.
Hokama H, Shenton ME, Nestor PG, Kikinis R, Levitt JJ, Metcalf D, Wible CG, O'Donnella BF, Jolesz FA, McCarley RW (1995) Caudate, putamen, and globus pallidus volume in schizophrenia: A quantitative MRI study. Psychiatry Research: Neuroimaging 61:209-229.
Holt DJ, Graybiel AM, Saper CB (1997) Neurochemical architecture of the human striatum. Journal of Comparative Neurology 384:1-25.

Hooks MS, Jones GH, Smith AD, Neill DB, Justice JB (1991) Response to novelty predicts the locomotor and nucleus accumbens dopamine response to cocaine. Synapse 9:121-128.
Hoops D, Flores C (2017) Making Dopamine Connections in Adolescence. Trends in Neurosciences 40:709-719.
Horga G, Cassidy CM, Xu X, Moore H, Slifstein M, Van Snellenberg JX, Abi-Dargham A (2016) Dopamine-related disruption of functional topography of striatal connections in unmedicated patients with schizophrenia. JAMA psychiatry 73:862-870.
Horn KE, Glasgow SD, Gobert D, Bull S-J, Luk T, Girgis J, Tremblay M-E, McEachern D, Bouchard J-F, Haber M (2013) DCC expression by neurons regulates synaptic plasticity in the adult brain. Cell reports 3:173-185.
Hübers A, Orekhov Y, Ziemann U (2008) Interhemispheric motor inhibition: its role in controlling electromyographic mirror activity. European Journal of Neuroscience 28:364-371.
Husain MM, McDonald WM, Doraiswamy PM, Figiel GS, Na C, Escalona PR, Boyko OB, Nemeroff CB, Krishnan KRR (1991) A magnetic resonance imaging study of putamen nuclei in major depression. Psychiatry Research: Neuroimaging 40:95-99.
Hutchison KE, Wood MD, Swift R (1999) Personality factors moderate subjective and psychophysiological responses to d-amphetamine in humans. Experimental and Clinical Psychopharmacology 7:493.
Jamuar SS, Schmitz-Abe K, D'Gama AM, Drottar M, Chan W-M, Peeva M, Servattalab S, Lam A-TN, Delgado MR, Clegg NJ (2017) Biallelic mutations in human DCC cause developmental split-brain syndrome. Nature Genetics 49:606-612.
Jaspers E, Byblow WD, Feys H, Wenderoth N (2016) The Corticospinal Tract: A Biomarker to Categorize Upper Limb Functional Potential in Unilateral Cerebral Palsy. Frontiers in Pediatrics 3.
Kaasinen V, Aalto S, Någren K, Rinne JO (2004) Insular dopamine D2 receptors and novelty seeking personality in Parkinson's disease. Movement Disorders 19:1348-1351.
Kalil K, Dent EW (2005) Touch and go: guidance cues signal to the growth cone cytoskeleton. Current Opinion in Neurobiology 15:521-526.
Kalivas PW, Stewart J (1991) Dopamine transmission in the initiation and expression of drug- and stress-induced sensitization of motor activity. Brain Research Reviews 16:223-244.
Kandel ER, Schwartz JH, Jessell TM, Siegelbaum SA, Hudspeth AJ (2012) Principles of Neural Science, Fifth Edition: McGraw-Hill Education.
Kang HJ, Kawasawa YI, Cheng F, Zhu Y, Xu X, Li M, Sousa AM, Pletikos M, Meyer KA, Sedmak G (2011) Spatio-temporal transcriptome of the human brain. Nature 478:483.
Kanouchi T, Yokota T, Isa F, Ishii K, Senda M (1997) Role of the ipsilateral motor cortex in mirror movements. Journal of Neurology, Neurosurgery & Psychiatry 62:629-632.
Keino-Masu K, Masu M, Hinck L, Leonardo ED, Chan SS, Culotti JG, Tessier-Lavigne M (1996) Deleted in Colorectal Cancer (DCC) encodes a netrin receptor. Cell 87:175-185.
Kennedy TE, Serafini T, De La Torre J, Tessier-Lavigne M (1994) Netrins are diffusible chemotropic factors for commissural axons in the embryonic spinal cord. Cell 78:425-435.
Keshavan MS, Diwadkar VA, DeBellis M, Dick E, Kotwal R, Rosenberg DR, Sweeney JA, Minshew N, Pettegrew JW (2002) Development of the corpus callosum in childhood, adolescence and early adulthood. Life Sciences 70:1909-1922.

Kieseppä T, Eerola M, Mäntylä R, Neuvonen T, Poutanen V-P, Luoma K, Tuulio-Henriksson A, Jylhä P, Mantere O, Melartin T, Rytsälä H, Vuorilehto M, Isometsä E (2010) Major depressive disorder and white matter abnormalities: A diffusion tensor imaging study with tract-based spatial statistics. Journal of Affective Disorders 120:240-244.
Kim JH, Lavan D, Chen N, Flores C, Cooper H, Lawrence AJ (2013) Netrin-1 receptor-deficient mice show age-specific impairment in drug-induced locomotor hyperactivity but still self-administer methamphetamine. Psychopharmacology 230:607-616.
Kohno M, Morales AM, Ghahremani DG, Hellemann G, London ED (2014) Risky decision making, prefrontal cortex, and mesocorticolimbic functional connectivity in methamphetamine dependence. JAMA psychiatry 71:812-820.
Kolodziej PA, Timpe LC, Mitchell KJ, Fried SR, Goodman CS, Jan LY, Jan YN (1996) frazzled encodes a Drosophila member of the DCC immunoglobulin subfamily and is required for CNS and motor axon guidance. Cell 87:197-204.
Konagaya Y, Mano Y, Konagaya M (1990) Magnetic stimulation study in mirror movements. Journal of neurology 237:107-109.
Konova AB, Moeller SJ, Tomasi D, Volkow ND, Goldstein RZ (2013) Effects of methylphenidate on resting-state functional connectivity of the mesocorticolimbic dopamine pathways in cocaine addiction. JAMA psychiatry 70:857-868.
Koolschijn P, van Haren NE, Lensvelt-Mulders GJ, Pol H, Hilleke E, Kahn RS (2009) Brain volume abnormalities in major depressive disorder: A meta-analysis of magnetic resonance imaging studies. Human brain mapping 30:3719-3735.
Korgaonkar MS, Grieve SM, Koslow SH, Gabrieli JD, Gordon E, Williams LM (2011) Loss of white matter integrity in major depressive disorder: Evidence using tract-based spatial statistical analysis of diffusion tensor imaging. Human brain mapping 32:2161-2171.
Krams M, Quinton R, Ashburner J, Friston K, Frackowiak R, Bouloux P-M, Passingham R (1999) Kallmann's syndrome mirror movements associated with bilateral corticospinal tract hypertrophy. Neurology 52:816-816.
Krams M, Quinton R, Mayston M, Harrison L, Dolan R, Bouloux P, Stephens J, Frackowiak R, Passingham R (1997) Mirror movements in X-linked Kallmann's syndrome. II. A PET study. Brain: a journal of neurology 120:1217-1228.
Lacerda ALT, Brambilla P, Sassi RB, Nicoletti MA, Mallinger AG, Frank E, Kupfer DJ, Keshavan MS, Soares JC (2005) Anatomical MRI study of corpus callosum in unipolar depression. Journal of Psychiatric Research 39:347-354.
Leday GG, Vértes PE, Richardson S, Greene JR, Regan T, Khan S, Henderson R, Freeman TC, Pariante CM, Harrison NA (2018) Replicable and coupled changes in innate and adaptive immune gene expression in two case-control studies of blood microarrays in major depressive disorder. Biological psychiatry 83:70-80.
Leinsinger GL, Heiss DT, Jassoy AG, Pfluger T, Hahn K, Danek A (1997) Persistent mirror movements: functional MR imaging of the hand motor cortex. Radiology 203:545-552.
Lenze E, Sheline Y (1999) Absence of Striatal Volume Differences Between Depressed Subjects With No Comorbid Medical Illness and Matched Comparison Subjects. American Journal of Psychiatry 156:1989-1991.
Lepage J-F, Beaulé V, Srour M, Rouleau G, Pascual-Leone A, Lassonde M, Théoret H (2012) Neurophysiological investigation of congenital mirror movements in a patient with agenesis of the corpus callosum. Brain Stimulation: Basic, Translational, and Clinical Research in Neuromodulation 5:137-140.

Lesnick TG, Papapetropoulos S, Mash DC, Ffrench-Mullen J, Shehadeh L, De Andrade M, Henley JR, Rocca WA, Ahlskog JE, Maraganore DM (2007) A genomic pathway approach to a complex disease: axon guidance and Parkinson disease. PLoS genetics 3:e98.

Lewis DA, Melchitzky DS, Sesack SR, Whitehead RE, Auh S, Sampson A (2001) Dopamine transporter immunoreactivity in monkey cerebral cortex: regional, laminar, and ultrastructural localization. Journal of Comparative Neurology 432:119-136.

Leyton M (2010) The neurobiology of desire: Dopamine and the regulation of mood and motivational states in humans. In: Pleasures of the brain. New York, NY, US: Oxford University Press.

Leyton M (2017) Altered dopamine transmission as a familial risk trait for addictions. Current opinion in behavioral sciences 13:130-138.

Leyton M, Boileau I, Benkelfat C, Diksic M, Baker G, Dagher A (2002) Amphetamine-induced increases in extracellular dopamine, drug wanting, and novelty seeking: a PET/[11C] raclopride study in healthy men. Neuropsychopharmacology 27:1027-1035.

Li JY, Espay AJ, Gunraj CA, Pal PK, Cunic DI, Lang AE, Chen R (2007) Interhemispheric and ipsilateral connections in Parkinson's disease: relation to mirror movements. Movement Disorders 22:813-821.

Lin K-L, Kobayashi M, Pascual-Leone A (2002) Effects of musical training on speech-induced modulation in corticospinal excitability. Neuroreport 13:899-902.

Livesey F (1999) Netrins and netrin receptors. Cellular and Molecular Life Sciences CMLS 56:62-68.

Livesey F, Hunt S (1997) Netrin and netrin receptor expression in the embryonic mammalian nervous system suggests roles in retinal, striatal, nigral, and cerebellar development. Molecular and Cellular Neuroscience 8:417-429.

Llambi F, Causeret F, Bloch-Gallego E, Mehlen P (2001) Netrin-1 acts as a survival factor via its receptors UNC5H and DCC. The EMBO Journal 20:2715-2722.

Lu H, Zou Q, Chefer S, Ross TJ, Vaupel DB, Guillem K, Rea WP, Yang Y, Peoples LL, Stein EA (2014) Abstinence from cocaine and sucrose self-administration reveals altered mesocorticolimbic circuit connectivity by resting state MRI. Brain connectivity 4:499-510.

Ly A, Nikolaev A, Suresh G, Zheng Y, Tessier-Lavigne M, Stein E (2008) DSCAM Is a Netrin Receptor that Collaborates with DCC in Mediating Turning Responses to Netrin-1. Cell 133:1241-1254.

Manitt C, Kennedy TE (2002) Where the rubber meets the road: netrin expression and function in developing and adult nervous systems. Progress in brain research 137:425-442.

Manitt C, Labelle-Dumais C, Eng C, Grant A, Mimee A, Stroh T, Flores C (2010) Peri-pubertal emergence of UNC-5 homologue expression by dopamine neurons in rodents. PLoS One 5:e11463.

Manitt C, Mimee A, Eng C, Pokinko M, Stroh T, Cooper HM, Kolb B, Flores C (2011) The netrin receptor DCC is required in the pubertal organization of mesocortical dopamine circuitry. The Journal of Neuroscience 31:8381-8394.

Manitt C, Eng C, Pokinko M, Ryan R, Torres-Berrio A, Lopez J, Yogendran S, Daubaras M, Grant A, Schmidt E (2013) DCC orchestrates the development of the prefrontal cortex during adolescence and is altered in psychiatric patients. Translational psychiatry 3:e338.

Manson SC, Palace J, Frank JA, Matthews PM (2006) Loss of interhemispheric inhibition in patients with multiple sclerosis is related to corpus callosum atrophy. Experimental brain research 174:728-733.
Marinelli M, White FJ (2000) Enhanced vulnerability to cocaine self-administration is associated with elevated impulse activity of midbrain dopamine neurons. Journal of Neuroscience 20:8876-8885.
Marsh AP, Heron D, Edwards TJ, Quartier A, Galea C, Nava C, Rastetter A, Moutard M-L, Anderson V, Bitoun P (2017) Mutations in DCC cause isolated agenesis of the corpus callosum with incomplete penetrance. Nature Genetics 49:511-514.
Mawdsley DJ, Cooper HM, Hogan BM, Cody SH, Lieschke GJ, Heath JK (2004) The Netrin receptor Neogenin is required for neural tube formation and somitogenesis in zebrafish. Developmental Biology 269:302-315.
Mayston MJ, Harrison LM, Stephens JA (1999) A neurophysiological study of mirror movements in adults and children. Annals of neurology 45:583-594.
Mayston MJ, Harrison LM, Quinton R, Stephens J, Krams M, Bouloux P (1997) Mirror movements in X-linked Kallmann's syndrome. I. A neurophysiological study. Brain: a journal of neurology 120:1199-1216.
Mehlen P, Rabizadeh S, Snipas SJ, Assa-Munt N, Salvesen GS, Bredesen DE (1998) The DCC gene product induces apoptosis by a mechanism requiring receptor proteolysis. Nature 395:801.
Méneret A, Depienne C, Riant F, Trouillard O, Bouteiller D, Cincotta M, Bitoun P, Wickert J, Lagroua I, Westenberger A (2014) Congenital mirror movements Mutational analysis of RAD51 and DCC in 26 cases. Neurology 82:1999-2002.
Menza MA, Golbe LI, Cody RA, Forman NE (1993) Dopamine-related personality traits in Parkinson's disease. Neurology 43:505-505.
Meyer BU, Röricht S, Woiciechowsky C (1998) Topography of fibers in the human corpus callosum mediating interhemispheric inhibition between the motor cortices. Annals of neurology 43:360-369.
Morales M, Pickel VM (2012) Insights to drug addiction derived from ultrastructural views of the mesocorticolimbic system. Annals of the New York Academy of Sciences 1248:71-88.
Müller K, Kass-Iliyya F, Reitz M (1997) Ontogeny of ipsilateral corticospinal projections: a developmental study with transcranial magnetic stimulation. Annals of neurology 42:705-711.
Newton JM, Sunderland A, Gowland PA (2005) fMRI signal decreases in ipsilateral primary motor cortex during unilateral hand movements are related to duration and side of movement. NeuroImage 24:1080-1087.
Nobuhara K, Okugawa G, Sugimoto T, Minami T, Tamagaki C, Takase K, Saito Y, Sawada S, Kinoshita T (2006) Frontal white matter anisotropy and symptom severity of late-life depression: a magnetic resonance diffusion tensor imaging study. Journal of Neurology, Neurosurgery & Psychiatry 77:120-122.
Ohtani T, Levitt JJ, Nestor PG, Kawashima T, Asami T, Shenton ME, Niznikiewicz M, McCarley RW (2014) Prefrontal cortex volume deficit in schizophrenia: a new look using 3 T MRI with manual parcellation. Schizophrenia research 152:184-190.

Okada N, Fukunaga M, Yamashita F, Koshiyama D, Yamamori H, Ohi K, Yasuda Y, Fujimoto M, Watanabe Y, Yahata N (2016) Abnormal asymmetries in subcortical brain volume in schizophrenia. Molecular psychiatry 21:1460.
Okbay A, Baselmans BM, De Neve J-E, Turley P, Nivard MG, Fontana MA, Meddens SFW, Linnér RK, Rietveld CA, Derringer J (2016) Genetic variants associated with subjective well-being, depressive symptoms, and neuroticism identified through genome-wide analyses. Nature genetics 48:624-633.
Osborne P, Halliday G, Cooper H, Keast J (2005) Localization of immunoreactivity for deleted in colorectal cancer (DCC), the receptor for the guidance factor netrin-1, in ventral tier dopamine projection pathways in adult rodents. Neuroscience 131:671-681.
Palmer LM, Schulz JM, Murphy SC, Ledergerber D, Murayama M, Larkum ME (2012) The cellular basis of GABAB-mediated interhemispheric inhibition. Science 335:989-993.
Pan CC, McQuoid DR, Taylor WD, Payne ME, Ashley-Koch A, Steffens DC (2009) Association analysis of the COMT/MTHFR genes and geriatric depression: An MRI study of the putamen. International Journal of Geriatric Psychiatry 24:847-855.
Parashos IA, Tupler LA, Blitchington T, Krishnan KRR Magnetic-resonance morphometry in patients with major depression. Psychiatry Research: Neuroimaging 84:7-15.
Paul LK, Brown WS, Adolphs R, Tyszka JM, Richards LJ, Mukherjee P, Sherr EH (2007) Agenesis of the corpus callosum: genetic, developmental and functional aspects of connectivity. Nature Reviews Neuroscience 8:287.
Paus T, Keshavan M, Giedd JN (2008) Why do many psychiatric disorders emerge during adolescence? Nature Reviews Neuroscience 9:947.
Pillai A, Howell KR, Ahmed AO, Weinberg D, Allen KM, Bruggemann J, Lenroot R, Liu D, Galletly C, Weickert CS, Weickert TW (2015) Association of serum VEGF levels with prefrontal cortex volume in schizophrenia. Molecular Psychiatry 21:686.
Pokinko M, Moquin L, Torres-Berrío A, Gratton A, Flores C (2015) Resilience to amphetamine in mouse models of netrin-1 haploinsufficiency: role of mesocortical dopamine. Psychopharmacology 232:3719-3729.
Pujol J, Vendrell P, Junqué C, Martí-Vilalta JL, Capdevila A (1993) When does human brain development end? Evidence of corpus callosum growth up to adulthood. Annals of neurology 34:71-75.
Rakic P, Yakovlev PI (1968) Development of the corpus callosum and cavum septi in man. Journal of Comparative Neurology 132:45-72.
Regli F, Filippa G, Wiesendanger M (1967) Hereditary mirror movements. Archives of neurology 16:620-623.
Reitz M, Müller K (1998) Differences between `congenital mirror movements' and `associated movements' in normal children: a neurophysiological case study. Neuroscience Letters 256:69-72.
Reyes S, Fu Y, Double KL, Cottam V, Thompson LH, Kirik D, Paxinos G, Watson C, Cooper HM, Halliday GM (2013) Trophic factors differentiate dopamine neurons vulnerable to Parkinson's disease. Neurobiology of aging 34:873-886.
Reynolds LM, Gifuni AJ, McCrea ET, Shizgal P, Flores C (2016) dcc haploinsufficiency results in blunted sensitivity to cocaine enhancement of reward seeking. Behavioural brain research 298:27-31.
Reynolds LM, Makowski CS, Yogendran SV, Kiessling S, Cermakian N, Flores C (2015) Amphetamine in adolescence disrupts the development of medial prefrontal cortex

dopamine connectivity in a DCC-dependent manner. Neuropsychopharmacology 40:1101-1112.
Reynolds LM, Pokinko M, Berrío AT, Cuesta S, Lambert LC, Pellitero EDC, Wodzinski M, Manitt C, Krimpenfort P, Kolb B (2018) DCC receptors drive prefrontal cortex maturation by determining dopamine axon targeting in adolescence. Biological Psychiatry 83:181-192.
Ridding M, Brouwer B, Nordstrom M (2000) Reduced interhemispheric inhibition in musicians. Experimental Brain Research 133:249-253.
Robinson TE, Berridge KC (2008) The incentive sensitization theory of addiction: some current issues. Philosophical Transactions of the Royal Society B: Biological Sciences 363:3137-3146.
Rosenzweig ES, Brock JH, Culbertson MD, Lu P, Moseanko R, Edgerton VR, Havton LA, Tuszynski MH (2009) Extensive spinal decussation and bilateral termination of cervical corticospinal projections in rhesus monkeys. Journal of Comparative Neurology 513:151-163.
Rouiller EM, Liang F, Moret V, Wiesendanger M (1991) Trajectory of redirected corticospinal axons after unilateral lesion of the sensorimotor cortex in neonatal rat; a phaseolus vulgaris-leucoagglutinin (PHA-L) tracing study. Experimental neurology 114:53-65.
Sachs-Ericsson NJ, Hajcak G, Sheffler JL, Stanley IH, Selby EA, Potter GG, Steffens DC (2017) Putamen Volume Differences Among Older Adults: Depression Status, Melancholia, and Age. Journal of Geriatric Psychiatry and Neurology 31:39-49.
Schmaal L, Veltman DJ, van Erp TG, Sämann P, Frodl T, Jahanshad N, Loehrer E, Tiemeier H, Hofman A, Niessen W (2016) Subcortical brain alterations in major depressive disorder: findings from the ENIGMA Major Depressive Disorder working group. Molecular psychiatry 21:806.
Schmaal L, Hibar D, Sämann P, Hall G, Baune B, Jahanshad N, Cheung J, van Erp T, Bos D, Ikram M (2017) Cortical abnormalities in adults and adolescents with major depression based on brain scans from 20 cohorts worldwide in the ENIGMA Major Depressive Disorder Working Group. Molecular psychiatry 22:900.
Schnitzler A, Kessler KR, Benecke R (1996) Transcallosally mediated inhibition of interneurons within human primary motor cortex. Experimental Brain Research 112:381-391.
Scholz J, Tomassini V, Johansen-Berg H (2014) Individual differences in white matter microstructure in the healthy brain. In: Diffusion MRI (Second Edition), pp 301-316: Elsevier.
Sharafaddinzadeh N, Bavarsad R, Yousefkhah M, Aleali A (2008) Familial mirror movements over five generations. Neurol India 56:482-483.
Shi M, Guo C, Dai JX, Ding YQ (2008) DCC is required for the tangential migration of noradrenergic neurons in locus coeruleus of mouse brain. Molecular and Cellular Neuroscience 39:529-538.
Shi M, Zheng M-H, Liu Z-R, Hu Z-L, Huang Y, Chen J-Y, Zhao G, Han H, Ding Y-Q (2010) DCC is specifically required for the survival of retinal ganglion and displaced amacrine cells in the developing mouse retina. Developmental Biology 348:87-96.
Shibasaki H, Sadato N, Lyshkow H, Yonekura Y, Honda M, Nagamine T, Suwazono S, Magata Y, Ikeda A, Miyazaki M, Fukuyama H, Asato R, Konishi J (1993) Both primary motor cortex and supplementary motor area play an important role in complex finger movement. Brain 116:1387-1398.

Shu T, Valentino KM, Seaman C, Cooper HM, Richards LJ (2000) Expression of the netrin-1 receptor, deleted in colorectal cancer (DCC), is largely confined to projecting neurons in the developing forebrain. Journal of Comparative Neurology 416:201-212.
Smeland OB, Wang Y, Frei O, Li W, Hibar DP, Franke B, Bettella F, Witoelar A, Djurovic S, Chen C-H (2018) Genetic Overlap Between Schizophrenia and Volumes of Hippocampus, Putamen, and Intracranial Volume Indicates Shared Molecular Genetic Mechanisms. Schizophrenia bulletin 44.
Sommer IEC, Ramsey NF, Kahn RS (2001) Language lateralization in schizophrenia, an fMRI study. Schizophrenia Research 52:57-67.
Srour M, Philibert M, Dion MH, Duquette A, Richer F, Rouleau GA, Chouinard S (2009) Familial congenital mirror movements: report of a large 4-generation family. Neurology 73:729-731.
Srour M, Rivière J-B, Pham JM, Dubé M-P, Girard S, Morin S, Dion PA, Asselin G, Rochefort D, Hince P (2010) Mutations in DCC cause congenital mirror movements. Science 328:592-592.
Sun KLW, Correia JP, Kennedy TE (2011) Netrins: versatile extracellular cues with diverse functions. Development 138:2153-2169.
Taber KH, Black DN, Porrino LJ, Hurley RA (2012) Neuroanatomy of dopamine: reward and addiction. The Journal of neuropsychiatry and clinical neurosciences 24:1-4.
Tomer R, Aharon-Peretz J (2004) Novelty seeking and harm avoidance in Parkinson's disease: effects of asymmetric dopamine deficiency. Journal of Neurology, Neurosurgery & Psychiatry 75:972-975.
Torres-Berrío A, Lopez JP, Bagot RC, Nouel D, Dal Bo G, Cuesta S, Zhu L, Manitt C, Eng C, Cooper HM (2017) DCC confers susceptibility to depression-like behaviors in humans and mice and is regulated by miR-218. Biological psychiatry 81:306-315.
Turner RS, Grafton ST, Votaw JR, Delong MR, Hoffman JM (1998) Motor subcircuits mediating the control of movement velocity: a PET study. Journal of Neurophysiology 80:2162-2176.
Ventura R, Alcaro A, Cabib S, Conversi D, Mandolesi L, Puglisi-Allegra S (2004) Dopamine in the medial prefrontal cortex controls genotype-dependent effects of amphetamine on mesoaccumbens dopamine release and locomotion. Neuropsychopharmacology : official publication of the American College of Neuropsychopharmacology 29:72-80.
Vezina P (2004) Sensitization of midbrain dopamine neuron reactivity and the self-administration of psychomotor stimulant drugs. Neuroscience & Biobehavioral Reviews 27:827-839.
Volenec A, Bhogal RK, Moorman JM, Leslie RA, Flanigan TP (1997) Differential expression of DCC mRNA in adult rat forebrain. Neuroreport 8:2913-2917.
Volkow ND, Rosen B, Farde L (1997) Imaging the living human brain: magnetic resonance imaging and positron emission tomography. Proceedings of the National Academy of Sciences of the United States of America 94:2787.
Vosberg DE, Zhang Y, Menegaux A, Chalupa A, Manitt C, Zehntner S, Eng C, DeDuck K, Allard D, Durand F (2018) Mesocorticolimbic Connectivity and Volumetric Alterations in DCC Mutation Carriers. Journal of Neuroscience:3251-3217.
Wahl M, Lauterbach-Soon B, Hattingen E, Jung P, Singer O, Volz S, Klein JC, Steinmetz H, Ziemann U (2007) Human Motor Corpus Callosum: Topography, Somatotopy, and Link between Microstructure and Function. The Journal of Neuroscience 27:12132-12138.

Ward J, Strawbridge RJ, Bailey ME, Graham N, Ferguson A, Lyall DM, Cullen B, Pidgeon LM, Cavanagh J, Mackay DF (2017) Genome-wide analysis in UK Biobank identifies four loci associated with mood instability and genetic correlation with major depressive disorder, anxiety disorder and schizophrenia. Translational psychiatry 7:1264.
Welniarz Q, Morel M-P, Pourchet O, Gallea C, Lamy J-C, Cincotta M, Doulazmi M, Belle M, Méneret A, Trouillard O (2017) Non cell-autonomous role of DCC in the guidance of the corticospinal tract at the midline. Scientific Reports 7:410.
Whitton AE, Treadway MT, Pizzagalli DA (2015) Reward processing dysfunction in major depression, bipolar disorder and schizophrenia. Current opinion in psychiatry 28:7.
Woodruff P, McManus I, David A (1995) Meta-analysis of corpus callosum size in schizophrenia. Journal of Neurology, Neurosurgery & Psychiatry 58:457-461.
Wray NR et al. (2018) Genome-wide association analyses identify 44 risk variants and refine the genetic architecture of major depression. Nature Genetics 50:668–681.
Wu JC, Buchsbaum MS, Johnson JC, Hershey TG, Wagner EA, Tung C, Lottenberg S (1993) Magnetic resonance and positron emission tomography imaging of the corpus callosum: size, shape and metabolic rate in unipolar depression. Journal of affective disorders 28:15-25.
Xu K, Wu Z, Renier N, Antipenko A, Tzvetkova-Robev D, Xu Y, Minchenko M, Nardi-Dei V, Rajashankar KR, Himanen J (2014) Structures of netrin-1 bound to two receptors provide insight into its axon guidance mechanism. Science 344:1275-1279.
Yan P, Qiao X, Wu H, Yin F, Zhang J, Ji Y, Wei S, Lai J (2016) An Association Study Between Genetic Polymorphisms in Functional Regions of Five Genes and the Risk of Schizophrenia. Journal of Molecular Neuroscience 59:366-375.
Yang Q, Huang X, Hong N, Yu X (2007) White matter microstructural abnormalities in late-life depression. International Psychogeriatrics 19:757-766.
Yasuno F, Suhara T, Sudo Y, Yamamoto M, Inoue M, Okubo Y, Suzuki K (2001) Relation among dopamine D2 receptor binding, obesity and personality in normal human subjects. Neuroscience Letters 300:59-61.
Zeng Y, Navarro P, Fernandez-Pujals AM, Hall LS, Clarke T-K, Thomson PA, Smith BH, Hocking LJ, Padmanabhan S, Hayward C (2017) A combined pathway and regional heritability analysis indicates NETRIN1 pathway is associated with major depressive disorder. Biological psychiatry 81:336-346.